8-2017

Design, Synthesis and Sustainable Applications of Animal Protein-Based Thermoset Polymers and Covalent Organic Frameworks

Xiaoyan Yu
Clemson University

DESIGN, SYNTHESIS AND SUSTAINABLE APPLICATIONS OF ANIMAL PROTEIN-BASED THERMOSET POLYMERS AND COVALENT ORGANIC FRAMEWORKS

A Dissertation
Presented to
the Graduate School of
Clemson University

In Partial Fulfillment
of the Requirements for the Degree
Doctor of Philosophy

---

by
Xiaoyan Yu
August 2017

Accepted by:
Srikanth Pilla, Committee Chair
Fadi Abu-farha
Craig Clemons
Mark Hoffman
Annel Greene

ABSTRACT

Extensive research has been undertaken in recent times on finding suitable, alternative, non-feed and non-fertilizer applications for proteinaceous materials in the animal rendering industry. In this regard, use of such proteins to derive plastics, especially thermoplastics and derived composites, has emerged as a potentially acceptable choice. However, the widespread use of such proteins for aforementioned applications is limited by their poor mechanical properties, high moisture absorption and their inherent odor. In this study, we have engineered, for the first time, high-strength, toughened thermoset polymers from proteinaceous materials obtained from the rendering industry so that they can be employed in high performance applications, such as in the automotive sector. However, the lack of compatibility between protein molecules and organic resins could not be ignored. Hence, in this study, we have also solved this problem by utilizing waterborne polyurethane as resins to react with protein molecules and form covalent-bonded interconnected hybrid polymers. To overcome the lack of compatibility, water soluble epoxy resin was also studied to crosslink with animal protein molecules.

Recycling of epoxy resin-based composites has widely gained attention among researchers and environmentalists as the major waste processing method for such composites is landfilling, which requires large areas of waste land. While alternative recycling pathways such as mechanical, pyrolysis and fluidized bed have been achieved, all such pathways have either been undertaken at a small scale, are highly energy-intensive, or are detrimental to the environment through other means. Here, we present a

new self-healing, repairable, and recyclable epoxy matrix with extendable usage time as well as increased life cycles. Moreover, urethane chain was introduced into the epoxy matrix as it helped achieve tunable, varying mechanical properties, with the copolymer possessing properties of both polyurethane and epoxy.

To understand the art of molecule architecture, an easy method to prepare graphitic material from synthesized polymer was described in this study. Polyazomethine was synthesized, activated at high temperature, referred to as nitrogen-doped carbon (NC) materials, and then used to purify water. TGA results directed the choice of annealing temperature. Raman spectra confirmed that the material was indeed graphite-similar, showing G and D bands at 1584 cm^{-1} and 1337 cm^{-1} respectively. Adsorption experiments and BET surface area measurements revealed that temperature of 750 ℃ or higher was efficient for annealing the material.

ACKNOWLEDGMENTS

I would like to thank many people I have worked with during my Ph.D. program. First and foremost, I would thank my research advisor Dr. Srikanth Pilla, without who my progress would not be possible. Dr. Srikanth Pilla will be my life long advisor and friend. Thanks to my committee members Dr. Annel Greene, Dr. Fadi Abu-farha, Dr. Mark Hoffman and Dr. Craig Clemens, whose insightful comments made finishing the dissertation an enriching experience.

I would like to acknowledge the financial support of ACREC (Animal Coproducts Research and Education Center) consortium at Clemson University.

Thanks to my parents Lanfang Dong and Laixin Yu for their unconditional love and support for every decision of mine in the pathway to pursue the Ph.D degree. Thanks to my brother Zhibo Yu, my sister-in-law Lihua Liu and my nephew Kaiyuan Yu for their continuous support and encouragement.

Thanks to Zeren Xu. He is my best friend in life and in research work. He has always been there for me through my Ph.D life.

Also thanks to my friends that I have met over these years: Xueyu Zhang, Qian Wang, Bin Xu, Zhe Wang, Zhiyuan Du, Darui Zhang, Ting Zheng, Vishnupriya Ramineni, Lirui Wang, Yuchen Zhang, Xin Wang, Lihua Jiang, Shuonan Xu, Chengqiang Zhan, Siyun Yang, Chenbo Dong, Yuan Jiang, Yueting Wu, Qiang Zhang, Xiaoning He.

TABLE OF CONTENTS

Page

LIST OF TABLES

LIST OF FIGURES

LIST OF ABBREVIATIONS

AP	Animal protein
BMI	Bismaleimide
HBP	Hyperbranched Polymer
WPU	Waterborne Polyurethane
E	Epoxy
P	Protein
WEP	Water soluble epoxy
5a	Copolymer with disulfide bond
5b	Copolymer without disulfide bond
NC	Nitrogen doped carbon
BET	Brunauer-Emmett-Teller
FTIR	Fourier transform infrared spectroscopy
SEM	Scanning electron microscopy
TGA	Thermogravimetric analysis
TEM	Transmission electron microscopy
XPS	X-ray photoelectron spectroscopy
2D	Two dimension
R-5a	Reprocessed copolymer 5a

CHAPTER ONE

INTRODUCTION

Thermosetting plastics play an important role across several industries in present times, such as automotive, aerospace and construction. This can be attributed to their good thermal and mechanical properties, high durability, excellent resistance to chemicals and moisture, and their unique properties due to their crosslinked network (1).

1.1 Bio-based Thermosetting Plastics: The Present Context

With increasing concerns regarding environmental degradation and its subsequent impacts on human health, studies on next-generation materials are focused increasingly towards sustainability, industrial ecology, eco-efficiency, and green chemistry. These principles have led researchers to focus on developing bio-based materials, especially in the plastics sector, especially with regard to producing bio-based polymers as alternatives to traditional petroleum-based plastics (2-4).

Extensive research has been undertaken in recent times on finding suitable, alternative, non-feed and non-fertilizer applications for these proteinaceous materials in the animal rendering industry. In this regard, use of such proteins to derive plastics, especially thermoplastics and derived composites, has emerged as a potentially acceptable choice. However, the widespread use of such proteins for aforementioned applications is limited by their poor mechanical properties, high moisture absorption and unpleasant inherent odor. Despite these issues, protein-based thermoset materials have attracted wide attention for plastic production in recent times. Most studies have targeted

functional groups of amino acid residues, such as primary amines, carboxyl, hydroxyl, and sulfhydryls. Among these studies, aldehydes (formaldehyde, glutaraldehyde, and glyoxal) are the most commonly used agents for chemical crosslinking of protein monomers (5-7). However, due to the chemical structure of these agents, release of toxic monomers remains unavoidable (6), which places obstacles in the use of animal protein-based plastics.

1.2 Motivation to study bio-based thermosetting plastics and organic frameworks

Developing high performance bio-based renewable thermosetting plastics needs one to take into consideration the lack of compatibility between the resin and the crosslinker. As is well known, such lack of compatibility in general leads to a compromise on properties and performance of a material system. It is this fundamental issue between the animal protein – extracted from poultry materials – and epoxy resin that is sought to be addressed in this work.

Even though partially bio-based thermosetting plastics were prepared, complete biodegradability could not be achieved and the plastic could only be used for one life cycle. To increase the number of life cycles of usage of such thermosetting plastics, reversible crosslinking reaction mechanism was introduced into the thermoset network. For instance, disulfide bond was chosen to realize the recyclable thermosetting network, while the combination of polyurethane and epoxy was simultaneously introduced to ensure comprehensive tunability of properties of the new copolymer.

With respect to the architecture of thermosetting network, the simplest 2D organic frameworks were designed and built in the lab. Since these frameworks were highly porous with large surface areas, their potential application in water purification and gas capture was also studied.

1.3 Goals of this work

Partially bio-based hybrid networks were obtained by preparing animal protein (after extraction from waste poultry byproducts) and combining it with traditional petroleum-based resins. Initially, traditional DGEBA epoxy was applied to crosslink the protein molecules, but this introduced a new problem of lack of compatibility between the epoxy and animal protein molecules. This lack of compatibility was due to the difference in nature of epoxy (hydrophobic) and animal protein molecules (hydrophilic). To overcome this issue, waterborne polyurethane (WPU) and water soluble epoxy were chosen and combined.

In addition to investigating bio-based resources as possible replacement to traditional petroleum-based thermoset resins, recyclability of thermoset networks was also studied. Hybrid polymers were synthesized for this purpose by combining flexible polyurethane and high strength epoxy. Finally, based on all the knowledge about thermoset networks, a fundamental attempt was made to better understand the art of molecule architecture via design and synthesis of 2D organic frameworks, as well as the potential for its use in water purification and gas capture applications.

1.4 Specific objectives of this thesis were:

- Energy-efficient protein extraction from poultry materials
- Applying epoxy resin to crosslink non-hydrolyzed animal protein to form thermosetting plastics
- Preparation of waterborne and animal protein hybrid polymer
- Development of water soluble epoxy and animal protein hybrid polymer to overcome the issue of compatibility
- Investigation on the recycling of thermosetting plastics
- Fundamental study on 2D organic frameworks and its sustainable application

REFERENCES

(1) Riccardi, C.; Adabbo, H.; Williams, R. Curing reaction of epoxy resins with diamines. J Appl Polym Sci 1984, 29, 2481-2492.

(2) Wool, R.; Sun, X. S. Bio-based polymers and composites; Academic Press: 2011; .

(3) Mohanty, A.; Misra, M.; Drzal, L. Sustainable bio-composites from renewable resources: opportunities and challenges in the green materials world. Journal of Polymers and the Environment 2002, 10, 19-26.

(4) Zheng, T.; Yu, X.; Pilla, S. Mechanical and moisture sensitivity of fully bio-based dialdehyde carboxymethyl cellulose cross-linked soy protein isolate films. Carbohydr. Polym. 2017, 157, 1333-1340.

(5) Park, S.; Bae, D.; Rhee, K. Soy protein biopolymers cross-linked with glutaraldehyde. J. Am. Oil Chem. Soc. 2000, 77, 879-884.

(6) Silva, R.; Elvira, C.; Mano, J.; San Roman, J.; Reis, R. Influence of β-radiation sterilisation in properties of new chitosan/soybean protein isolate membranes for guided bone regeneration. J. Mater. Sci. Mater. Med. 2004, 15, 523-528.

(7) Marqui é, C. Chemical reactions in cottonseed protein cross-linking by formaldehyde, glutaraldehyde, and glyoxal for the formation of protein films with enhanced mechanical properties. J. Agric. Food Chem. 2001, 49, 4676-4681.

CHAPTER TWO

LITERATURE REVIEW: PROTEIN DERIVED THERMOSETTING PLASTICS

2.1 Introduction

Thermosetting plastics play an important role across multiple industries such as automotive, aerospace and construction, which can be attributed to its good thermal and mechanical properties, high durability, and excellent chemical and moisture resistance, combined with its unique properties due to its crosslinked network structure (1). Commonly used thermosetting plastics for commercial applications include epoxy (2), polyurethane (3) and phenolics (4). Epoxy is the most-preferred due to its ease of curing, good elasticity and exceptional chemical resistance compared to other resins. Thermosetting polyurethane elastomer exhibits low temperature flexibility and shape memory (5), while phenolics are easy to mold, brittle, strong and hard (6). The wide range of properties of these thermosetting plastics promotes their application across various sectors.

Production of thermosetting plastics till date is mostly dependent on crude oil production. As is well known, crude oil is a limited nonrenewable resource that is spread unevenly across the world (7). Thus, the price and availability of crude oil can significantly affect the market for thermosetting plastics, driving the need to urgently develop new thermosetting plastics based on renewable resources. Recent years have witnessed an increase in studies on bio-resource based plastics that combine traditional crude oil-based polymer with biopolymers obtained from plants (8), animal byproducts

(9), and others. Such bio-resources can be added to thermosetting network as fillers (10) or as chemical bond connected chains (11), depending on the reaction mechanisms.

Addition of bio-resources, even if as replacement to traditional thermosetting polymer networks, not only provides solutions to the problem of nonrenewable nature of materials for such polymers, but also generates new opportunities for achieving recyclability of thermosetting plastics (12). Various bio-based renewable materials have been reported in literature with regard to preparing thermosetting plastics. Plant oils are now being considered as the most important renewable source for the production of bio-based thermoset plastics. While epoxidized soybean oil (ESO) – synthesized via epoxidation of general soybean oil – stands out among plant oils as the most commonly used (13), other epoxidized plant oils reported in past studies include epoxidized versions of sunflower oil (14), triglyceride oil (15), and palm oil (16).

After cellulose and plant oils, lignin remains the most abundant naturally occurring macromolecule (17). Traditionally, lignin has been viewed as a waste material available in large quantity derived from wood pulp in the paper industry. However, very little quantity of lignin is utilized for specific applications, while most of it is generally burnt, resulting in air pollution. Most forms of lignin have an aromatic and crosslinked structure, along with the presence of many functional groups such as ether and hydroxyl groups, depending on their origin and the technology used for their extraction (18).

Rapid development has occurred in the fields of biotechnology and organic chemistry, leading to the emergence of new bio-based materials, including from animal sources. Among these, proteins remain the most widely used bio-based material, although

most of it is used as food. Protein molecules contain various functional groups that possess the potential to form 3D architecture with other chemical molecules. Some resins such as epoxy, phenolic and polyurethane have been studied to prepare thermosetting plastic materials combined with proteins.

2.2 Epoxy resins

Epoxy resins have been used across several industries over several decades, and cover a large ratio of thermosetting materials with their unique crosslinked network structure formed with curing agent and stimuli like heating, UV and sonication. Epoxy ring is the functional group in epoxy resins, and it is highly active and can react with some other functional groups such as –OH, -NH_2, -COOH, -SH and –NH- to form inter-connective bonds. Figure 1 shows the reaction mechanism between epoxy and these functional groups. In some cases, it also needs the involvement of a catalyst to promote the crosslinking reaction. As reported, all these functional groups can be found in protein molecules, which means that these reaction mechanisms are valid for reactions between protein molecules and epoxy.

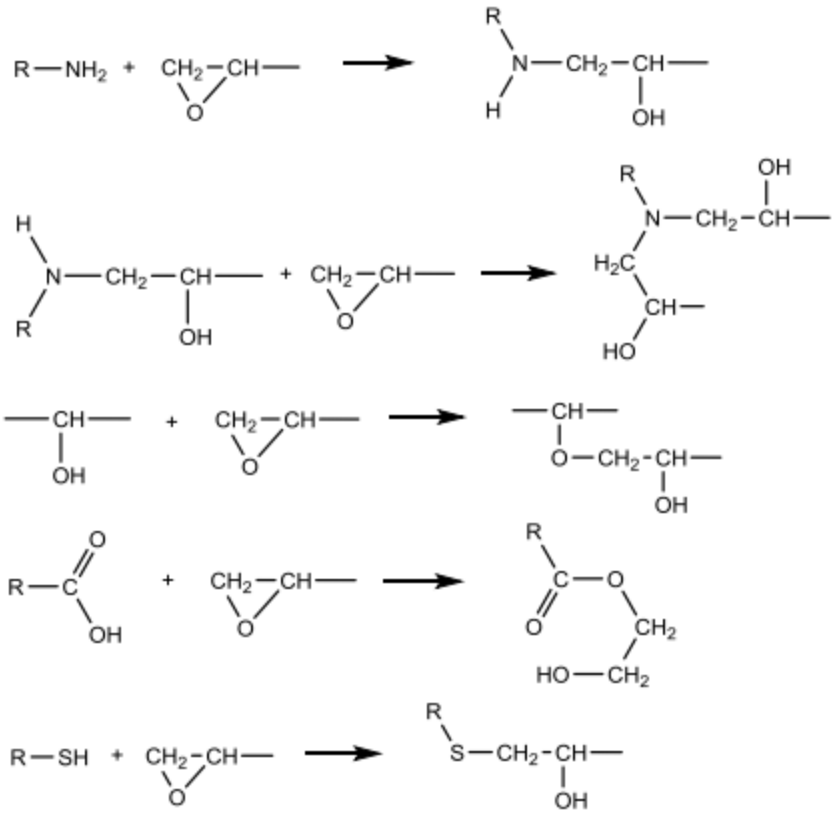

Figure 2.1 Reaction mechanism of protein molecule with epoxy (19)

Plant oils have been studied as epoxy resins for a long duration that report their various properties, such as for deoxidized soybean oils (20) and deoxidized linseed oils (21). Synthesis of monomers as well as polymers from plant fats and oils has already found some industrial applications, and recent developments in this field offer promising new opportunities. Besides epoxy resins, new value-added applications have also been obtained for other bio-resources. For instance, proteins have been reported as crosslinkers (crosslinking agents) in epoxy curing processes in the literature reviewed (19, 22, 23).

Wang et al. prepared canola protein isolate-poly(glycidyl methacrylate) conjugates-based adhesives through free radical polymerization mechanism (22).

Poly(glycidyl methacrylate) was grafted onto alpha-carbon of the peptide backbone, and secondary structure changes were observed based on results obtained by 13C CP/MAS NMR spectroscopy. This adhesive showed competitive adhesive strength and improved water resistance (81.97 % increase) compared with denatured canola protein-based adhesive, due to the covalent bond formed between protein molecules, grafted polymer chains and the wooden surface. Addition of polymer chains to biomolecules not only contributed to the improvement in adhesive strength, but also improved its thermal properties. This study addressed the application of canola protein in preparation of thermosetting plastics.

Wang et al. (23) synthesized soy protein isolate (SPI)-epoxy castor oil-hydroxypropyl cellulose-based thermosetting films, which was fully bio-based, and showed the formation of covalent bond between SPI and castor oil. Both tensile strength and elongation at break showed increase upon the addition of epoxy castor oil and hydroxypropyl cellulose compared to pure soy protein isolate films. This was due to the covalent bond formed between epoxy groups of epoxy castor oil and amino groups of SPI through ring opening reaction. They confirmed that hydroxypropyl cellulose was completely compatible with the SPI matrix. This report showed how soy protein could be used in the preparation of thermoset materials. Xia et al. (24) prepared soy protein isolate-based films cross-linked by epoxidized soybean oil – a fully bio-based thermoset material. Tensile modulus, tensile strength, 10 % offset yield strength and water resistance of ESO-modified SPI-based films showed significantly improvement upon addition of soy protein. Dastidar et al. (67) developed a novel chemistry scheme to

prepare soy flour-based thermoset resin without the use of any external crosslinker. The resultant crosslinked (thermosetting) soy protein resin showed enhanced mechanical and thermal properties along with reduced moisture absorption. When reinforced with strong microfibrillated cellulose, they can thus produce fully sustainable and biodegradable green composites.

Mekonnen et al. (19) reported using hydrolyzed animal protein as crosslinker for Bisphenol A diglycidyl ether (DGEBA) to prepare thermosetting plastics. The animal protein was hydrolyzed under high temperature and high pressure prior to further usage. Competitive performance was showed in the produced specimen. The same mechanism was applied in this process as that used in studies on canola protein and soy protein.

As the most popularly studied resin for protein-based thermosetting plastics, epoxy resin provides a good basis for the development of wide application of protein-based plastics. In future, introduction of water-based epoxy could help solve the compatibility problem between hydrophobic epoxy and hydrophilic protein molecules, further enhancing the properties of protein-epoxy based thermosetting plastics.

2.3 Aldehydes resins

Aldehydes such as glutaraldehyde, glyoxal and formaldehyde, have been used to crosslink many proteins, such as soy protein (25) (26), cottonseed protein (27), sunflower protein isolate (28) and whey proteins (29). Following this, many studies have focused on enhancing properties of such protein/aldehyde-based films. The reaction mechanism between proteins and aldehydes in such studies involves reaction between amino groups

(abundantly available in protein chains) and aldehyde groups (of aldehydes) to form the crosslinking network. Thermal and mechanical properties of the crosslinked network have been shown to be much better than those of individual protein isolate compressed films.

Hernández-Muñoz et al. (30) reported the effect of crosslinking agents, glutaraldehyde (GTA), glyoxal (GLY) and formaldehyde (FA) on relevant properties of films based on glutenin-rich fraction from commercial wheat gluten (80% protein). The results showed that the highest tensile strength values were obtained using FA, followed by GTA and GLY. Glass transition temperature of crosslinked films was observed to shift to slightly higher values upon the use of crosslinking agents.

Ting et al. (31) prepared dialdehyde carboxymethyl cellulose (DCMC) crosslinked soy protein isolate (SPI) films by solvent casting method. In this study, significant increase in tensile strength was observed (up to 218 %), which suggests the occurrence of highly effective crosslinking between SPI and DCMC. Impressive improvement in tensile strength compared to other dialdehyde polysaccharide crosslinking agents such as dialdehyde starch was likely caused of higher compatibility of DCMC with SPI, as was further confirmed by SEM images. Crosslinking also leads to reduction in water vapor permeability and moisture content, along with an increase in insoluble mass percentage, indicating improvement in water resistance of these bio-based protein films. The thermal stability of protein films was improved after crosslinked by DCMC.

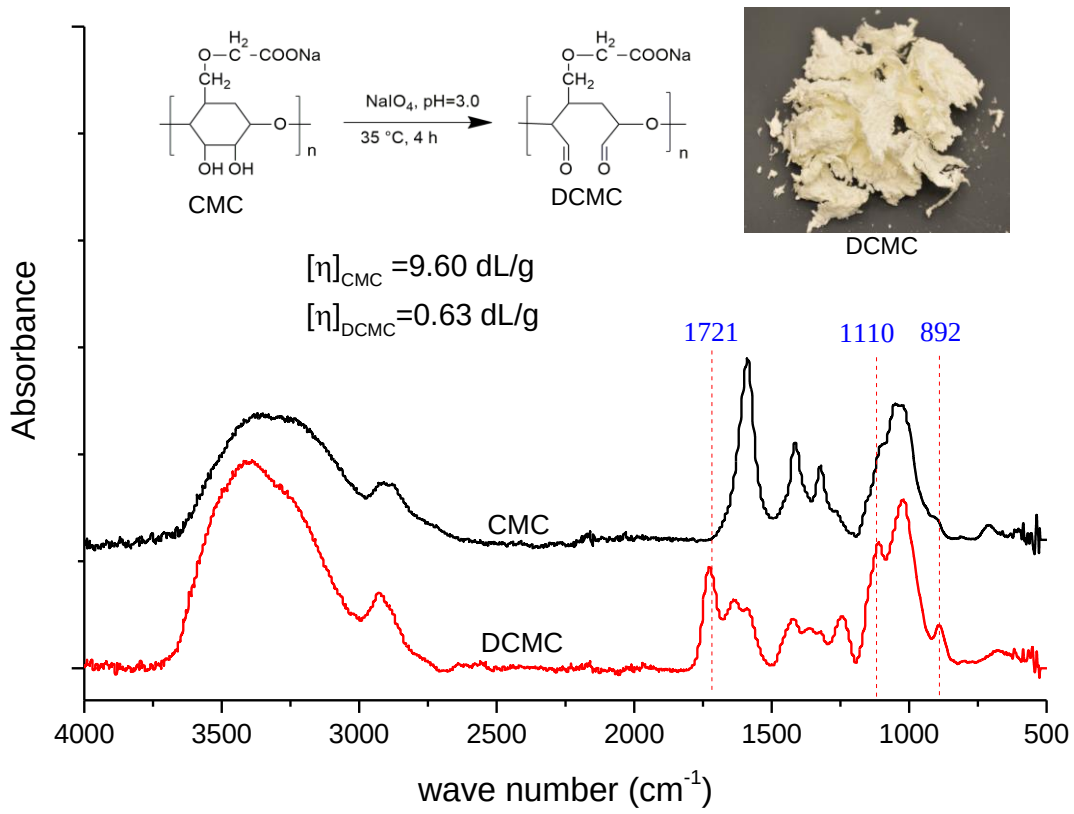

Figure 2.2 Reaction mechanism between DCMC and soy protein isolate (31).

Orliac et al. reported films prepared by using aldehydes crosslinked sunflower protein isolate. They studied the effects of additives on mechanical properties, hydrophobicity and water uptake of thermo-moulded films. Various crosslinked or hydrophobic components (aldehydes, plant tannins, alcohols and fatty acids) were added and the properties of films obtained with those of control films (containing no additives other than plasticizer) were compared. Use of octanoic acid resulted in high tensile strength (7 MPa), whereas use of octanol resulted in great increase in tensile elongation

(54 %). Plant tannins gave films with properties similar to those obtained with aldehydes, but without any toxicity.

Generally, phenol-aldehyde resins were applied to form thermosetting plastics with more enhanced properties than small aldehyde monomers. Phenolic resins have been introduced in commercial applications for more than a decade, mainly due to desirable characteristics such as superior mechanical strength, high heat resistance and dimensional stability, as well as high resistance against various solvents, acids and water (32-35). Phenolic resins can be synthesized under both acidic and alkaline conditions (36). Recently, alternative phenolic resins have been reported from renewable resources like cashew nut shell liquid (37), lignin (38) and tannin compounds that are extracted from the wood, bark, leaves and galls of plants (39). Cashew nut shell liquid is a major economical source of naturally occurring phenols. Commercial lignin forms are available as co-products among the various types of chemical pulping processes in the paper industry (40). Tannin compounds show strong ability to interact with carbohydrates and proteins, converting the skin into leather (41).

Ford Motor Company was the first major company to utilize blends of phenol–formaldehyde resin and soybean meal for automotive applications (42) 80 years ago. This inspires the widespread usage of bio-based renewable resources for preparing thermosetting plastics. Good properties of protein-phenol–formaldehyde resin are mainly due to the formation of crosslinked structure. However, there remain grave concerns about using aldehyde resins to crosslink protein molecules to prepare thermoset films due

to the toxicity of aldehyde molecules that cannot be ignored, as this can restrict their wide application in food industries (43).

2.4 Polyurethane resins

Polyurethane (PU) shows high performance as elastomer and excellent properties as thermoplastic materials (44). In general, polyurethane polymers contain a significant number of urethane linkages (–NH-COO–), regardless of the macromolecule (45). Its impressive thermal and mechanical properties have made PU become among the most widely used polymers in various industries, such as aerospace, automotive, packing and home decoration. Such widespread applications of PU have been accompanied by growing concerns regarding its toxicity in recent times. Some investigations on developing new, non-toxic PU have achieved pleasing results, such as waterborne polyurethane (WPU) (46) and non-isocyanate synthesis strategy (47). WPU has been used to prepare hybrid polymer with protein molecules in recent years (48-52).

As early as 2004, Wang et al. (48) prepared crosslinked casein/waterborne polyurethane sheets by adding 1-10 wt. % ethanedial. Results indicated that crosslinked blend sheets exhibited a certain degree of miscibility and higher tensile strength and water resistance compared to WPU, casein or non-crosslinked blend of WPU and casein. Moreover, they prepared soy protein isolate (SPI)/waterborne polyurethane composites with enhanced mechanical properties and biodegradability (49). They prepared crosslinked SPI/WPU sheets by mixing SPI, glycol diglycidyl ether (EGDE) and WPU in aqueous solutions and then cast and cured at room temperature. The results revealed that

crosslinked SPI/WPU plastics with EGDE concentrations of 2–4 wt. % exhibited high miscibility, good mechanical properties, and water resistivity. In addition, crosslinked sheets could be biodegradable, and half-life of biodegradation for a sheet crosslinked with 3 wt. % EGDE was calculated as being less than 1 month.

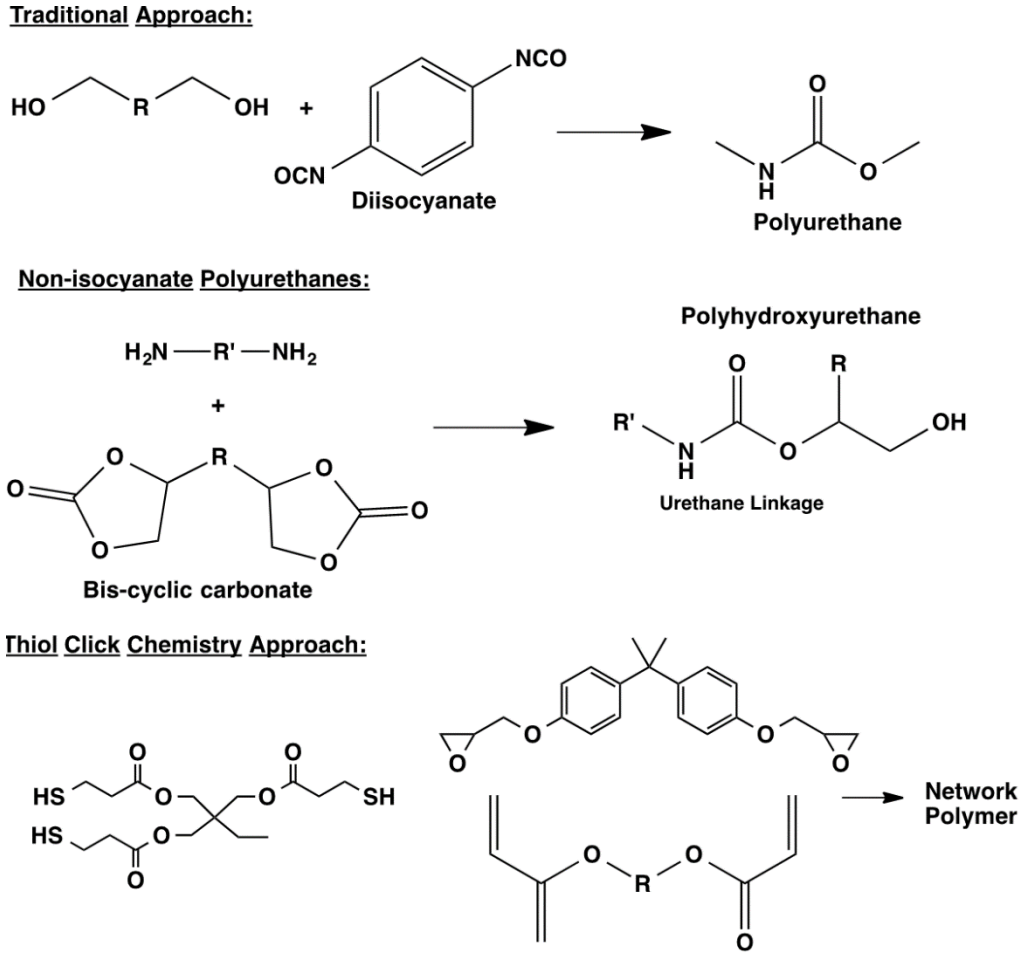

Figure 2.3 Synthesis of polyurethane where R and R' are of aliphatic or aromatic nature (66).

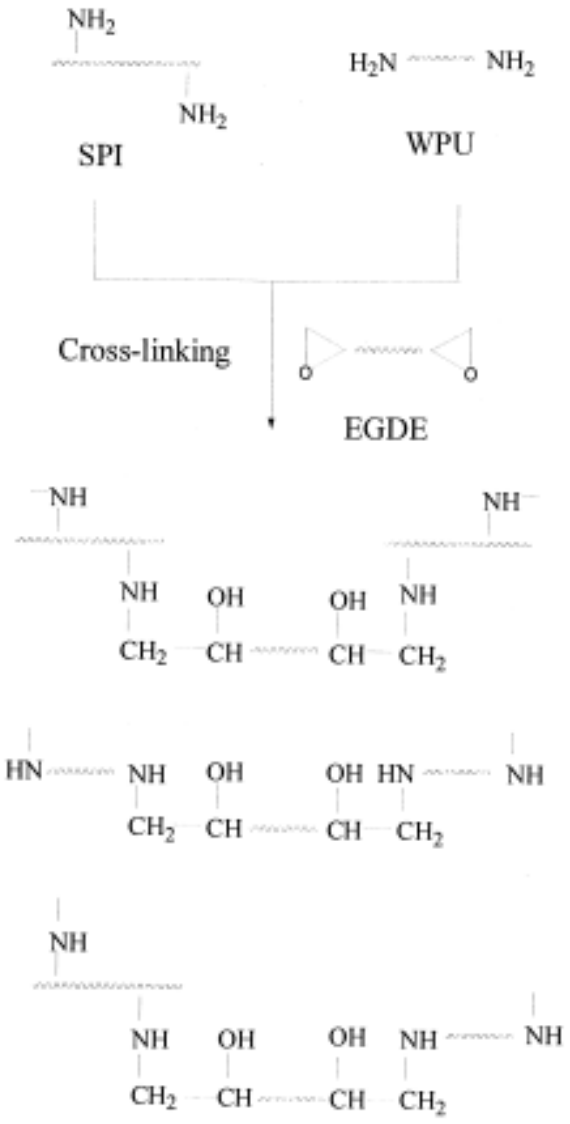

Figure 2.4 Reaction mechanism between polyurethane and protein molecules (49)

Tian et al. (50) developed biodegradable SPI/WPU composite with good flexibility and water resistance. SPI and WPU were connected via intermolecular hydrogen bonds, leading to the resultant blending films exhibiting fine compatibility. Furthermore, flexibility, water resistance and mechanical properties of soy protein-based films in water showed significant improvement. More importantly, SPI/WPU blend films

showed much lower cytotoxicity than WPU, making them potentially useful as biomedical materials. Zhang et al. (51) fabricated poly(butylene adipate) (PBA)-based WPU/SPI blend films with strong intermolecular interactions between WPU and SPI, which provides them chance to form homogeneous structure. The resultant films exhibited high performance on water resistance, flexibility, thermal and mechanical properties. SPI has been used to prepare composites with WPU in various studies.

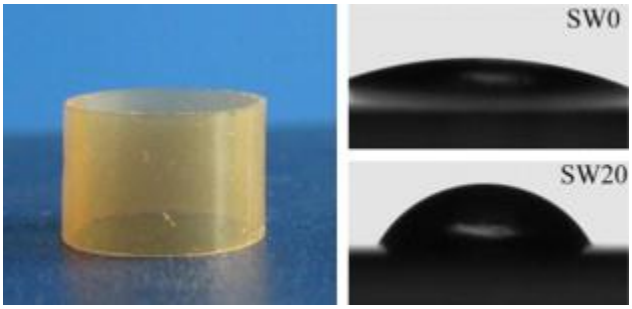

Figure 2.5 Water resistance properties showing improvement upon addition of polyurethane to protein films (50)

Different than epoxy resins that show lack of compatibility with protein molecules, waterborne polyurethane can react with protein molecules in aqueous solution. All aforementioned reports/studies that involved the formation of hybrid polymers showed better mechanical properties and water resistance of hybrid polymers compared to original protein films. On the other hand, these hybrid films also showed biodegradability and better biocompatibility than polyurethane polymers (51).

2.5 Cellulose resins

Another widely applied crosslinking resin for preparing protein-based thermoset plastics is cellulose. All the above-mentioned methods to modify proteins bring with them safety concerns with regard to food packaging applications. Carbomethoxy cellulose (CMC), among the most important derivatives of cellulose, is a typical anionic polysaccharide that has been widely used as a stabilizer in food (53), and can be a suitable additive for enhancing properties of SPI films. CMC is fully human safe and is derived from water-soluble cellulose. Hence, it has been used as additives to enhance properties in the fields from foodstuffs, cosmetics, and pharmaceuticals to products for the paper and textile industries (54). CMC chains are linear β (1→4)-linked glucopyranose residues. CMC shows amphiphilic characteristics as it contains a hydrophobic polysaccharide backbone and many hydrophilic carboxyl groups. It has been applied in a number of tunable film formulations due to its non-toxicity, biocompatibility, biodegradability, hydrophilicity, and good film-forming ability (55). It is different than other epoxy resins, ensuring that there is no issue of compatibility between cellulose and proteins.

Zaleska et al. (56) reported the preparation of CMC-casein complexes through electrosynthesis at 12 V from aqueous mixtures of components. The use of electrosynthesis led to the formation of complexes that involved peptide bonds of casein and carboxylic groups of CMC. Components of these complexes interacted with each other solely via involvement of electrical charges, van der Waals and dispersion forces, with the complexes exhibiting semi-crystalline nature. Lii et al. (57) reported using CMC

to form complexes by electrosynthesis. The complexes showed high stability due to the change in ionic strength and pH, along with possessing good emulsifying properties and high thermal stability.

Girard et al. (58) reported using CMC to crosslink whey proteins and form a new complex. The higher protein load of WPI/CMC emulsions and visual observations indicated that WPI/CMC complexes had greater emulsifying properties against coalescence than whey proteins. However, complexes enhanced the flocculation of oil droplets. Su et al. (59) prepared carboxymethyl cellulose/soy protein isolate blend edible films crosslinked by Maillard reactions, with the film being made from food grade CMC and SPI. Water sensitivity of films showed decrease with increase in CMC content, even as such blending of CMC with SPI was seen to cause improvement in properties, which has been attributed to the Maillard reaction occurring between CMC and SPI. The films developed in this work have been suggested to be suitable for low moisture foods and pharmaceutical products.

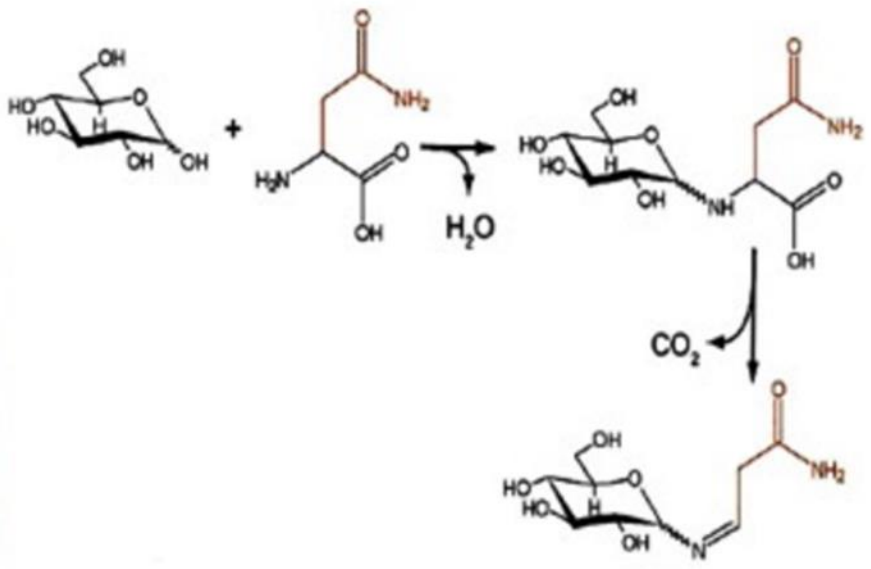

Figure 2.6 Reaction mechanism between CMC and whey protein molecules (59)

CMC was also used to prepare thermoset plastic films with various gelatin (60-62).The reaction mechanism is similar to that of CMC with whey proteins. All past studies on this aspect show improvement in properties by preparing blend films compared to pure protein films. In summary, cellulose resin can be used to prepare thermoset plastics with proteins. In future, the range of applications for which proteins can be used may be even larger.

2.6 Conclusions and Outlook

Thermosetting plastics are high-performance plastics with high density of crosslinked networks that result in high modulus and strength, good durability, and excellent thermal and chemical resistance, making them ideal for industrial applications. In this review, an emphasis is made to summarize some resins used to crosslink proteins

and form thermosetting plastics. Renewable resources provide a variety of new structures as thermosetting materials. Recent years have witnessed particular attention on protein-based thermosetting materials. Consisting of amino acids with a wide range of chain lengths, proteins have the potential to form thermoset plastics with various functional groups other than epoxy, aldehydes, polyurethane and cellulose. These proteins can be obtained from animal or plant products and byproducts.

Other than amine and carboxyl groups, there are several other different functional groups, such as hydroxyl and disulfide bond, that exist in protein molecules. These functional groups may introduce new reaction potential for protein. For instance, disulfide bond has been reportedly used as reversible reaction for thermosetting plastics (63-65). Through further research on protein-based thermosetting plastics, it may be possible to provide more economic value other than feeding or disposing for rendered animal proteins.

REFERENCES

(1) Riccardi, C.; Adabbo, H.; Williams, R. Curing reaction of epoxy resins with diamines. *J Appl Polym Sci* **1984**, *29*, 2481-2492.

(2) Lee, H.; Neville, K. Handbook of epoxy resins. **1967**.

(3) Hebert, E. A.; Morgan, W. E.; Snell, D. *Multilayer golf ball with a thin thermoset outer layer* **1999**.

(4) Trindade, W. G.; Hoareau, W.; Razera, I. A.; Ruggiero, R.; Frollini, E.; Castellan, A. Phenolic thermoset matrix reinforced with sugar cane bagasse fibers: attempt to develop a new fiber surface chemical modification involving formation of quinones followed by reaction with furfuryl alcohol. *Macromolecular Materials and Engineering* **2004**, *289*, 728-736.

(5) Wang, Z.; Pinnavaia, T. J. Nanolayer reinforcement of elastomeric polyurethane. *Chemistry of Materials* **1998**, *10*, 3769-3771.

(6) Kamal, M. R. Thermoset characterization for moldability analysis. *Polymer Engineering & Science* **1974**, *14*, 231-239.

(7) Kilian, L. Not all oil price shocks are alike: Disentangling demand and supply shocks in the crude oil market. **2006**.

(8) Wang, S.; Sue, H.; Jane, J. Effects of polyhydric alcohols on the mechanical properties of soy protein plastics. *Journal of Macromolecular Science, Part A: Pure and Applied Chemistry* **1996**, *33*, 557-569.

(9) Mekonnen, T.; Mussone, P.; El‐Thaher, N.; Choi, P. Y.; Bressler, D. C. Thermosetting proteinaceous plastics from hydrolyzed specified risk material. *Macromolecular Materials and Engineering* **2013**, *298*, 1294-1303.

(10) Fombuena, V.; Bernardi, L.; Fenollar, O.; Boronat, T.; Balart, R. Characterization of green composites from biobased epoxy matrices and bio-fillers derived from seashell wastes. *Mater Des* **2014**, *57*, 168-174.

(11) Wang, S.; Sue, H.; Jane, J. Effects of polyhydric alcohols on the mechanical properties of soy protein plastics. *Journal of Macromolecular Science, Part A: Pure and Applied Chemistry* **1996**, *33*, 557-569.

(12) González, A.; Strumia, M. C.; Igarzabal, C. I. A. Cross-linked soy protein as material for biodegradable films: Synthesis, characterization and biodegradation. *J. Food Eng.* **2011**, *106*, 331-338.

(13) Meier, M. A.; Metzger, J. O.; Schubert, U. S. Plant oil renewable resources as green alternatives in polymer science. *Chem. Soc. Rev.* **2007**, *36*, 1788-1802.

(14) Bouchareb, B.; Benaniba, M. T. Effects of epoxidized sunflower oil on the mechanical and dynamical analysis of the plasticized poly (vinyl chloride). *J Appl Polym Sci* **2008**, *107*, 3442-3450.

(15) Crivello, J.; Narayan, R. Epoxidized triglycerides as renewable monomers in photoinitiated cationic polymerization. *Chemistry of materials* **1992**, *4*, 692-699.

(16) Rosli, W. W.; Kumar, R.; Zah, S. M.; Hilmi, M. M. UV radiation curing of epoxidized palm oil–cycloaliphatic diepoxide system induced by cationic photoinitiators for surface coatings. *European Polymer Journal* **2003**, *39*, 593-600.

(17) Stewart, D. Lignin as a base material for materials applications: Chemistry, application and economics. *Industrial crops and products* **2008**, *27*, 202-207.

(18) Raquez, J.; Deléglise, M.; Lacrampe, M.; Krawczak, P. Thermosetting (bio) materials derived from renewable resources: a critical review. *Progress in Polymer Science* **2010**, *35*, 487-509.

(19) Mekonnen, T.; Mussone, P.; El‐Thaher, N.; Choi, P. Y.; Bressler, D. C. Thermosetting proteinaceous plastics from hydrolyzed specified risk material. *Macromolecular Materials and Engineering* **2013**, *298*, 1294-1303.

(20) Teng, G.; Soucek, M. D. Epoxidized soybean oil-based ceramer coatings. *J. Am. Oil Chem. Soc.* **2000**, *77*, 381-387.

(21) Motawie, A.; Hassan, E.; Manieh, A.; Aboul‐Fetouh, M.; El‐Din, A. F. Some epoxidized polyurethane and polyester resins based on linseed oil. *J Appl Polym Sci* **1995**, *55*, 1725-1732.

(22) Wang, C.; Wu, J.; Bernard, G. M. Preparation and characterization of canola protein isolate–poly (glycidyl methacrylate) conjugates: A bio-based adhesive. *Industrial Crops and Products* **2014**, *57*, 124-131.

(23) Wang, L.; Li, J.; Zhang, S.; Shi, J. Preparation and Characterization of All-Biomass Soy Protein Isolate-Based Films Enhanced by Epoxy Castor Oil Acid Sodium and Hydroxypropyl Cellulose. *Materials* **2016**, *9*, 193.

(24) Xia, C.; Wang, L.; Dong, Y.; Zhang, S.; Shi, S. Q.; Cai, L.; Li, J. Soy protein isolate-based films cross-linked by epoxidized soybean oil. *RSC Advances* **2015**, *5*, 82765-82771.

(25) Jane, J.; Lim, S.; Paetau, I.; Spence, K.; Wang, S. In *Biodegradable plastics made from agricultural biopolymers;* ACS Publications: 1994; .

(26) Rhim, J.; Gennadios, A.; Weller, C. L.; Cezeirat, C.; Hanna, M. A. Soy protein isolate–dialdehyde starch films. *Industrial Crops and Products* **1998**, *8*, 195-203.

(27) Marquie, C.; Aymard, C.; Cuq, J. L.; Guilbert, S. Biodegradable packaging made from cottonseed flour: formation and improvement by chemical treatments with gossypol, formaldehyde, and glutaraldehyde. *J. Agric. Food Chem.* **1995**, *43*, 2762-2767.

(28) Orliac, O.; Rouilly, A.; Silvestre, F.; Rigal, L. Effects of additives on the mechanical properties, hydrophobicity and water uptake of thermo-moulded films produced from sunflower protein isolate. *Polymer* **2002**, *43*, 5417-5425.

(29) Galietta, G.; Di Gioia, L.; Guilbert, S.; Cuq, B. Mechanical and thermomechanical properties of films based on whey proteins as affected by plasticizer and crosslinking agents. *J. Dairy Sci.* **1998**, *81*, 3123-3130.

(30) Hernández-Muñoz, P.; Villalobos, R.; Chiralt, A. Effect of cross-linking using aldehydes on properties of glutenin-rich films. *Food Hydrocoll.* **2004**, *18*, 403-411.

(31) Zheng, T.; Yu, X.; Pilla, S. Mechanical and moisture sensitivity of fully bio-based dialdehyde carboxymethyl cellulose cross-linked soy protein isolate films. *Carbohydr. Polym.* **2017**, *157*, 1333-1340.

(32) Ghosh, N.; Kiskan, B.; Yagci, Y. Polybenzoxazines—new high performance thermosetting resins: synthesis and properties. *Progress in polymer Science* **2007**, *32*, 1344-1391.

(33) Nair, C. R. Advances in addition-cure phenolic resins. *Progress in Polymer Science* **2004**, *29*, 401-498.

(34) Gardziella, A.; Pilato, L. A.; Knop, A. *Phenolic resins: chemistry, applications, standardization, safety and ecology*; Springer Science & Business Media: 2013; .

(35) Knop, A.; Pilato, L. A. *Phenolic resins: chemistry, applications and performance*; Springer Science & Business Media: 2013; .

(36) Campbell, A. G.; Walsh, A. R. The present status and potential of kraft lignin-phenol-formaldehyde wood adhesives. *The Journal of Adhesion* **1985**, *18*, 301-314.

(37) Tyman, J. H.; Johnson, R.; Muir, M.; Rokhgar, R. The extraction of natural cashew nut-shell liquid from the cashew nut (Anacardium occidentale). *J. Am. Oil Chem. Soc.* **1989**, *66*, 553-557.

(38) Turunen, M.; Alvila, L.; Pakkanen, T. T.; Rainio, J. Modification of phenol–formaldehyde resol resins by lignin, starch, and urea. *J Appl Polym Sci* **2003**, *88*, 582-588.

(39) Kim, S.; Kim, H. Curing behavior and viscoelastic properties of pine and wattle tannin-based adhesives studied by dynamic mechanical thermal analysis and FT-IR-ATR spectroscopy. *J. Adhes. Sci. Technol.* **2003**, *17*, 1369-1383.

(40) Sena-Martins, G.; Almeida-Vara, E.; Duarte, J. Eco-friendly new products from enzymatically modified industrial lignins. *Industrial crops and products* **2008**, *27*, 189-195.

(41) Martinez, S. Inhibitory mechanism of mimosa tannin using molecular modeling and substitutional adsorption isotherms. *Mater. Chem. Phys.* **2003**, *77*, 97-102.

(42) Rosenthal, F. Cottonseed meal in phenolic plastics. *Industrial & Engineering Chemistry* **1942**, *34*, 1154-1157.

(43) Krochta, J. M.; Mulder-Johnston, D. Edible and biodegradable polymer films: challenges and opportunities. *Food technology (USA)* **1997**.

(44) Yoon, P. J.; Han, C. D. Effect of thermal history on the rheological behavior of thermoplastic polyurethanes. *Macromolecules* **2000**, *33*, 2171-2183.

(45) Zia, K. M.; Bhatti, H. N.; Bhatti, I. A. Methods for polyurethane and polyurethane composites, recycling and recovery: a review. *React Funct Polym* **2007**, *67*, 675-692.

(46) Kim, B. K.; Lee, J. C. Waterborne polyurethanes and their properties. *Journal of polymer science part A: polymer chemistry* **1996**, *34*, 1095-1104.

(47) Delebecq, E.; Pascault, J.; Boutevin, B.; Ganachaud, F. On the versatility of urethane/urea bonds: reversibility, blocked isocyanate, and non-isocyanate polyurethane. *Chem. Rev.* **2012**, *113*, 80-118.

(48) Wang, N.; Zhang, L.; Lu, Y.; Du, Y. Properties of crosslinked casein/waterborne polyurethane composites. *J Appl Polym Sci* **2004**, *91*, 332-338.

(49) Wang, N.; Zhang, L.; Gu, J. Mechanical properties and biodegradability of crosslinked soy protein isolate/waterborne polyurethane composites. *J Appl Polym Sci* **2005**, *95*, 465-473.

(50) Tian, H.; Wang, Y.; Zhang, L.; Quan, C.; Zhang, X. Improved flexibility and water resistance of soy protein thermoplastics containing waterborne polyurethane. *Industrial Crops and Products* **2010**, *32*, 13-20.

(51) Zhang, M.; Song, F.; Wang, X.; Wang, Y. Development of soy protein isolate/waterborne polyurethane blend films with improved properties. *Colloids and surfaces B: biointerfaces* **2012**, *100*, 16-21.

(52) Tong, X.; Luo, X.; Li, Y. Development of blend films from soy meal protein and crude glycerol-based waterborne polyurethane. *Industrial Crops and Products* **2015**, *67*, 11-17.

(53) Toğrul, H.; Arslan, N. Carboxymethyl cellulose from sugar beet pulp cellulose as a hydrophilic polymer in coating of mandarin. *J. Food Eng.* **2004**, *62*, 271-279.

(54) Schmitt, C.; Sanchez, C.; Desobry-Banon, S.; Hardy, J. Structure and technofunctional properties of protein-polysaccharide complexes: a review. *Crit. Rev. Food Sci. Nutr.* **1998**, *38*, 689-753.

(55) Toğrul, H.; Arslan, N. Extending shelf-life of peach and pear by using CMC from sugar beet pulp cellulose as a hydrophilic polymer in emulsions. *Food Hydrocoll.* **2004**, *18*, 215-226.

(56) Zaleska, H.; Tomasik, P. Formation of carboxymethyl cellulose–casein complexes by electrosynthesis. *Food Hydrocoll.* **2002**, *16*, 215-224.

(57) Lii, C.; Chen, H.; Lu, S.; Tomasik, P. Electrosynthesis of κ-carrageenan complexes with gelatin. *Journal of Polymers and the Environment* **2003**, *11*, 115-121.

(58) Girard, M.; Turgeon, S.; Paquin, P. Emulsifying Properties of Whey Protein - Carboxymethylcellulose Complexes. *J. Food Sci.* **2002**, *67*, 113-119.

(59) Su, J.; Huang, Z.; Yuan, X.; Wang, X.; Li, M. Structure and properties of carboxymethyl cellulose/soy protein isolate blend edible films crosslinked by Maillard reactions. *Carbohydr. Polym.* **2010**, *79*, 145-153.

(60) Hosseini, S. F.; Rezaei, M.; Zandi, M.; Ghavi, F. F. Preparation and functional properties of fish gelatin–chitosan blend edible films. *Food Chem.* **2013**, *136*, 1490-1495.

(61) Al-Hassan, A.; Norziah, M. Starch–gelatin edible films: Water vapor permeability and mechanical properties as affected by plasticizers. *Food Hydrocoll.* **2012**, *26*, 108-117.

(62) Kanmani, P.; Rhim, J. Physical, mechanical and antimicrobial properties of gelatin based active nanocomposite films containing AgNPs and nanoclay. *Food Hydrocoll.* **2014**, *35*, 644-652.

(63) Xu, Y.; Chen, D. A Novel Self‐Healing Polyurethane Based on Disulfide Bonds. *Macromolecular Chemistry and Physics* **2016**.

(64) Zheng, M.; Aslund, F.; Storz, G. Activation of the OxyR transcription factor by reversible disulfide bond formation. *Science* **1998**, *279*, 1718-1721.

(65) Li, Y.; Xiao, K.; Luo, J.; Xiao, W.; Lee, J. S.; Gonik, A. M.; Kato, J.; Dong, T. A.; Lam, K. S. Well-defined, reversible disulfide cross-linked micelles for on-demand paclitaxel delivery. *Biomaterials* **2011**, *32*, 6633-6645.

(66) Leitsch, E.; Goliath, B.; Kun, L.; Tian, L., William, H.; Karl, S.; and John. T.; Nonisocyanate thermoplastic polyhydroxyurethane elastomers via cyclic carbonate aminolysis: critical role of hydroxyl groups in controlling nanophase separation. *ACS Macro Letters* **2016** 5.4, 424-429.

(67) Dastidar, T.G.; Netravali, A.N.; A soy flour based thermoset resin without the use of any external crosslinker. *Green Chemistry* **2013** 15.11, 3243-3251.

CHAPTER THREE

ENERGY-EFFICIENT PROCESSING OF RENDERED ANIMAL PROTEINS AS VALUE ADDED BIO-CROSSLINKED IN HIGH-STRENGTH THERMOSETS

ABSTRACT

Extensive research has been undertaken in recent times on finding suitable, alternative, non-feed and non-fertilizer applications for these materials in the animal rendering industry. In this regard, to increase the economic value, use of such proteins to derive plastics, especially thermoplastics and derived composites, has emerged as a potentially acceptable choice. However, widespread use of such proteins for this purpose is limited by its poor mechanical properties, high moisture absorption and its inherent odor. In this study, we have engineered, for the first time, high-strength, toughened thermoset polymers from proteinaceous materials obtained from the rendering industry, so that they can be employed in high performance applications, such as in the automotive sector.

3.1 Introduction

With the development of society and economy, the study of next generation materials is more focused on sustainability, industrial ecology, eco-efficiency, and green chemistry. These principles have led researchers to focus on developing bio-based materials, especially in the plastics sector, with an increasing focus on producing bio-based polymers as alternatives to traditional petroleum based plastics (1-3). In most cases, bio-based materials incorporate industrial products, while avoiding the use of food, feed

or materials produced from renewable agricultural and forestry feed stocks, such as wood, wood wastes and residues, grasses, or crop wastes. In this context, the use of bioproducts in plastic production increases its biodegradability, while also reducing the waste and pollution caused by such byproducts. This enhances the attractiveness of proteinaceous materials as potential precursors for producing eco-friendly plastics (4). Extensive research in recent times towards finding suitable, alternative, non-feed and non-fertilizer applications for proteinaceous materials in the rendering industry have emerged. A potential alternative has emerged in the form of producing plastics from such proteins, especially thermoplastics and derived composites. Simultaneously, poor mechanical properties, high moisture absorption and its inherent odor have limited the widespread use of such proteins, especially in high-performance structural applications.

Several studies have been undertaken to investigate the properties and behavior of plastics derived from animal proteins. Chen et al. (5) developed thermoplastic films from milk proteins for use as protective layer on food items, but observed poor mechanical properties as a limiting factor for their use in such applications. A detailed understanding of the molecular basis of uncertainty is thus needed for efficient engineering of desired films. Wu et al. (6) modified zein protein using PCL-HDI to induce toughness combined with hydrophobicity, though not to levels desired for commercial applications. They observed significant deterioration in strength and stiffness of zein protein upon the incorporation of PCL-HDI. Similarly, Kim et al. (7) undertook crosslinking of zein protein via use of 1-[3-dimethylamino-propyl]-3-ethyl-carbo-diimide hydrochloride (EDC) and N-hydroxy-succi-nimide (NHS), but did not achieve properties desired for

high-performance applications. Sharma et al. (8) developed feathermeal protein-based biodegradable polymers blended with whey and albumin, and investigated their thermo-physical and mechanical properties. While they achieved success in enhancing the modulus of the protein, this was accompanied by reduction in toughness. In addition, the hydrophilic nature of the polymer proved detrimental to its processing by expediting its thermal degradation, leading to inferior properties. While this may seem good from the viewpoint of economic value, it remains a perplexing strategy as variable temperature profiles lead to inefficient thermal management in such highly sensitive animal proteins. This in turn ensures thermal degradation of proteins, resulting in significant decrement in their mechanical properties, thereby limiting its application base to low-performance and perhaps, low economic value applications.

On the other hand, preparation of protein-based thermoset materials has attracted wide attention in recent times. Most of these studies have targeted protein functional groups of amino acid residues – primary amines, carboxyl, hydroxyl, and sulfhydryls. Among these studies, aldehydes (formaldehyde, glutaraldehyde, and glyoxal) are the most commonly used agents for chemical crosslinking of protein monomers (9-11). However, due to the chemical structure of these agents, release of toxic monomers remains unavoidable (10), which places obstacles in the use of animal protein-based plastics. Furthermore, Mekonnen et al. (12, 13) developed crosslinked thermoset resins from animal proteins by applying hydrolyzed peptides molecule to crosslinked DGEBA. Despite demonstrating enhancement in tensile modulus, the study showed significant compromise on strength and strain-at-break – parameters critical for structural

applications. This might have been due to poor cure kinetics, which needs to be strategically investigated. Furthermore, hydrolysis of protein was undertaken at high pressure and high temperature, which is energy-intensive and leads to an increase in process cost.

Due to restrictions on reducing greenhouse gas (GHG) emissions, automakers are forced to work on approaches focused on improving fuel economy. Many strategies have been explored in this regard, such as the development of hybrid vehicles (14-18) and electric vehicles (19, 20), and the application of new lightweight metals (21-24) and composites (25, 26). Based on this, incorporation of rendered animal protein-based plastics in automotive manufacturing helps increasing the economic value of animal byproducts, while also providing a new candidate for manufacturing lightweight automobiles. In this study, we designed an energy-efficient, and cost-effective process to extract and purify rendered animal proteins that are employed as bio-based crosslinking agents for developing high-strength, toughened thermoset polymers for high-performance applications, such as in the automotive sector. IR spectra were used to confirm the occurrence of successful reaction between the animal protein and DGEBA. Thermal and mechanical properties were studied for the final product – thermoset plastics. Reaction kinetics study was performed to investigate the reaction energy for this research.

3.2 Materials and Methods

3.2.1. Materials:

The original sample – used in this study – was Poultry by-product meal (Feed grade) provided byAnimal Co-product Research and Education Center. Total protein content ratio of the sample was labeled as not less than 56 % by dry weight basis. Diglycidyl ether of bisphenol A (DGEBA) epoxy resin, NaCl, Na_2HPO_4, KH_2PO_4 and $MgCl_2$ were purchased from Sigma-Aldrich (USA). Hexane and Bismaleimide was purchased from VWR (USA). All chemicals were used without further processing. Filter paper used in our study is obtained from Whatman (USA) (Whatman #4, D = 11 cm, pore size 20-25 μm) and was used in as-received state. The dialysis membrane (d = 3000) was purchased from Thermo Fisher Scientific. Hyperbranched polymer (Boltron H30) was purchased from Perstorp, Toledo, USA.

3.2.2. Proteinaceous Material Extraction:

Protein was extracted from the poultry meal and salt solution mixture by controlling its pH value. Every 100 g sample of the poultry meal was treated with 450 mL salt solution containing 18 g NaCl (or $MgCl_2$), 4.1 g KH_2PO_4, and 4.3 g Na_2HPO_4, according to the method used by Park et. Al (9). Dialysis process was applied to separate the salt from the protein sample. Protein/salt solution was filled into the dialysis membrane bag and then placed in enough water for 4 h, during which the water was changed every hour. The employment of non-hydrolyzed protein extraction procedure in this study makes this process cost-effective and energy-efficient compared to the traditional high temperature and high pressure protein extraction process.

3.2.3. Thermoset Polymer Preparation:

Protein samples, prepared from the previous extraction step, were used to crosslink the DGEBA epoxy resin. Epoxy resin was pre-heated to 55 ℃ in the oven for 30 min. Protein was dried in vacuum oven for 2 h at 100 ℃ and then mixed with epoxy by stirring at 60 ℃ for 2 h in different animal protein/DGEBA ratios. The prepared mixture was then cast in silicon (Si) mold (consisting of tensile geometries as per ASTM D-638 type V) at 150 ℃ for 5 h.

3.2.4. ATR-FTIR Spectroscopy:

Attenuated Total Reflectance-Fourier Transform-Infrared (ATR-FTIR) Spectroscopy was performed on a Thermo-Nicolet Magna 550 FTIR Spectrometer in combination with a Thermo-Spectra Tech Foundation Series Diamond ATR accessory, with the angle of incidence being 50 °. ATR-FTIR spectra were obtained for the mixture before curing and the product after curing.

3.2.5. Differential Scanning Calorimetry (DSC):

Differential scanning calorimetry (DSC) analysis was conducted to investigate the curing behavior of protein/epoxy mixture using a thermal analyzer (Q2000, TA Instruments, USA) under nitrogen (N_2) atmosphere. Experiments were performed with sample weights ranging from 6 to 10 mg. In dynamic experiments, samples were heated from 25 to 275 ℃ at various heating rates (i.e., 2, 5, 10, 15 and 20 ℃ /min). Reaction heat was calculated based on the total area under the exothermal peak of the DSC graph.

3.2.6. Thermo-gravimetric Analysis (TGA):

TGA measurement was performed using a TGA Q5000 instrument (TGA Q5000) under nitrogen flow at a heating rate of 10 ℃/min to study thermal degradation behavior of protein-based plastics. About 8 mg of plastic samples were heated at 10 ℃/min over the temperature range of 30-600 ℃ in nitrogen atmosphere.

3.2.7. Mechanical Properties:

Tensile strength and elongation-at-break were measured using Instron Universal Testing Machine (Model 1125) at a cross-head speed of 50 mm/min, with 30 mm grip separation. Testing was undertaken using the procedure prescribed as per the relevant ASTM standards.

3.3 Results and Discussion

3.3.1. Protein Cross-linking Reactions:

Many functional groups are present in protein molecular chains. Among these, the main groups that could react with DGEBA include amines (-NH_2), carboxyls (-COOH), sulfhydryls (-SH), hydroxyl (-OH), and carbonyls (-CHO). Reactions between these functional groups and epoxy have been reported elsewhere in literature (27). Scheme 1.A shows the reaction mechanism of these major functional groups with the epoxy group, while Scheme 1.B shows the schematic flow of crosslinking reaction between animal protein molecular chains and DGEBA. Upon curing at elevated temperature, the

crosslinked network was formed, and protein-based thermoset materials were prepared via this mechanism showed enhanced mechanical properties compared to most conventional thermoplastics.

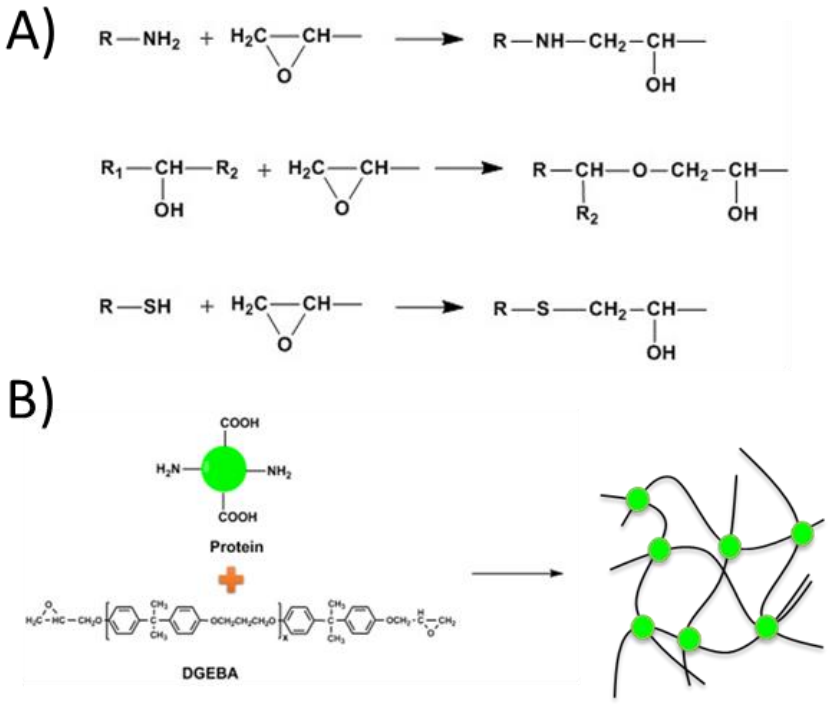

Scheme 3.1: A) Reaction mechanism of Protein/Epoxy curing, B) Schematic of the crosslinking reaction process

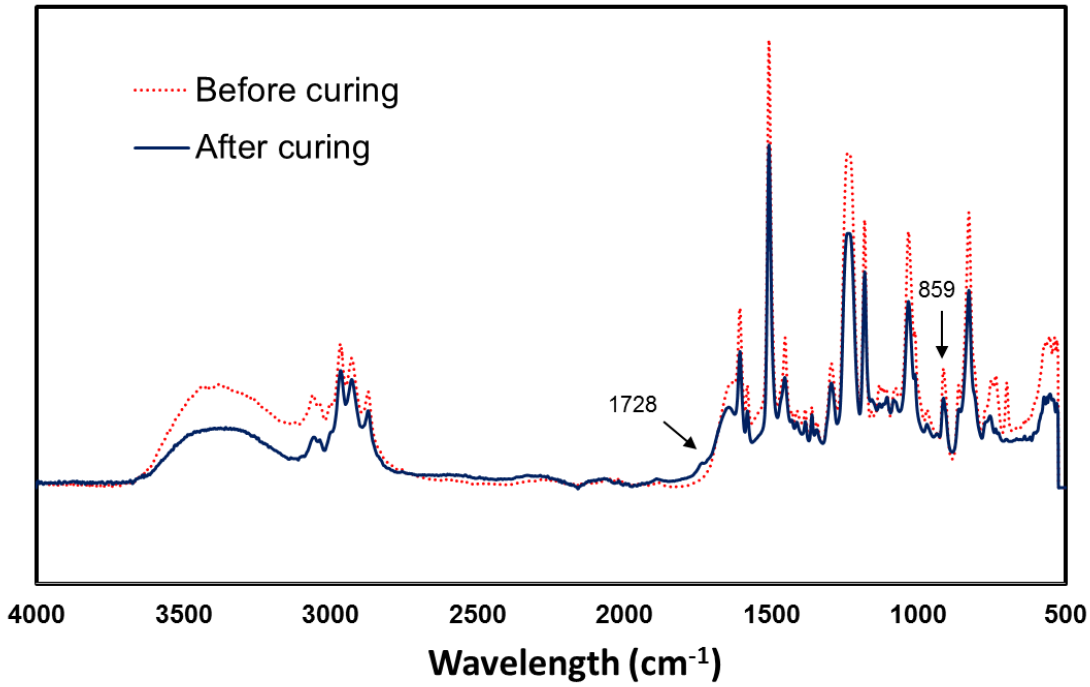

Figure 3.1 Typical FTIR spectra for pre-cured and post-cured protein/epoxy mixture. (Animal protein weight ratio is 30 wt %).

IR spectra were obtained for the chemical mixture – prior to and after the occurrence of the crosslinking reaction – in the wavelength of 500-4000 cm^{-1} for two reasons: (a) to compare changes in the functional group (if any); and (b) to verify that crosslinking between animal protein molecular chains and DGEBA was successful (as shown in Figure 3.1 The successful nature of crosslinking is clearly indicated by the new absorption peak obtained at ~ 1728 nm that corresponds to the ester group formed by the curing of DGEBA and protein functional groups present in the crosslinking agent. Moreover, the peak at ~ 859 nm – corresponding to the epoxy group – shows reduction in its intensity upon crosslinking, indicating a decrease in the concentration of epoxy groups

upon reaction with the animal protein. Thus, a comparison of the IR spectra prior to and after curing confirmed the successful nature of crosslinking reaction between the animal protein and the epoxy.

3.3.2. Protein/epoxy Ratio Optimization:

In almost all applications it is used for, epoxy undergoes curing, often through the application of a crosslinking agent. Variation in the epoxy resin or crosslinking agent used has been reported to cause variation in the mechanical properties of thermosets obtained (28) with the addition of very low or high amount of crosslinking agent observed to cause deterioration in mechanical properties of thermosets. This makes it prudent to investigate the optimal ratio of epoxy resin and crosslinking agent used. Differential scanning calorimetry (DSC) is a convenient and widely used method by researchers to monitor the heat change during heating of thermoplastics (29, 30) and investigate the kinetics of curing reactions observed for thermoset epoxy resins (31).

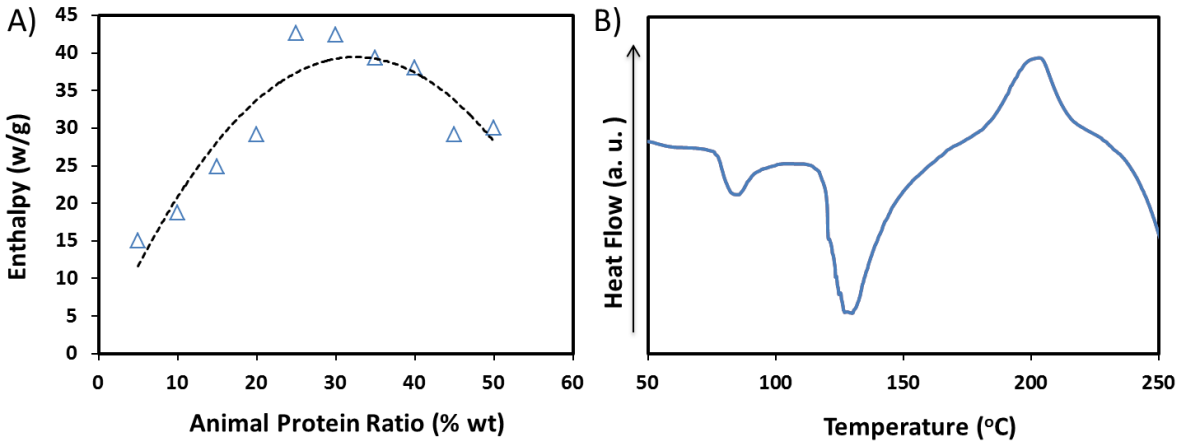

Figure3.2 A) Plot showing variation in reaction heat (enthalpy) with increasing of protein weight ratio DSC curves for protein ratio 30 wt.%; B) DSC curves for protein weight ratio 30 wt.%.

For this work, animal protein was used as the crosslinking agent for epoxy resins, and was added in varying amounts (ranging from 5 to 50 wt. %) to optimize the extent of crosslinking in epoxy using the DSC method. In this study, we have treated the total area under the exothermal peak as total reaction heat for crosslinking. Since reaction heat corresponding to the reaction conversion is positive (32, 33), values of reaction heat at different protein weight ratios have been plotted in Figure 3.2 A, which indicates the highest reaction heat being obtained for the mixture containing around 30 wt. % protein and 70 wt. % epoxy. Thus, based on the DSC results, we chose the 30 wt. % protein ratio as the optimal proportion for this study.

Figure 3.2 B shows the DSC curve for the optimal animal protein/epoxy ratio in this study. As the heat release peak centered at ～ 200 ℃ can be attributed to the

crosslinking reaction peak, the DSC curve provides yet another evidence of the occurrence of crosslinking reaction during the heating of the protein/epoxy mixture (34).

3.3.3. Dynamic Curing Behavior:

The major reactions that occur between DGEBA and functional groups present in the protein have been discussed in the section on protein crosslinking reactions. Mekonnen et al. (12) have studied cure kinetics involving the use of hydrolyzed protein to cure epoxy resin through non-isothermal DSC measurement. Similar to Mekonnen's study (35), we assumed the reaction rate to be proportional to the heat flow recorded, and treated the exothermal maximum peak temperature value as the one corresponding to the highest reaction rate, using it to calculate the activation energy (Ea). We also used a widely-applied activation energy calculation pathway – the Kissinger equation method – that assumes the curing reaction as a first-order reaction, dependent on temperature, and independent of conversion. E_a and the pre-exponential factor (A) can be calculated using the maximum exothermic peak temperature (T_p) and heating rate (β) (36), using the following expression:

$$-\ln\left(\frac{\beta}{T_P^2}\right) = \frac{E_a}{RT_P} - \ln\left(\frac{AR}{E_a}\right)$$

where R is the universal gas constant (8.314 J/mol). The plot drawn between $\ln(\beta/T_P^2)$ and $1/RT_P$ for all heating rates shows a linear regression (Fig.3.B). In this plot,

slope of the line is E_a and the y-intercept of the line is $\ln(AR/E_a)$. Fig.3.A shows five curing peaks at different cure heating rates (2, 5, 10, 15 and 20 ℃/min). According to Fig.3.A, peak temperature or the highest reaction temperature is affected by the heating rate. After collecting the peak values and plotting them in Fig.3.B, we calculated the reaction activation energy (E_a) by fitting the line with all curing peak values, and found it to be equal to 28.267 KJ/mol, which is much smaller than the curing activation energy reported (35) with similar animal protein/epoxy ratio ($\sim 70 \mathrm{KJ/mol}$). Table 1 lists the Kissinger parameter values obtained through our calculations. Generally, lower reaction activation energy indicates easier reaction process. Thus, the crosslinking process in this study is more accessible than previously reported in literature (35).

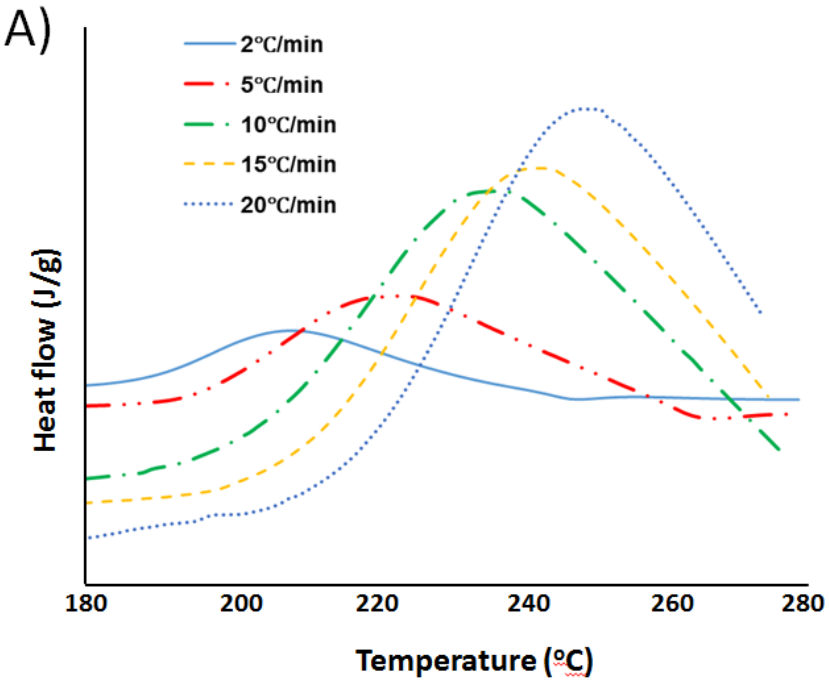
A)
2°C/min
5°C/min
10°C/min
15°C/min
20°C/min
Heat flow (J/g)
180
200
220
240
260
280
Temperature (°C)

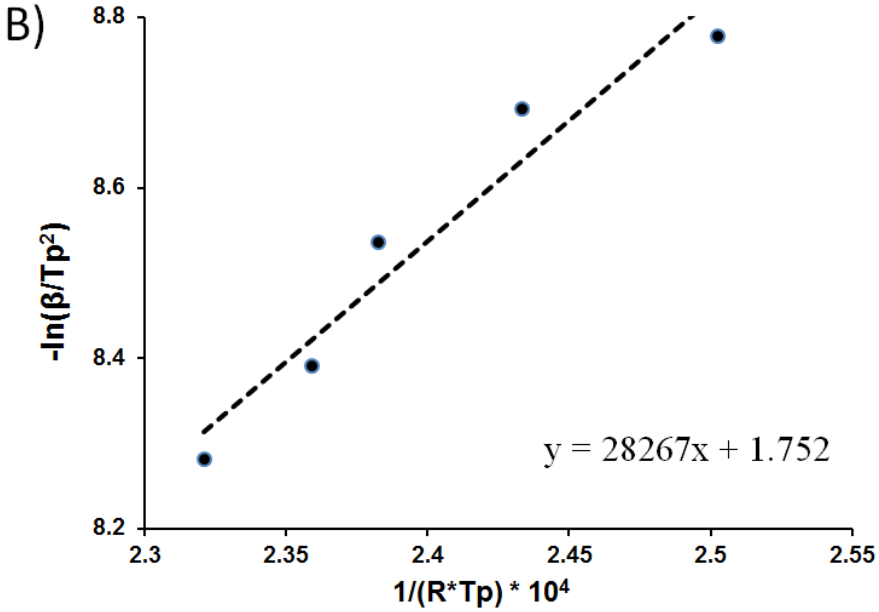
B)
8.8
8.6
8.4
8.2
-ln(β/Tp²)
y = 28267x + 1.752
2.3
2.35
2.4
2.45
2.5
2.55
1/(R*Tp) * 10⁴

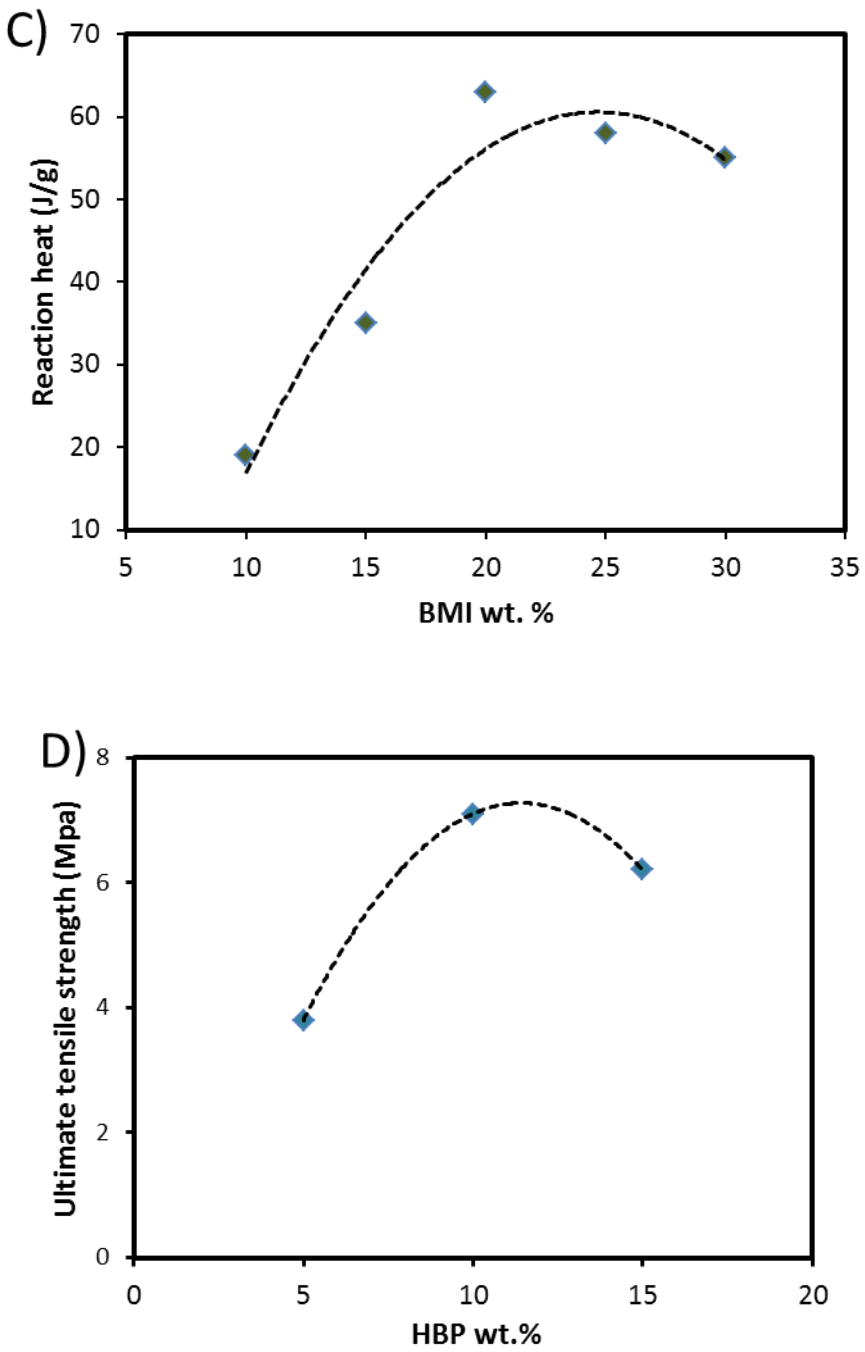

Figure 3.3 A) DSC curves (exo up),B) constructed Kissinger plots for Protein:DGEBA ratio as 7:3, C) BMI ratio optimization and D) HBP ratio optimization

Table 3.1 Calculated Kissinger Parameters and initial degradation temperatures (Ti), char yields, temperature first and second at DTG peaks of E/P, E/P/BP, E/P/BMI and E/P/BMI/HBP

Sample	β (ºC/min)	T_i (K)	T_p (K)	E_a (J/mol)	A (s^{-1})
DGEBA/Protein (30 wt.%)	2	460.48	480.63	28267	589
	5	468.30	484.28		
	10	475.86	504.79		
	15	482.30	509.89		
	20	489.11	518.21		

3.3.4. Optimization of Mechanical Properties:

Since the protein molecule is too large to be a crosslinking agent and is also brittle, cured protein/epoxy samples are also found to be brittle. Hence, this study investigated on improving the properties of cured protein/epoxy samples by introducing a unique reaction mechanism involving bismaleimide (BMI) and hyperbranched polymers (HBP). BMI possesses high crosslinking ability, high thermal stability, high glass transition temperature, superior specific strength modulus, and excellent fire resistance (Dinakaran and Alagar, 2002; Wetzel et al., 2006). Scheme 2.A shows the reaction mechanism for BMI added to the protein/epoxy reaction system. HBPs are ultra-branched polydisperse molecules at the nanometer scale. Due to their nano-size, HBPs help to constrain matrix deformation as they interact better with the polymer microstructure upon reaching nearly molecular dimensions (39). Scheme 2.B shows the final structure of the thermoset polymer obtained after adding HBP to the reaction system, as the latter helps to enhance

the impact strength or toughening effect of the resultant matrix. Prior to testing mechanical properties, the optimal addition ratio of BMI was tested for the protein/epoxy matrix. For this purpose, the reaction heat was calculated using the same method as described in the section on calculating the reaction activation energy. Figure 3.3 C shows variation in reaction heat with increase in BMI weight ratio. Based on this plot, it can be observed that reaction heat is proportional to reaction conversion, and thus 20 wt. % of BMI content was obtained as its optimal content value. Hence, this value was chosen in this study for further experiments. The hyperbranched polymer addition ratio was optimized by comparing the ultimate tensile strength with tensile tests as shown in Fig.3.D. 5, 10 and 15 wt.% animal protein was added to the epoxy/animal protein mixture, respectively. It clearly shows that the optimal HBP percentage is around 10%, at which the ultimate tensile strength is maximum. Thus, in the following investigations, we choose 20%BMI and 10% HBP to enhance the properties of the polymer networks.

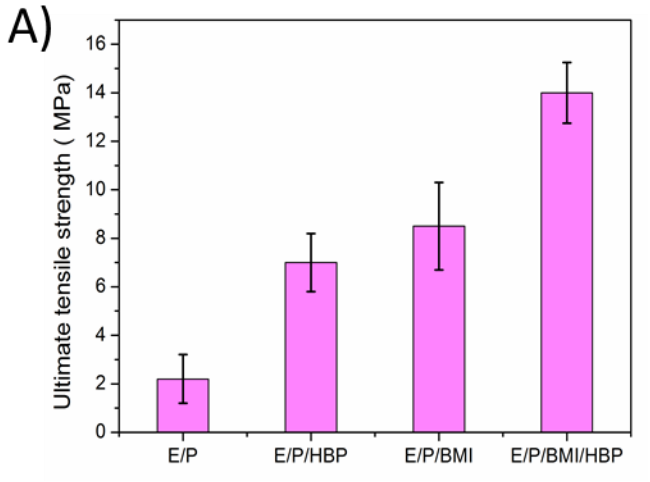
A)
Ultimate tensile strength (MPa)
0
2
4
6
8
10
12
14
16
E/P
E/P/HBP
E/P/BMI
E/P/BMI/HBP

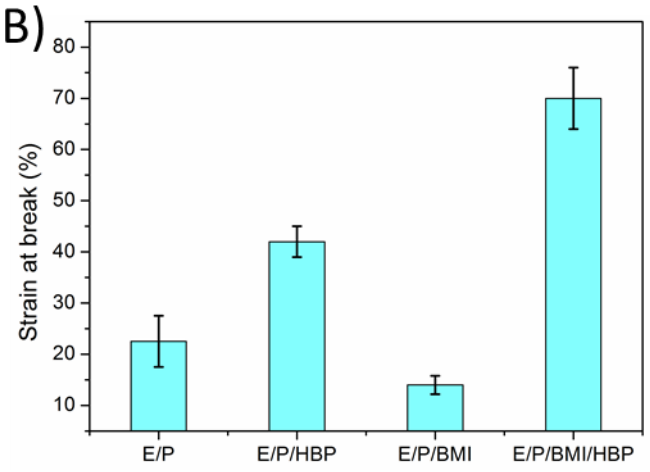
B)
Strain at break (%)
10
20
30
40
50
60
70
80
E/P
E/P/HBP
E/P/BMI
E/P/BMI/HBP

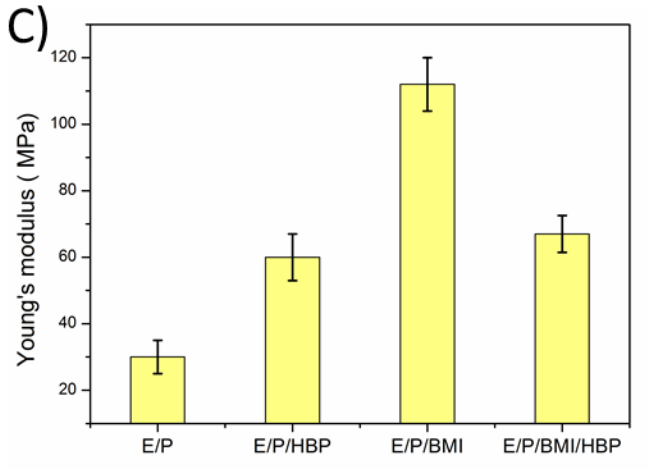
C)
Young's modulus (MPa)
20
40
60
80
100
120
E/P
E/P/HBP
E/P/BMI
E/P/BMI/HBP

Figure 3.4 A) Ultimate tensile strength; B) Elongation-at-break; and C) Young's modulus for protein/epoxy (unfilled), protein/epoxy/BMI, protein/epoxy/HBP, protein/epoxy/BMI/HBP cured polymer.

Figure 3.4 shows improvement in mechanical properties upon the addition of either or both of BMI (20 wt. %) and HBP (10 wt. %). While the addition of either BMI or HBP was observed to cause increase in the ultimate tensile strength (UTS) of the polymer, addition of both HBP and BMI led to its UTS value reaching 14 MPa – comparable to that of soybean protein-based plastics (40). Addition of HBP was seen to increase the elongation-at-break (or strain-at-break), while the addition of BMI reduced its elongation-at-break, as indicated by Fig.4.B, which may be due to increase in crosslinking density. The addition of BMI promotes the formation of intermolecular connections, which increased crosslinking density and caused smaller strain-at-break with higher ultimate tensile strength (37, 38). Furthermore, the modulus of epoxy/protein/BMI combination was observed to be the highest among all combinations. Thus, addition of HBP was observed to cause enhancement in modulus, strength and strain-at-break of the epoxy-protein thermoset matrix, while the addition of BMI led to increase in modulus and strength along with decline in the strain-at-break of the matrix. This result follows the report that the addition of HBP would increase the tensile strength and elongation-at-break, since HBP could increase the crosslinking density and reduce the free volume in the final polymer network (41). However, simultaneous addition of BMI and HBP was observed to result in complementary properties, i.e., superior strength and strain-at-break.

Compared to ~70MPa in a similar study reported by Mekonnen et al (12), our results shows large compromise in ultimate tensile strength. This is due to the application of non-hydrolyzed animal protein as crosslinkers in our study. The functional groups density increases effectively when the animal protein is hydrolyzed to small peptides, which increases the crosslinking density of the polymer network. However, such hydrolysis also comes at an expense since it is an energy-intensive process due to the employment of high pressure and high temperature. As such, while hydrolyzed protein leads to enhanced strength, it leads to an increase in process cost, thereby augmenting the overall product cost.

3.3.5. Thermal Stability:

To evaluate thermal stability of four different combinations, TGA of samples was undertaken in nitrogen (N_2) atmosphere over the temperature range of 30-600 ℃. Initial degradation temperatures (Ti), cited as the characteristic temperature to assess thermal stability, were measured as the temperature at which 5 % of the sample undergoes degradation, and have been listed in Table 1. A comparison of the Ti values of the four combinations shows that addition of HBP led to reduction in thermal stability, while the addition of BMI did not lead to any compromise on thermal stability.

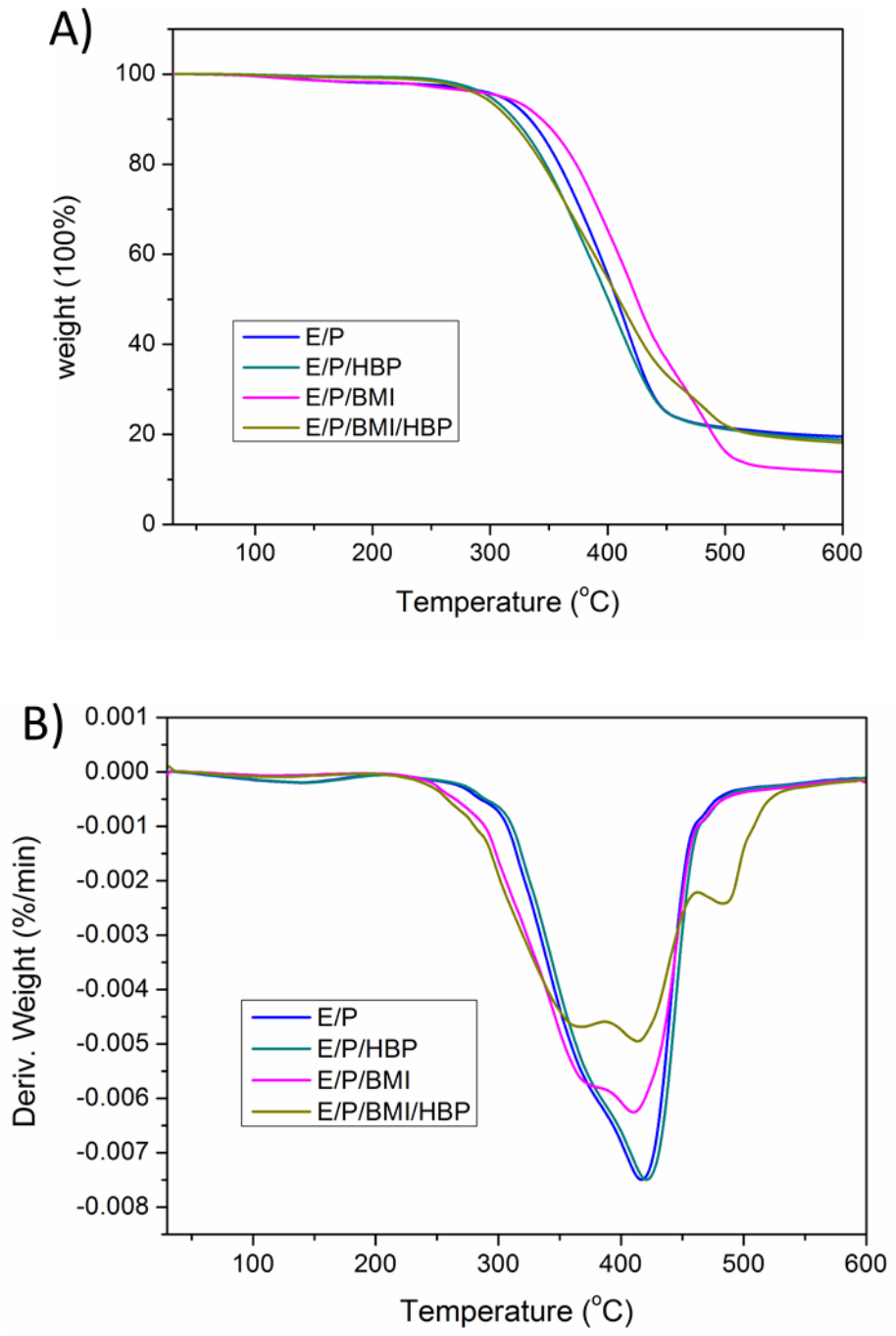

Figure 3.5 A) thermogravimetric analysis (TGA) B) Derivative thermogravimetric analysis of protein/epoxy resin cured either with BMI or HBP added.

It is well known that a longer polymer chain possesses lower thermal stability than a shorter polymeric chain (42). This explains the easier degradation of E/P/BMI/HBP combination compared to the unmodified epoxy/protein combination. Figure 3.5 B shows a typical derivative thermal degradation pattern of protein-based polymers. The maximum degradation heating temperatures were observed to be close for all chosen combinations, ranged from 408.9 to 419.6 ℃. Two peaks (T_{max}^{1} and T_{max}^{2}) have been shown in the DTG curves for E/P combinations, indicating the presence of unreacted animal protein in the system, and its absence in combinations where HBP or BMI were added.

3.4 Conclusions

This work demonstrates a method for preparation of rendered animal protein-based high-strength polymers through a low energy-intensive method. Animal protein was used for crosslinking with DGEBA without the use of any hydrolysis process. This process was observed to guarantee the conversion of waste protein to an environment-friendly plastic for usage, while achieving the desired mechanical performance upon the addition of BMI and HBP to the reaction system. However, thermal properties of the obtained polymer need significant improvement, even as significant space exists for further improvement in mechanical properties of the protein-based polymer.

ACKNOWLEDGMENTS

The authors would like to acknowledge the financial support of ACREC (Animal Co-product Research and Education Center) at Clemson University. The authors are also grateful to Kimberly Ivey for her assistance in conducting TGA and FTIR tests.

REFERENCES

(1) Wool, R.; Sun, X. S. *Bio-based polymers and composites*; Academic Press: 2011; .

(2) Mohanty, A.; Misra, M.; Drzal, L. Sustainable bio-composites from renewable resources: opportunities and challenges in the green materials world. *Journal of Polymers and the Environment* **2002**, *10*, 19-26.

(3) Zheng, T.; Yu, X.; Pilla, S. Mechanical and moisture sensitivity of fully bio-based dialdehyde carboxymethyl cellulose cross-linked soy protein isolate films. *Carbohydr. Polym.* **2017**, *157*, 1333-1340.

(4) Shen, L.; Haufe, J.; Patel, M. K. Product overview and market projection of emerging bio-based plastics PRO-BIP 2009. *Report for European polysaccharide network of excellence (EPNOE) and European bioplastics* **2009**, *243*.

(5) Chen, H. Functional properties and applications of edible films made of milk proteins. *J. Dairy Sci.* **1995**, *78*, 2563-2583.

(6) Wu, Q.; Yoshino, T.; Sakabe, H.; Zhang, H.; Isobe, S. Chemical modification of zein by bifunctional polycaprolactone (PCL). *Polymer* **2003**, *44*, 3909-3919.

(7) Kim, S.; Sessa, D.; Lawton, J. Characterization of zein modified with a mild cross-linking agent. *Industrial Crops and Products* **2004**, *20*, 291-300.

(8) Sharma, S.; Hodges, J. N.; Luzinov, I. Biodegradable plastics from animal protein coproducts: feathermeal. *J Appl Polym Sci* **2008**, *110*, 459-467.

(9) Park, S.; Bae, D.; Rhee, K. Soy protein biopolymers cross-linked with glutaraldehyde. *J. Am. Oil Chem. Soc.* **2000**, *77*, 879-884.

(10) Silva, R.; Elvira, C.; Mano, J.; San Roman, J.; Reis, R. Influence of β-radiation sterilisation in properties of new chitosan/soybean protein isolate membranes for guided bone regeneration. *J. Mater. Sci. Mater. Med.* **2004**, *15*, 523-528.

(11) Marqui é, C. Chemical reactions in cottonseed protein cross-linking by formaldehyde, glutaraldehyde, and glyoxal for the formation of protein films with enhanced mechanical properties. *J. Agric. Food Chem.* **2001**, *49*, 4676-4681.

(12) Mekonnen, T.; Mussone, P.; El‐Thaher, N.; Choi, P. Y.; Bressler, D. C. Thermosetting proteinaceous plastics from hydrolyzed specified risk material. *Macromolecular Materials and Engineering* **2013**, *298*, 1294-1303.

(13) Mekonnen, T. H.; Mussone, P. G.; Stashko, N.; Choi, P. Y.; Bressler, D. C. Recovery and characterization of proteinacious material recovered from thermal and alkaline hydrolyzed specified risk materials. *Process Biochemistry* **2013**, *48*, 885-892.

(14) Jalil, N.; Kheir, N. A.; Salman, M. A rule-based energy management strategy for a series hybrid vehicle. *American Control Conference, 1997. Proceedings of the 1997.* **1997**, 1, 689-693.

(15) Liu, J.; Peng, H. Modeling and control of a power-split hybrid vehicle. *IEEE Trans. Control Syst. Technol.* **2008**, *16*, 1242-1251.

(16) Zhang, X.; Ivanco, A.; Tao, X.; Wagner, J.; Filipi, Z. Optimization of the Series-HEV Control with Consideration of the Impact of Battery Cooling Auxiliary Losses. *SAE International Journal of Alternative Powertrains* **2014**, *3*, 234-243.

(17) Zhang, X.; Filipi, Z. Optimal Supervisory Control of the Series HEV with Consideration of Temperature Effects on Battery Fading and Cooling Loss. *SAE International Journal of Alternative Powertrains* **2016**, *5*, 299-307.

(18) Zhang, X.; Filipi, Z. *Computationally Efficient Li-Ion Battery Aging Model for Hybrid Electric Vehicle Supervisory Control Optimization* **2017**. SAE conference paper.

(19) Callon, M. In *The sociology of an actor-network: The case of the electric vehicle;* Mapping the dynamics of science and technology; Springer: 1986; pp 19-34.

(20) Wang, C.; Stielau, O. H.; Covic, G. A. Design considerations for a contactless electric vehicle battery charger. *IEEE Trans. Ind. Electron.* **2005**, *52*, 1308-1314.

(21) Kaufman, J. G.; Rooy, E. L. *Aluminum alloy castings: properties, processes, and applications*; Asm International: 2004; .

(22) Wang, B.; Deng, L.; Adrien, C.; Guo, N.; Xu, Z.; Li, Q. Relationship between textures and deformation modes in Mg–3Al–1Zn alloy during uniaxial tension. *Mater Charact* **2015**, *108*, 42-50.

(23) Xin, R.; Liu, D.; Xu, Z.; Li, B.; Liu, Q. Changes in texture and microstructure of friction stir welded Mg alloy during post-rolling and their effects on mechanical properties. *Materials Science and Engineering: A* **2013**, *582*, 178-187.

(24) Xin, R.; Guo, C.; Xu, Z.; Liu, G.; Huang, X.; Liu, Q. Characteristics of long {10-12} twin bands in sheet rolling of a magnesium alloy. *Scr. Mater.* **2014**, *74*, 96-99.

(25) Ashori, A. Wood–plastic composites as promising green-composites for automotive industries! *Bioresour. Technol.* **2008**, *99*, 4661-4667.

(26) Yebi, A.; Ayalew, B.; Pilla, S.; Yu, X. Model-Based Robust Optimal Control for Layer-By-Layer Ultraviolet Processing of Composite Laminates. *Journal of Dynamic Systems, Measurement, and Control* **2017**, *139*, 021008.

(27) Opalički, M.; Kenny, J. M.; Nicolais, L. Cure kinetics of neat and carbon‐fiber‐reinforced TGDDM/DDS epoxy systems. *J Appl Polym Sci* **1996**, *61*, 1025-1037.

(28) d'Almeida, J.; Monteiro, S. The resin/hardener ratio as a processing parameter for modifying the mechanical behaviour of epoxy-matrix/glass microsphere composites. *Composites Sci. Technol.* **1998**, *58*, 1593-1598.

(29) Averous, L.; Moro, L.; Dole, P.; Fringant, C. Properties of thermoplastic blends: starch–polycaprolactone. *Polymer* **2000**, *41*, 4157-4167.

(30) Davarpanah, M. A.; Mirkouei, A.; Yu, X.; Malhotra, R.; Pilla, S. Effects of incremental depth and tool rotation on failure modes and microstructural properties in Single Point Incremental Forming of polymers. *J. Mater. Process. Technol.* **2015**, *222*, 287-300.

(31) Barton, J. The application of differential scanning calorimetry (DSC) to the study of epoxy resin curing reactions. *Epoxy resins and composites I* **1985**, 111-154.

(32) Horie, K.; Mita, I.; Kambe, H. Calorimetric investigation of polymerization reactions. I. Diffusion‐controlled polymerization of methyl methacrylate and styrene. *Journal of Polymer Science Part A‐1: Polymer Chemistry* **1968**, *6*, 2663-2676.

(33) Riccardi, C.; Adabbo, H.; Williams, R. Curing reaction of epoxy resins with diamines. *J Appl Polym Sci* **1984**, *29*, 2481-2492.

(34) Bigi, A.; Cojazzi, G.; Panzavolta, S.; Rubini, K.; Roveri, N. Mechanical and thermal properties of gelatin films at different degrees of glutaraldehyde crosslinking. *Biomaterials* **2001**, *22*, 763-768.

(35) El-Thaher, N.; Mekonnen, T.; Mussone, P.; Bressler, D.; Choi, P. Nonisothermal DSC study of epoxy resins cured with hydrolyzed specified risk material. *Ind Eng Chem Res* **2013**, *52*, 8189-8199.

(36) Kissinger, H. E. Reaction kinetics in differential thermal analysis. *Anal. Chem.* **1957**, *29*, 1702-1706.

(37) Dinakaran, K.; Alagar, M. Preparation and characterization of bismaleimide (N, N′‐bismaleimido‐4, 4′‐diphenyl methane)–unsaturated polyester modified epoxy intercrosslinked matrices. *J Appl Polym Sci* **2002**, *85*, 2853-2861.

(38) Wetzel, B.; Rosso, P.; Haupert, F.; Friedrich, K. Epoxy nanocomposites–fracture and toughening mechanisms. *Eng. Fract. Mech.* **2006**, *73*, 2375-2398.

(39) Kanimozhi, K.; Sethuraman, K.; Selvaraj, V.; Alagar, M. Development of ricehusk ash reinforced bismaleimide toughened epoxy nanocomposites. *Front. Chem.* **2014**, *2*, 65, DOI: 10.3389/fchem.2014.00065 [doi].

(40) Zhang, J.; Mungara, P.; Jane, J. Mechanical and thermal properties of extruded soy protein sheets. *Polymer* **2001**, *42*, 2569-2578.

(41) Luo, L.; Meng, Y.; Qiu, T.; Li, X. An epoxy‐ended hyperbranched polymer as a new modifier for toughening and reinforcing in epoxy resin. *J Appl Polym Sci* **2013**, *130*, 1064-1073.

(42) Gu, A.; Liang, G. Thermal degradation behaviour and kinetic analysis of epoxy/montmorillonite nanocomposites. *Polym. Degrad. Stab.* **2003**, *80*, 383-391.

CHAPTER FOUR

PREPARATION AND PROPERTIES OF WATERBORNE POLYURETHANE AND ANIMAL PROTEIN BASED HYBRID FILMS

ABSTRACT

The past decades have witnessed impressive development of protein based plastics. Extensive research has been undertaken in recent times on finding suitable, alternative, non-feed and non-fertilizer applications for these materials as well as increasing the economic values of these proteins. In this regard, use of such proteins to derive plastics, especially thermoplastics and derived composites, has emerged as a potentially acceptable choice. However, the compatibility problem between protein molecules and organic resins could not be ignored. In this study, we solved this problem by utilizing waterborne polyurethane as resins to react with protein molecules and form the covalent bonded interconnected hybrid polymers.

4.1 Introduction

Polyurethane (PU) exhibits high performance as elastomer and excellent properties as a thermoplastic material (1). Its impressive thermal and mechanical properties have made PU among the most widely used polymers in various industries, such as in the aerospace, automotive, packing and home decorating sectors. The rapid increase in usage of PU across multiple sectors has led to increasing attention on its toxicity. Attempts have been made towards developing novel, non-toxic forms of PU, some of which have achieved pleasant results, such as waterborne polyurethane (WPU)

(2) and PU forms synthesized via non-isocyanate strategy (3). With regard to commercial uses, organic solvent-based traditional PU forms have been gradually replaced by eco-friendly, health-friendly, waterborne PU (2). Several studies undertaken in recent years have focused on enhancing properties of WPU, such as via the addition of graphene (4), nanoclay(5) or carbon nanotube(6) to obtain WPU-based nanocomposites. All such studies have shown improvement in thermal and mechanical properties of WPUs, but have also ignored the issue of non-biodegradability of PU and its subsequent degrading impact on our environment. Researchers have taken initiatives in recent times to enhance the biodegradability and biocompatibility of WPU through addition of biomass to the WPU matrix via physical mixing or the formation of new intermolecular bonds.

Plastics derived from soybean protein isolate (SPI) – be it individual SPI films or SPI films combined with other chemicals such as aldehydes (7) and WPU to form hybrid materials – have gained significant attention among researchers in this regard. As early as 2004, Wang et. al prepared crosslinked soy protein isolate (SPI)/WPU composite sheets by mixing SPI, glycol diglycidyl ether (EGDE) and WPU in aqueous solutions, and then cast and cured these sheets at room temperature (8). The resultant sheets were found to be biodegradable, and exhibited good mechanical properties. Tian et al. developed biodegradable SPI/WPU composites, and found strong bonding between SPI and WPU due to the presence of intermolecular hydrogen bonds that ensured good flexibility and enhanced water resistance of the composite (9). Zhang et al. fabricated poly(butylene adipate) (PBA)-based WPU/SPI-blended films, and observed strong intermolecular interactions between WPU and SPI, that allowed for the formation of a homogeneous

structure. The resultant films obtained were observed to exhibit high water resistance, high flexibility, and excellent thermal and mechanical properties (10).

Even as SPI has been used to prepare composites with WPU in various academic studies, no research has been undertaken till date on preparing WPU-based composites using animal protein. This is because in comparison to SPI, extracted animal proteins are complicated, not only in terms of their structure and components, but also due to the potential presence of bio-contaminats such as bacteria. Mekonnen et al. prepared thermosetting plastics based on hydrolyzed and bovine spongiform encephalopathy (BSE)-contaminated animal protein (11). Animal protein molecules contain various functional groups, such as amines ($–NH_2$, and -NH-), sulfyl (-SH), carboxylic acid (-COOH) and hydroxyl (–OH) groups. These functional groups provide good opportunities for the formation of animal protein/WPU composites due to strong intermolecular bonds between the constituents, as such bonds result in the obtainment of a uniform structure and enhanced properties compared to mere physical blending.

In our previous studies, we have developed a new, energy-efficient method for extracting protein isolate from the poultry meal (chapter 3). We have utilized the animal protein extracted via this method to prepare thermosetting plastics, and then enhanced the mechanical properties of these plastics through addition of BMI and HBP. In this paper, we report a new study on WPU/animal protein extraction-based hybrid polymer films possessing enhanced mechanical properties. The occurrence of successful intermolecular bonding between WPU and animal protein was confirmed via Fourier Transform Infra-red (FTIR) Spectroscopy and Ultraviolet (UV)-visible spectrometry. Mechanical

properties and thermal stability were investigated by tensile test and thermo-gravimetric analysis (TGA) respectively. Fracture surface morphology was studied using Scanning Electron Microscopy (SEM).

The principal scientific benefit of this study lies in the use of animal proteins for the development of high-strength waterborne polyurethane composites for automotive coating/painting and other applications. Polyurethanes are widely used in the manufacture of cars due to the benefits they offer in terms of comfort, protection and energy conservation via lowering of weight and consequent enhancement in fuel economy. The new hybrid polymers processed in this study exhibit better mechanical performance compared to pure WPU films, while showing enhanced recyclability and sustainability.

The proposed novel WPU films processed in this study can be suitable for use as interior and exterior coating materials in cars. While providing high gloss and resistance to scratches and corrosion, combined with durability, to a car's exterior, such films are also ideal for use in car cushions due to their light weight, high strength, and durable nature. Moreover, animal protein/WPU composites have better biocompatibility compared to pure WPU films, making them vastly suitable for a larger number of applications vis-à-vis pure WPU. With the rapidly increasing global automobile sales and increasing focus on lightweighting to achieve improved fuel economy, R&D units of automotive manufacturers are focusing exclusively on developing innovative composites

possessing multi-functional and structural properties. Given the extensive application of PU in the automotive industry and the recurring problems associated with recycling of vehicles, our new protein-WPU hybrid polymer has a large potential consumer market.

4.2 Materials and Experimental

4.2.1 Materials

The original sample used in this study was Poultry by-product meal (Feed grade) provided by Animal Co-product Research and Education Center., with its total protein content ratio labeled as being not less than 56 % on dry weight basis. Diglycidyl ether of bisphenol A (DGEBA) epoxy resin, sodium chloride (NaCl), disodium phosphate (Na_2HPO_4), mono-potassium phosphate (KH_2PO_4) and magnesium chloride ($MgCl_2$) were purchased from Sigma-Aldrich, USA. Hexane (C_6H_{14}) was purchased from VWR. All chemicals were used without further processing. Filter paper used in our study was purchased from Whatman, USA (Whatman #4, D = 11 cm, pore size of 20-25 μm), and was used in as-received state. Dialysis membrane used in this study (d = 3000) was purchased from Thermo Fisher Scientific.

Tolylene-2,4-diisocyanate (TDI) (95 %) and polyethylene glycol 1000 (PEG) (100g/l, H2O) was purchased from Sigma-Aldrich, while dimethylol propionic acid (DMPA), triethylamine (TEA) and acetone were obtained from VWR, USA. TDI was

distilled prior to its use, while PEG and DMPA were vacuum-dried before usage. TEA and acetone were treated with 3 Å molecular sieves to dehydrate them.

4.2.2. Proteinaceous Material Extraction

Initially, poultry meat-salt solution was prepared by mixing 100 g sample of the poultry meal sample with 450 mL salt solution containing 18 g NaCl, 4.1 g KH_2PO_4, and 4.3 g Na_2HPO_4 as per the method described by Park et. al (13). Following this, dialysis process was applied to separate the salt from the meat sample in order to extract the protein from this solution mixture by controlling its pH value. Protein/salt solution was filled into the dialysis membrane bag, after which the bag was placed in enough water for 4 h, during which the water was changed every hour. The use of hydrolysis procedure in this study for animal protein extraction makes this process cost-effective and energy-efficient when compared to traditional protein extraction processes that are undertaken at high temperatures and pressures.

4.2.3. Preparation of WPU/Animal protein hybrid films

Extracted animal protein (3 g) and glycerol (1 g) were dissolved in distilled water (50 ml) with constant stirring and heated to 70 ℃ for 30 min. The pH of the solution was adjusted to 10 $\pm$0.1 via use of 1 M ammonia solution using a digital pH analyzer. The solution was then heated to 90 ℃ for 30 min to denature the animal protein. The resultant protein solution was then cooled to room temperature prior to its further use.

TDI (10 g, 0.056 mol) and PEG (30 g, 0.03 mol) were introduced into a three-neck flask equipped with a thermometer, mechanical stirrer and a condenser tube. The resultant mixture obtained was heated to 75 ℃ for 1 h and stirred continuously, after which DMPA (1.34 g, 0.01 mol) was added to the mixture. The mixture was stirred at 85 ℃ for 3 h, and then cooled to 40 ℃, after which 15 g of acetone was added to it to reduce the viscosity of the pre-polymer. Following this, TEA (1.05 g, 0.01 mol) was added to the mixture to neutralize the carboxylic acid groups of DMPA, subsequent to which 350 g of distilled (DI) water was added to the mixture and stirred.

WPU dispersion was then mixed with animal protein solution and stirred at 40 ℃. The mixture was degassed in a vacuum tank and then cast in a silicon (Si) mold. The mixture was dried under room temperature in ambient conditions for 72 hours. The animal protein content was kept at 2, 4, 6, 8, 10, and 12 wt. % in the hybrid polymer matrix.

4.2.4. Characterization

4.2.4.1 ATR-FTIR Spectroscopy:

Attenuated Total Reflectance Flourier Transform Infra-red (ATR-FTIR) Spectroscopy was performed on a Thermo-Nicolet Magna 550 FTIR spectrometer in combination with a Thermo-Spectra Tech Foundation Series Diamond ATR accessory, with the angle of incidence being 50 °. ATR-FTIR spectra were obtained for animal protein, WPU, and WPU/animal protein hybrid polymer.

4.2.4.2 UV–vis spectrophotometer:

Optical transmittance (Tr) of the hybrid polymer films was measured using a UV–vis spectrophotometer (Lambda 900, Perkin Elmer) at wavelengths ranging from 200-800 nm.

4.2.4.3 Differential Scanning Calorimetry (DSC):

Differential scanning calorimetry (DSC) analysis was conducted to investigate the curing behavior of protein/epoxy mixture using a thermal analyzer (Q2000, TA Instruments, USA) under nitrogen (N_2) atmosphere. DSC experiments were undertaken on samples weighing 6-10 mg. In dynamic DSC experiments, samples were heated from 25 to 275 ℃ at various heating rates (2, 5, 10, 15 and 20 ℃ /min). In each case, reaction heat was calculated based on the total area under the exothermal peak of the DSC graph.

4.2.4.4 Thermo-gravimetric Analysis (TGA):

TGA measurements were undertaken using a TGA Q5000 instrument (TGA Q5000) under nitrogen (N_2) flow at a heating rate of 10 ℃/min to study thermal degradation behavior of animal protein-based polymers processed in this study. About 8 mg of hybrid polymer samples were heated at 10 ℃/min over the temperature range of 30-600 ℃ in nitrogen (N_2) atmosphere.

4.2.4.5 Scanning Electron Microscopy:

Hybrid WPU/SPI polymer films were frozen in liquid nitrogen and broken, after which the fractured film surfaces were placed on the Scanning Electron Microscopy (SEM) sample holder and sputtered with 1.5 nm thick layer of gold. Fracture surface morphology was characterized using SEM to analyze the miscibility and compatibility of WPU and animal protein.

4.2.4.6 Mechanical Properties:

Tensile strength and elongation-at-break of animal protein-based WPU films were measured using Instron Universal Testing Machine (Model 1125) at cross-head speed of 50 mm/min, with 30 mm grip separation. All procedures were based on the relevant ASTM standards.

4.3 Results and discussion

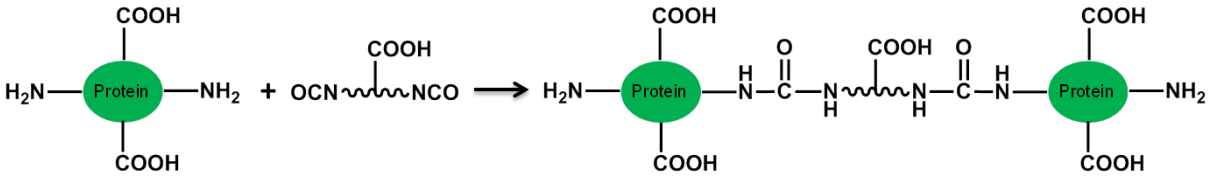

Scheme 4.1 The crosslinking reaction mechanism between WPU and animal protein

Scheme 1 shows the crosslinking reaction mechanism between WPU and animal protein. As is well-known (14), both amine and carboxyl functional groups can be found in animal protein molecules. WPU pre-polymer possesses active -NCO groups, which

can easily react with -NH2 in the animal protein molecules (15). Upon the completion of this reaction, a crosslinked network is obtained, which has been named by us as the WPU/animal protein hybrid polymer.

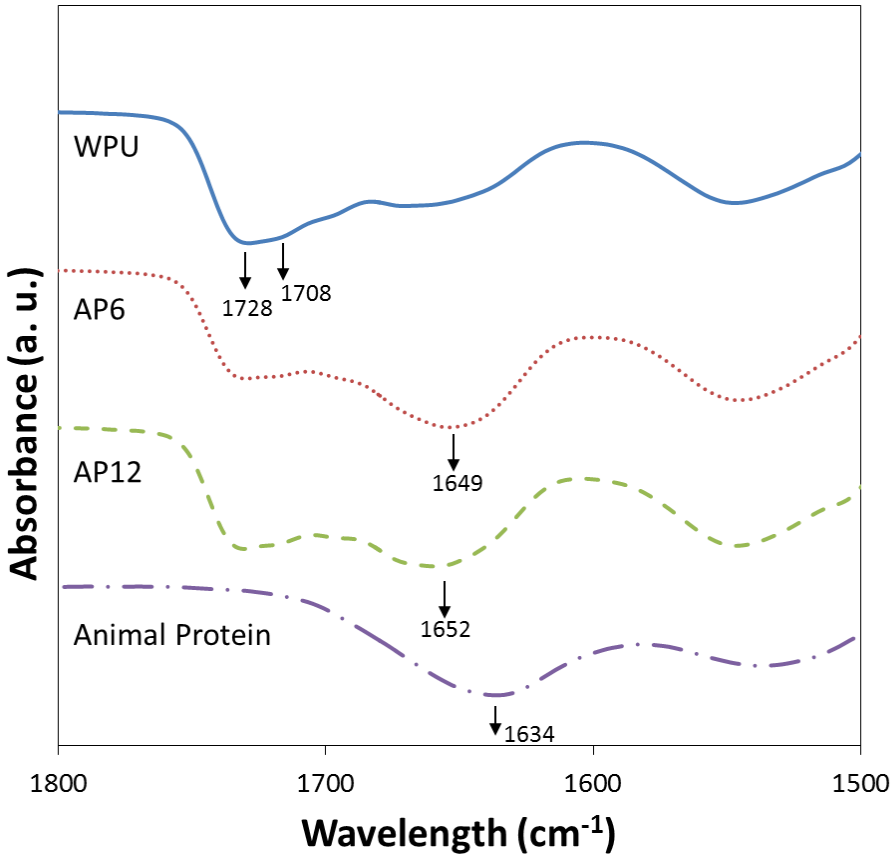

Figure 4.1 FTIR spectra of pure WPU, animal protein 6 wt.% (AP6) and animal protein 12wt. % (AP12) animal protein added, pure animal protein.

FTIR spectra of WPU, AP6, AP12 and animal protein has been shown in Figure 1. The region between 1750 cm^{-1} and 1700 cm^{-1} corresponds to carbonyl stretching, and in this study, showed two prominent peaks at 1728 cm^{-1} and 1708 cm^{-1}, corresponding to the

free –C=O bond and the O=C–O-H bond in WPU respectively. Furthermore, absorptivity coefficient of hydrogen-bonded carbonyl in WPU was observed to be higher than that of the non-hydrogen bonded carbonyl (16). The higher intensity of free carbonyl peaks indicated that most carbonyls in WPU were not hydrogen-bonded, thus allowing for the formation of an intermolecular hydrogen bond with amine groups present in animal proteins, as shown in Figure 1. With regard to animal proteins, FTIR spectra showed characteristic peaks of amide I group centered at 1634 cm^{-1}, which could be attributed to the stretching of C=O bond. Addition of WPU was observed to result in a shift of this peak to a higher wavelength, indicating strong intermolecular interactions between WPU and protein. In summary, FTIR results confirmed the formation of successful intermolecular bonding between WPU and animal protein.

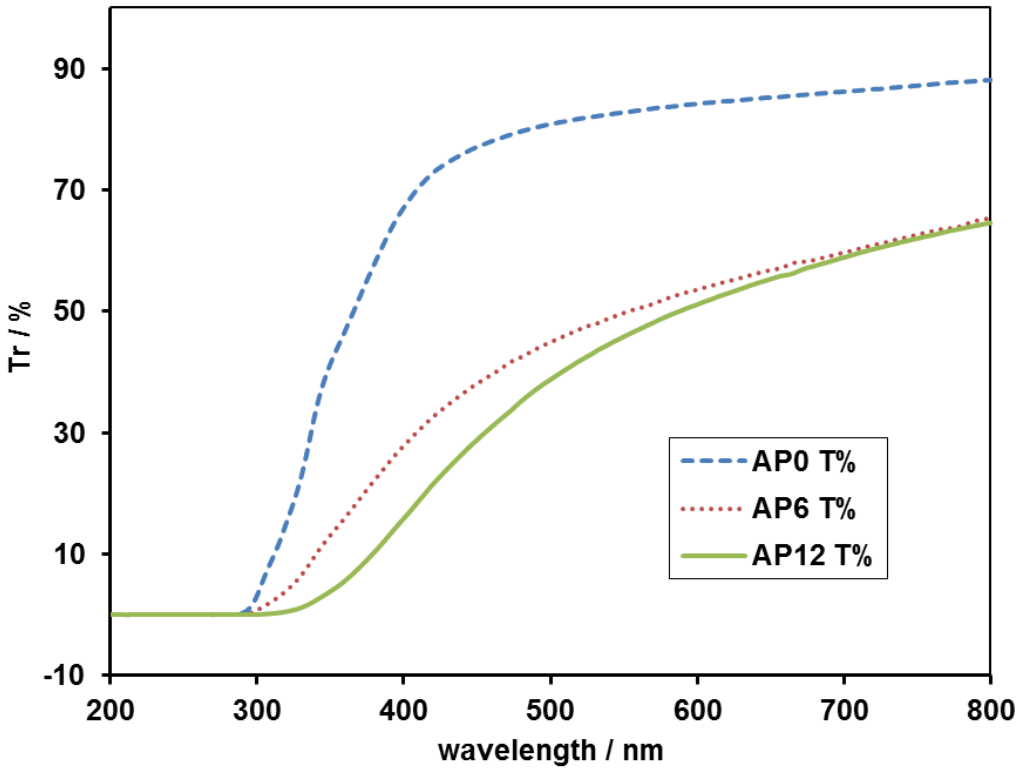

Figure 4.2 Dependence of the optical transmittance (Tr) on wavelength for different animal protein content of the WPU and WPU/animal protein composite.

To investigate optical properties and miscibility of the two constituents of the WPU/animal protein hybrid polymer, UV-visible microscopy tests were performed for pure WPU (AP0), AP6 and AP12. According to Figure 2, all films exhibited the highest optical transmittance at wavelength of 800 nm, which reduced gradually with change in wavelength to smaller values. At wavelength values of less than 300 nm, optical transmittance reached zero, indicating that the samples were mostly opaque. Optical transparency of materials can be regarded as an auxiliary criterion to judge the compatibility of blends and interfacial interactions (17). The results in Figure 2 confirm

good miscibility between animal protein and WPU in the hybrid polymer, and may have been caused by the hydrophilic properties of both animal protein and WPU. With regard to compatibility, animal protein-WPU combination showed better performance when compared to the animal protein-DGEBA combination.

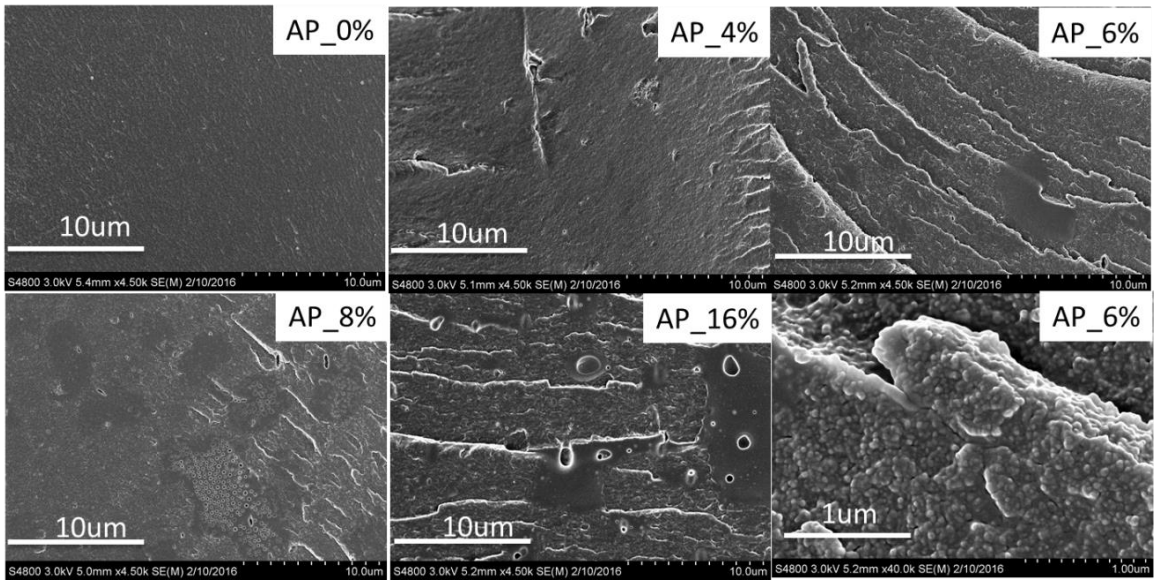

Figure 4.3 SEM photographs of the cross sections of the pure WPU, 4%, 8% and 16% animal protein added.

Figure 4.3 shows the fracture surface SEM images of AP_0 % (WPU), AP_4 %, AP_6 %, AP_8 %, AP_16 % and AP_6 % zoom-in. SEM images of pure WPU films indicated an even and homogeneous surface, while for WPU films with less than 8 wt. % animal protein content, cross-section of the hybrid polymer seemed to be highly homogeneous, which indicated good miscibility between the two components. At protein concentrations higher than 8 wt. %, fracture surface was observed to be uneven, with

noticeable interfacial separation of components observed to occur. Moreover, the animal protein particle size of AP_16 % seems larger than in case of hybrid polymer combinations containing smaller amounts of animal protein. However, this is expected to be mitigated by refining the fabrication process via modulating the mixing time and force.

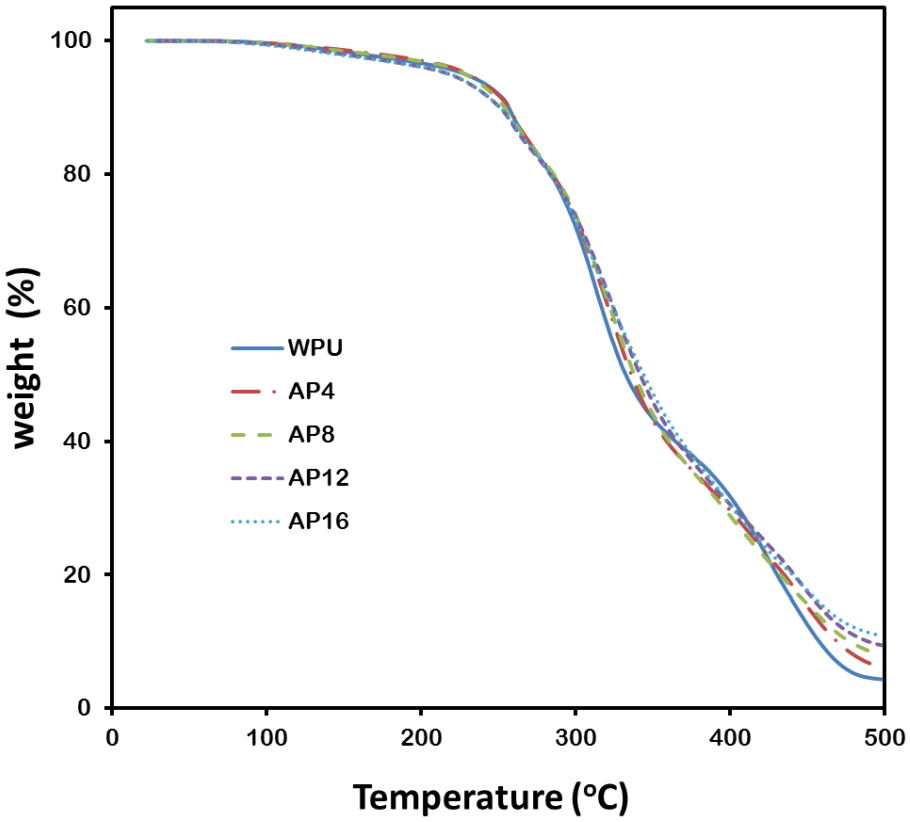

Figure 4.4 TGA spectra of WPU, AP4, AP8, AP12 and AP16

Table 4.1 Thermal properties summary of WPU, AP2, AP4, AP6, AP8, AP12 and AP16 based on DSC and TGA results

Animal protein (wt.%)	T_g (°C)	T_m (°C)	The change of melting heat capacity ΔC_p ($J \cdot g^{-1} \cdot K^{-1}$)	T_i at 5% loss (°C)	T_{ii} at 10% loss (°C)	Char %
0	42.614	123.354	0.9979	228	256	4.367
2	44.552	123.786	3.3263	-	-	-
4	47.445	124.034	4.5135	230	257	6.178
6	49.009	124.318	10.004	-	-	-
8	50.175	123.839	10.864	229	254	8.042
12	50.572	125.042	7.0603	217	251	9.457
16	-	125.101	12.743	218	251	10.900

Figure 4.4 shows the dependence of weight loss on temperature for films heated from room temperature to 500 ℃ in N_2 atmosphere. For all films, residual weight was observed to reduce with increase in temperature. While the temperature at which 5 % and 10 % weight loss were observed to occur was found to reduce by tiny amounts at higher animal protein weight content, residual weight in TGA at 500 ℃ showed the opposite trend. TGA data in Table 1 demonstrates no change in thermal stability of WPU upon the addition of animal protein and formation of the composite.

DSC results have been summarized in Table 1. Glass transition temperature (T_g) of pristine WPU is ~ 42.614 ℃. For WPU/animal protein hybrid polymer, a single T_g value was observed to shift to a higher temperature with increase in animal protein content, indicating the successful nature of crosslinking reaction between WPU and animal protein molecules. Similarly, a single value was observed for melting point (T_m), along with an increase in melting heat capacity with increase in animal protein content, further proving the successful formation of the hybrid polymer network.

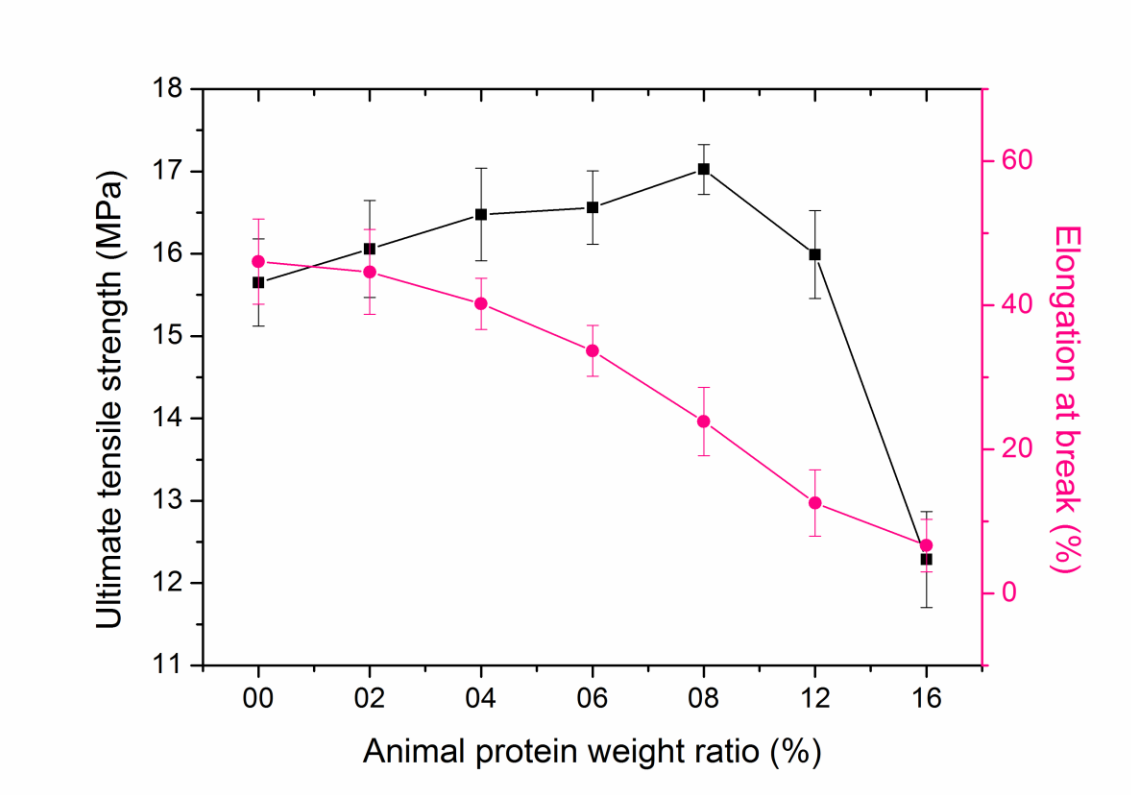

Figure 4.5 Ultimate tensile stress and Elongation (strain at break), of pure WPU and different weight ratio protein added hybrid polymers.

Investigation of mechanical properties of WPU/animal protein hybrid polymers was undertaken via tensile testing, and the results have been shown in Figure 4.5. As can be clearly seen, ultimate tensile strength (UTS) of the polymer did not show any change till the addition of animal protein up to 12 wt. % content; however, further increase in animal protein content was observed to result in a minor decrease in UTS of the hybrid polymer. In contrast, increase in animal protein content was observed to result in an increase in the elongation-at-break of the hybrid polymer. As has been reported elsewhere, elongation-at-break tends to reduce with increase in crosslinking density (18).

A similar result can be seen in Figure 5, indicating that a higher animal protein content results in higher crosslinking density, consistent with the trend observed for UTS of the hybrid polymer. In sum, addition of animal protein to WPU led to enhancement in mechanical properties of WPU due to the formation of crosslinked matrix till the animal protein content was up to 8 wt. %. Further addition of animal protein was observed to result in deterioration in mechanical properties of the hybrid polymer/composite.

4.4 Conclusion

An elastic WPU/animal protein hybrid polymer was prepared by adding animal protein to crosslink waterborne polyurethane pre-polymer through casting and evaporation process. The reaction mechanism between -NCO and -NH2 has been reported earlier, but it has been used for the first time to apply animal proteins as crosslinking agent for WPU. The hydrophilic properties of both animal protein and WPU ensured excellent compatibility between the two constituents of WPU/animal protein hybrid films, while the formation of highly crosslinked matrix resulted in significant improvement in mechanical properties of WPU. Moreover, the addition of animal proteins – highly renewable, environment-friendly materials – into the WPU matrix is expected to improve the biocompatibility of the WPU system. Hence, with its suite of attractive properties due to the addition of animal proteins, the resultant hybrid PU is likely to have wide applicability in diverse fields, including in the automotive industry.

REFERENCES

(1) Yoon, P. J.; Han, C. D. Effect of thermal history on the rheological behavior of thermoplastic polyurethanes. *Macromolecules* **2000**, *33*, 2171-2183.

(2) Kim, B. K.; Lee, J. C. Waterborne polyurethanes and their properties. *Journal of polymer science part A: polymer chemistry* **1996**, *34*, 1095-1104.

(3) Delebecq, E.; Pascault, J.; Boutevin, B.; Ganachaud, F. On the versatility of urethane/urea bonds: reversibility, blocked isocyanate, and non-isocyanate polyurethane. *Chem. Rev.* **2012**, *113*, 80-118.

(4) Lee, Y. R.; Raghu, A. V.; Jeong, H. M.; Kim, B. K. Properties of waterborne polyurethane/functionalized graphene sheet nanocomposites prepared by an in situ method. *Macromolecular Chemistry and Physics* **2009**, *210*, 1247-1254.

(5) Kim, B. K.; Seo, J. W.; Jeong, H. M. Morphology and properties of waterborne polyurethane/clay nanocomposites. *European Polymer Journal* **2003**, *39*, 85-91.

(6) Kuan, H.; Ma, C. M.; Chang, W.; Yuen, S.; Wu, H.; Lee, T. Synthesis, thermal, mechanical and rheological properties of multiwall carbon nanotube/waterborne polyurethane nanocomposite. *Composites Sci. Technol.* **2005**, *65*, 1703-1710.

(7) Zheng, T.; Yu, X.; Pilla, S. Mechanical and moisture sensitivity of fully bio-based dialdehyde carboxymethyl cellulose cross-linked soy protein isolate films. *Carbohydr. Polym.* **2017**, *157*, 1333-1340.

(8) Wang, N.; Zhang, L.; Gu, J. Mechanical properties and biodegradability of crosslinked soy protein isolate/waterborne polyurethane composites. *J Appl Polym Sci* **2005**, *95*, 465-473.

(9) Tian, H.; Wang, Y.; Zhang, L.; Quan, C.; Zhang, X. Improved flexibility and water resistance of soy protein thermoplastics containing waterborne polyurethane. *Industrial Crops and Products* **2010**, *32*, 13-20.

(10) Zhang, M.; Song, F.; Wang, X.; Wang, Y. Development of soy protein isolate/waterborne polyurethane blend films with improved properties. *Colloids and surfaces B: biointerfaces* **2012**, *100*, 16-21.

(11) Mekonnen, T.; Mussone, P.; El‐Thaher, N.; Choi, P. Y.; Bressler, D. C. Thermosetting proteinaceous plastics from hydrolyzed specified risk material. *Macromolecular Materials and Engineering* **2013**, *298*, 1294-1303.

(12) Austin, D.; Dinan, T. Clearing the air: The costs and consequences of higher CAFE standards and increased gasoline taxes. *J. Environ. Econ. Manage.* **2005**, *50*, 562-582.

(13) Park, S. K.; Bae, D.; Hettiarachchy, N. Protein concentrate and adhesives from meat and bone meal. *J. Am. Oil Chem. Soc.* **2000**, *77*, 1223-1227.

(14) Chen, R. J.; Zhang, Y.; Wang, D.; Dai, H. Noncovalent sidewall functionalization of single-walled carbon nanotubes for protein immobilization. *J. Am. Chem. Soc.* **2001**, *123*, 3838-3839.

(15) Hepburn, C. In *Reaction rates, catalysis and surfactants;* Polyurethane elastomers; Springer: 1992; pp 107-121.

(16) Coleman, M. M.; Lee, K. H.; Skrovanek, D. J.; Painter, P. C. Hydrogen bonding in polymers. 4. Infrared temperature studies of a simple polyurethane. *Macromolecules* **1986**, *19*, 2149-2157.

(17) Kumar, R.; Liu, D.; Zhang, L. Advances in proteinous biomaterials. *Journal of Biobased Materials and Bioenergy* **2008**, *2*, 1-24.

(18) Remunan-Lopez, C.; Bodmeier, R. Mechanical, water uptake and permeability properties of crosslinked chitosan glutamate and alginate films. *J. Controlled Release* **1997**, *44*, 215-225.

CHAPTER FIVE

THERMOSETTING PLASTICS DERIVED FROM WATER SOLUBLE EPOXY AND ANIMAL PROTEIN

ABSTRACT

Epoxy resin-based composites have been widely used across various industries, beginning with their use initially in making small components that has now extended to producing whole bodies of structures across the aeronautical, construction and wind energy sectors. Today, they have even gained prominence as potential replacement for metals in a number of industries. Traditional petroleum-based epoxy resins show impressive properties due to the high density of their crosslinked structure, but this is also accompanied by their none bio-degradable nature that leads to environmental issues regarding their disposal. Renewable resources like wood, protein, lignin and cellulose-based epoxy composites have attracted a lot of attention in recent years as potential alternatives to petroleum-based epoxy resins. However, among these alternatives, researchers have ignored a significant problem while working on protein-based epoxy composites – lack of compatibility between hydrophobic epoxy and hydrophilic proteins. The present study explores the means to overcome this problem by undertaking the reaction in aqueous solution.

5.1 Introduction

Epoxy resins play an important role across several industries on account of their high flexibility for being tailored to achieve desired properties, such as high modulus and

strength, durability, and excellent thermal and chemical resistance – achieved by the high density of their crosslinked structure. Traditional petroleum-based plastics are well-known for their high durability, and have been used across multiple industrial applications. However, the finite nature of petroleum resources poses a problem with regard to the sustainability of use of petroleum-based resins, especially given the likely outlook of rise in their prices in the future. Also, after the end of life-cycle of such resins, achieving environmental degradability and decomposition over a short time is difficult and can lead to further environmental problems such as air and soil pollution, in addition to their role in global warming (1-5). Hence, it is critical to innovate and utilize a novel, sustainable series of plastics that are made using renewable resources and that possess the potential to be biodegradable (6). In this regard, plant-based materials have been widely studied, but similar studies on developing plastics using animal by-products are relatively scarce. This is especially important in light of the increasing disease outbreaks among cattle, such as the emergence of Bovine Spongiform Encephalopathy (7, 8). On the other side, extra economic values of the animal byproduct gained a lot attraction recently. Therefore, it becomes imperative to develop new applications that work towards using animal by-products as well as such wasted meat.

In this context, some studies have been undertaken to investigate the properties and behavior of plastics derived from animal proteins. Chen et al. (9) developed thermoplastic films from milk proteins for use as protective layer on food items, but observed poor mechanical properties as a limiting factor for their use in such applications. A detailed understanding at the molecular level is thus needed for efficient engineering of

desired films. Wu et al. (10) modified zein protein using PCL-HDI to induce toughness combined with hydrophobicity, though not to the levels desired for commercial applications. They observed significant deterioration in strength and stiffness of zein protein upon the incorporation of PCL-HDI. Similarly, Kim et al. (11) undertook crosslinking of zein protein via use of 1-[3-dimethylamino-propyl]-3-ethyl-carbo - diimide hydrochloride (EDC) and N-hydroxy-succi-nimide (NHS), but did not achieve properties desired for high-performance applications. Sharma et al. (12) developed feathermeal protein-based biodegradable polymers blended with whey and albumin, and investigated their thermo-physical and mechanical properties. While they achieved success in enhancing modulus of the protein, this was accompanied by reduction in toughness. In addition, the hydrophilic nature of the polymer proved detrimental to its processing by expediting its thermal degradation, leading to inferior properties. While this may seem good from the viewpoint of economic value, it remains a perplexing strategy as variable temperature profiles lead to inefficient thermal management in such highly sensitive animal proteins. This in turn ensures thermal degradation of proteins, resulting in significant decrement of mechanical properties, thereby limiting its application base to low-performance and perhaps, low economic value applications. Recently, Mekkonnen et al. (13) derived thermoset materials using protein extraction from polluted meat and crosslinked these with epoxy resins. BSE-polluted meat was treated with pH-controlled aqueous solutions under high temperature and high pressure conditions to kill the virus and hydrolyze the protein, after which the protein was extracted from the mixture. Hydrolyzed animal protein was used as crosslinking agent

for epoxy resin to form the interconnected network. As reported, the final thermoset plastic exhibited good mechanical and thermal properties.

In our previous papers included in chapter 3 and chapter 4, we applied animal protein as crosslinker to prepare thermoset materials with DGEBA and enhanced its properties by adding Bismaleimide and hyperbranched polymers. All these studies focused on the enhancement of mechanical and thermal properties of animal protein-derived plastic, but none of them tried to overcome the fundamental compatibility problem of the protein used with epoxy resins. The biggest obstacle to the development of protein-based thermoset plastics is this very lack of compatibility that arises because protein molecules are hydrophilic while traditional DEGBA is hydrophobic, and has been clearly shown using Scanning Electron Micrographs (SEM) in previous studies. It usually results in phase separation, thereby affecting the properties. To overcome this problem, in this work, we applied water soluble epoxy resin (WEP) to crosslink with animal protein molecules and form the crosslinked network. The reaction mechanism has been clearly shown. Fourier Transform Infra-red (FTIR) Spectroscopy was used to characterize the change in the functional group after the crosslinking reaction. Scanning Electron Micrograph (SEM) was used to observe the microstructures of cross-sectional surface. Thermo-gravimetric analysis (TGA) was undertaken to study thermal properties of all compounds, while tensile test was performed to study mechanical properties of as-produced hybrid films.

5.2 Materials and Experimental

5.2.1 Materials

The original sample – used in this study – was Poultry by-product meal (Feed grade) provided byAnimal Co-product Research and Education Center at Clemson University. Total protein content ratio of the sample was labeled as not less than 56 % by dry weight basis. Diglycidyl ether of bisphenol A (DGEBA) epoxy resin, NaCl, Na_2HPO_4, KH_2PO_4 and $MgCl_2$ were purchased from Sigma-Aldrich, USA. Hexane was purchased from VWR, USA. All chemicals were used without further processing. Filter paper used in our study was obtained from Whatman, USA (Whatman #4, D = 11 cm, pore size 20-25 μm) and used in as-received state. Dialysis membrane (d = 3000) was purchased from Thermo Fisher Scientific. Water-based acrylic epoxy was purchased from Vital Coat (Tallahassee, FL, USA) and used without further processing.

5.2.2. Proteinaceous material extraction

Protein was extracted from the poultry meal and salt solution mixture by controlling its pH value. Every 100 g sample of the poultry meal was treated with 450 mL salt solution containing 18 g NaCl (or $MgCl_2$), 4.1 g KH_2PO_4, and 4.3 g Na_2HPO_4, according to the method used by Park et al. (14) Dialysis process was applied to separate the salt from the protein sample. Protein/salt solution was filled into the dialysis membrane bag and then placed in enough water for 4 h, during which water was changed every hour. Employment of non-hydrolyzed protein extraction procedure in this study makes this process cost-effective and energy-efficient when compared to traditional high-temperature, high-pressure protein extraction processes.

5.2.3. Preparation of WEP/Animal protein hybrid films

Animal protein extraction (3 g) and glycerol (1 g) were dissolved in distilled water (50 ml) at constant stirring and heated to 70 ^{o}C for 30 min. pH of the solution was adjusted to 10 $\pm$0.1 using 1 M ammonia solution and digital pH analyzer. The solution was then heated to 90 oC for 30 min to denature the animal protein. The resultant protein solution was then cooled to room temperature before further use.

50 ml water-based acrylic epoxy solution was heated at 60 ^{o}C till no change in weight was observed, indicating that the solution had fully dried. The final solid part was then weighed and density of the solution was calculated. Proper amount of water-based acrylic epoxy solution and animal protein solution was introduced in a glass beaker, varying the net epoxy/protein ratio as 0/100, 98.5/1.5, 95/5, and 92.5/7.5. The mixture was thoroughly mixed by stirring on a hot plate for 1 h under 60^{o}C. The mixture was then degassed in a vacuum chamber (till no bubbles were visible), and then poured on to a flat silicon mold. The mixture was subsequently dried in room temperature for 48 h and then dried at 60^{o}C for 2 h. The final membrane was cut into 1 cm x 5 cm specimen and kept in vacuum condition for testing.

5.2.4. Characterization

5.2.4.1 ATR-FTIR Spectroscopy

Thin films at varying weight ratios of WEP/animal protein were prepared for the purpose of analysis in this work. Attenuated Total Reflectance Flourier Transform-Infrared (ATR-FTIR) Spectroscopy was performed on Thermo-Nicolet Magna 550 FTIR

spectrometer in combination with Thermo-Spectra Tech Foundation Series Diamond ATR accessory; with the angle of incidence being 50 º. ATR-FTIR spectra were obtained for animal protein, WPU, and WPU/animal protein hybrid polymer.

5.2.4.2 Thermo-gravimetric Analysis (TGA)

TGA measurement was performed using a TGA Q5000 instrument (TGA Q5000) under nitrogen flow at a heating rate of 10 ℃/min to study thermal degradation behavior of protein-based plastics. About 8 mg of plastic samples were heated at 10 ℃/min over the temperature range of 30-600 ℃ in nitrogen atmosphere. The temperature at which the slope of weight loss versus temperature curve starts to increase was considered as the temperature of initiation of degradation.

5.2.4.3. Scanning Electron Microscopy (SEM)

Thin films at varying weight ratios of WEP/animal protein were frozen in liquid nitrogen and broken quickly. Fractured surface of the films was placed on a SEM holder. Specimen mounts were then coated with 60 % gold and 40 % palladium for 60 s at 45 mA current in a sputter coater (Desk II, Denton Vacuum, Moorestown, NJ). Hitachi S4800 SEM was used to perform microstructure analysis. Fracture surface morphology of coated specimen was characterized by SEM to show miscibility and compatibility of WPU and animal protein.

5.2.4.4. Mechanical properties

Ultimate tensile strength, modulus and elongation-at-break were measured using Instron Universal Testing Machine (Model 1125) at cross-head speed of 30 mm/min with 30 mm grip separation. Procedures followed were in conformance with ASTM standards.

5.3 Results and discussion

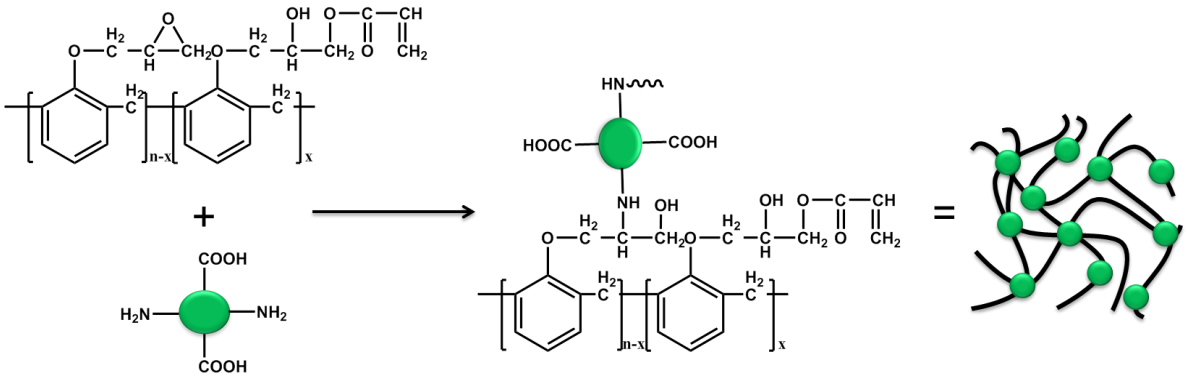

: Animal protein molecule

Scheme 1 Crosslinking mechanism between WEP and animal protein

Crosslinking mechanism between WEP and animal protein molecules is shown in Scheme 1. As reported before (15), both amine and carboxyl functional groups can be found in animal protein molecules. When it comes to crosslinking with epoxy groups, amine groups are more active than carboxyl groups under the reaction conditions. During crosslinking, epoxy ring in water-based acrylic epoxy opens and connects with amine groups, along with simultaneous formation of new hydroxyl groups in the final product. After crosslinking, water-based acrylic epoxy and animal protein formed a new networking to produce thermoset plastics. We refer to this network as "WEP/animal protein hybrid polymer".

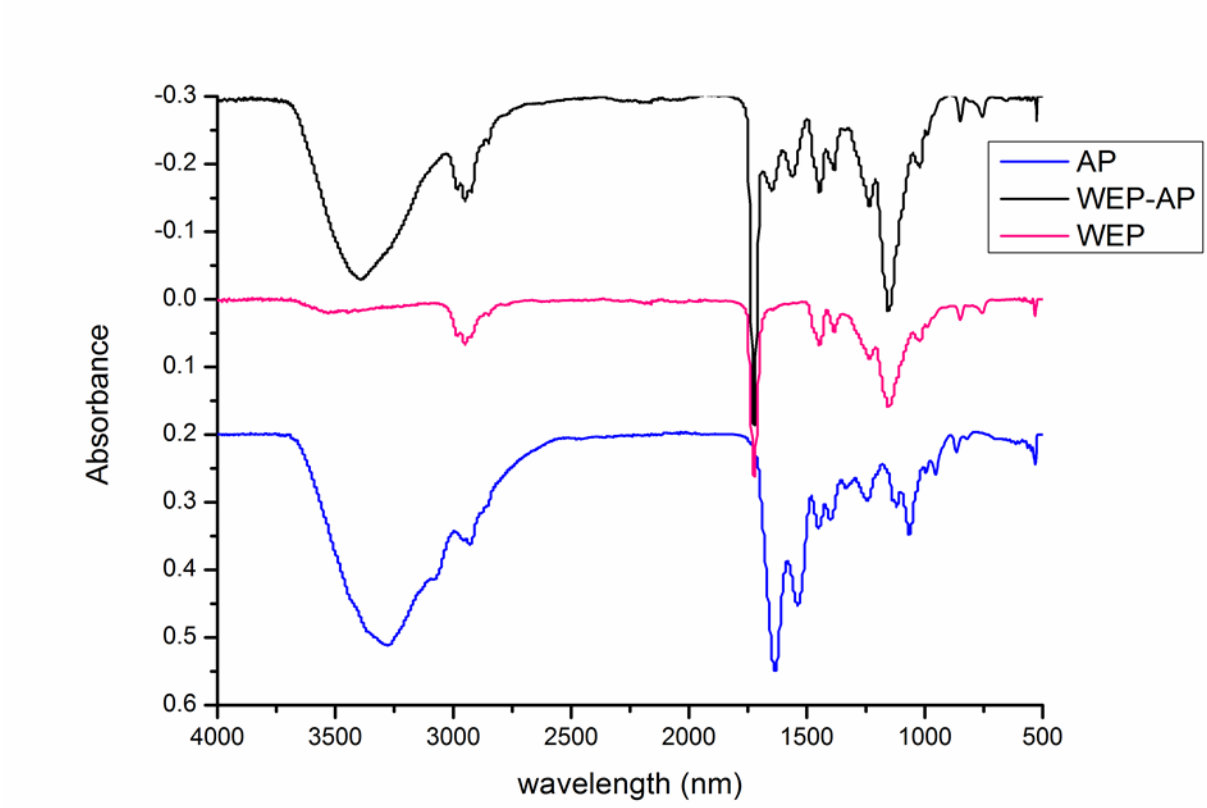

Figure 5.1 FTIR spectra of pure animal protein, WEP/animal protein (5 wt. %) hybrid polymer and pure WEP.

FTIR spectra of pure animal protein, WEP/animal protein (5 wt. %) hybrid polymer and pure WEP has been shown in Figure 5.1. On comparing the above three spectra, it shows that a new peak around -1500 cm-1 was observed for WEP/animal protein (5 wt. %) hybrid polymer, which could be the direct evidence of the formation of chemical linkage (new ester group), as initially proposed. For animal protein, FTIR spectra showed characteristic peaks of amide I (which can be attributed to C=O stretching), centered around 1634 cm^{-1}. Addition of WEP was found to lead to shifting of this peak to higher wavelength to ~ 1720 cm-1, indicating strong intermolecular

interactions between WPU and protein (16). In summary, FTIR results confirmed successful intermolecular bond formation between WEP and animal protein.

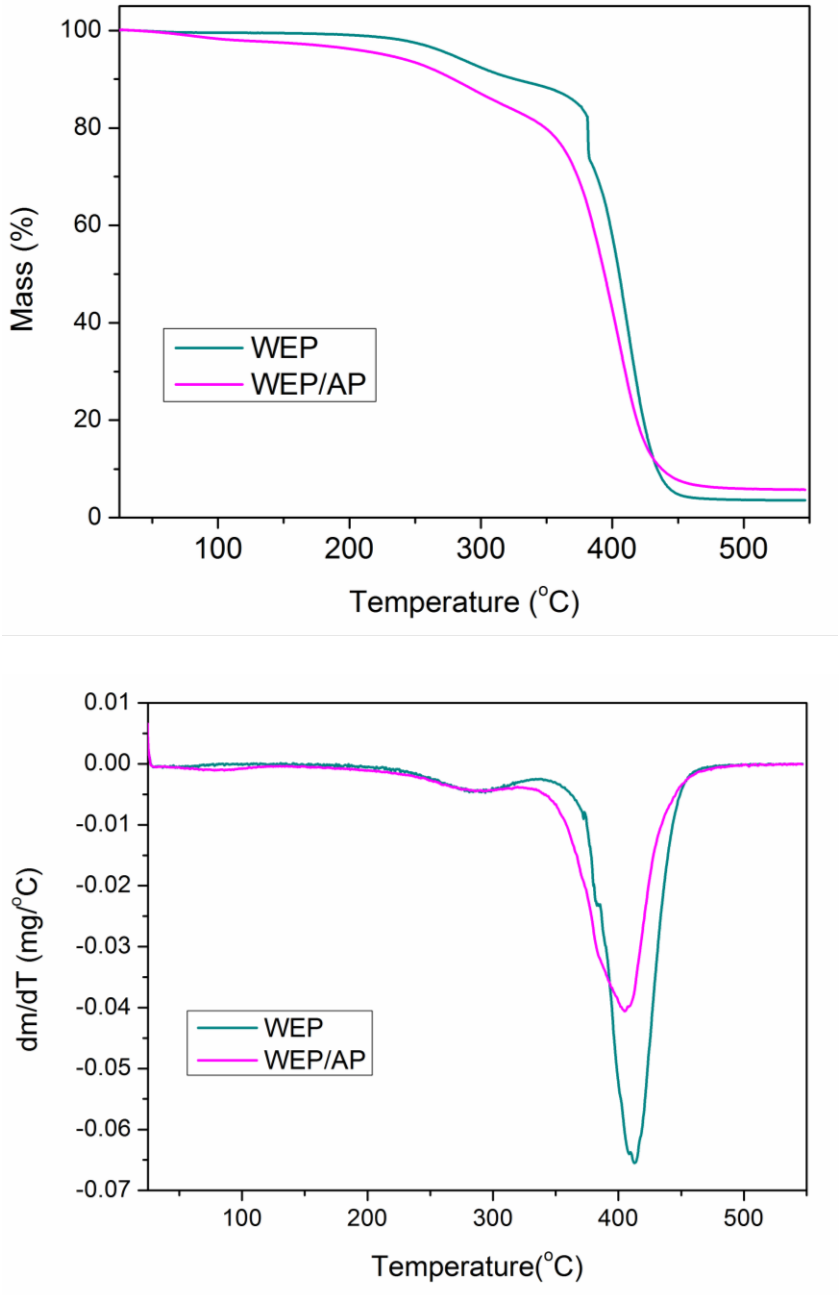

Figure 5.2 TGA spectra of WEP/AP (5 wt. %) hybrid polymer

Figure 5.2 shows the dependence of weight loss on temperature upon heating WEP and WEP/Animal protein hybrid films from room temperature to 550^{o}C in N_2 atmosphere. Residual weight showed decrease with increase in temperature for all films. The temperature at 5 % and 20 % weight loss showed reduction for WEP/Animal protein hybrid polymers, mainly due to evaporation of moisture present in animal protein. Both pure WEP and hybrid polymer showed significant weight loss upon being heated to 250^{o}C, along with a sharp decrease in weight at 350^{o}C, indicating the initiation of their decomposition. However, residual weight at 500^{o}C showed the opposite result, clearly indicating the residual weight for WEP/Animal protein hybrid polymer to be much larger than that of pure WEP. Above all, a minimal depletion in thermal stability was observed upon the introduction of AP (animal protein) into WE system. However, this was expected to be negligible and was expected to be compensated by the enhancement of mechanical properties obtained by crosslinking. Moreover, through precise process engineering, this inadequacy is supposed to be overcome. Efforts in this direction are also being carried out.

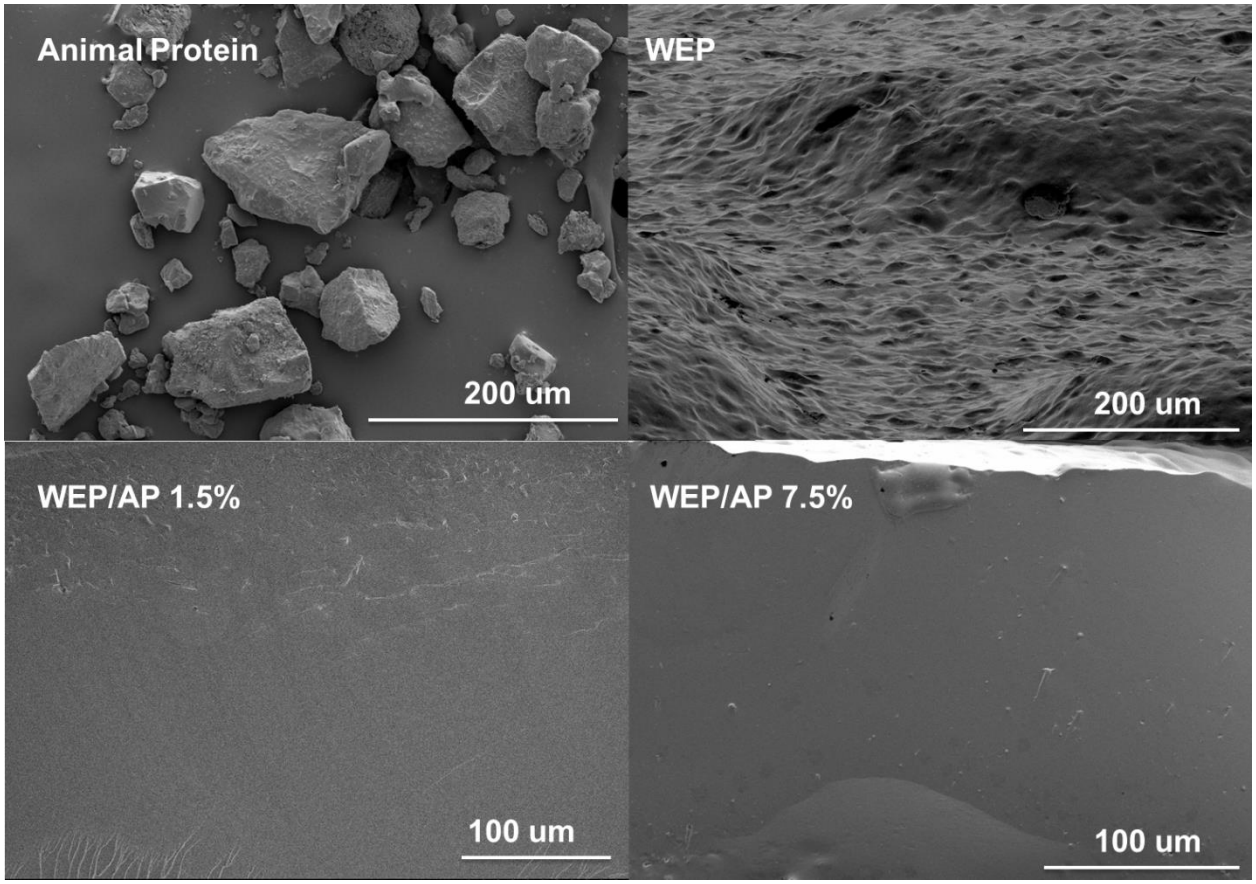

Figure 5.3 SEM images of WEP/AP (wt. %) hybrid polymer

Figure 5.3 shows the morphology of pure animal protein powders and fracture surface SEM images of pure WEP, WEP/AP wt. (AP - 1.5 wt. %) and WEP/AP wt. (AP - 7.5 wt. %). SEM images of animal protein powder show all dimensions below 200 um, which can be attributed to the grinding process after extraction from poultry materials. Pure WEP film was prepared by drying water-based acrylic epoxy water solution, and showed porous and uneven structure. This morphology was possibly caused by the aggregation of non-crosslinked molecules. Addition of animal protein to water-based acrylic epoxy solution, followed by its subsequent curing, led to the films showing a

more even, smooth cross-section. This can be explained by the role of animal protein as a crosslinker in the final product matrix and the high density of the resultant molecule due to the interconnection structure whereby strong, numerous bonds exist between animal protein molecule and water-based acrylic epoxy. Thus, after curing, newly formed crosslinked thermoset films show more smooth fracture surfaces than that of pure water-based acrylic epoxy solution dried films.

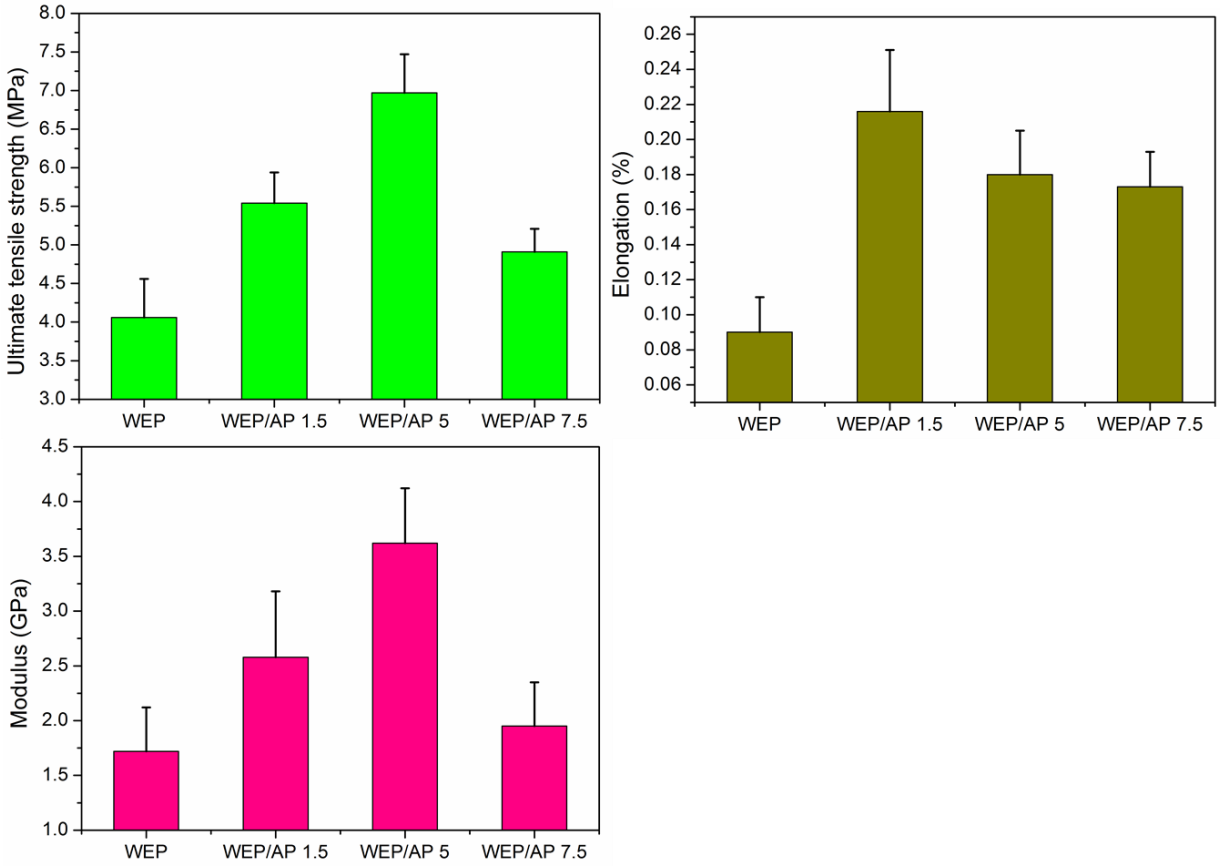

Figure 5.4 Ultimate tensile stress and Elongation (strain at break), of pure WEP and different weight ratio protein added hybrid polymers.

Investigation of mechanical properties of WEP/animal protein hybrid polymers was undertaken via tensile test and has been summarized in Figure 5.4. The figure clearly shows that increase in ultimate tensile strength upon addition of animal protein to WEP matrix till 5 wt. % of animal protein, followed by subsequent decrease with increase in animal protein content. Similar results were obtained for modulus. Increase in both parameters can be explained by the crosslinking of animal protein and water-based acrylic epoxy solution. Crosslinking leads to increase in crosslinking density, which results in a decrease in elongation-at-break and increase in ultimate tensile strength and modulus. Pure water-based acrylic epoxy solution dried films showed the lowest values for ultimate tensile strength, elongation and modulus, which is in agreement with SEM images that show highly porous structure for pure water-based acrylic epoxy solution dried films, which will lead to poor mechanical properties.

5.4 Conclusion

Elastic WEP/animal protein hybrid polymer films were prepared by adding different animal protein weight ratios to water-based acrylic epoxy solution through casting and evaporation processes. The reaction mechanism between –NH2 group in animal protein molecules and epoxy groups in water-based acrylic epoxy solution has been shown. This is the first work that uses water-based acrylic epoxy to solve the compatibility problem between hydrophilic animal protein and hydrophobic epoxy. Addition of animal protein to water-based acrylic epoxy solution led to increase in crosslinking density and reduction in porosity. Formation of highly crosslinked matrix

was found to result in significant improvement in mechanical properties. Thus, the compatibility problem between hydrophilic animal protein and hydrophobic epoxy was solved by changing the epoxy to water-based acrylic epoxy solution. This novel reaction system is based on the traditional reaction mechanism between amine groups and epoxy groups. However, it will definitely help in developing and promoting the wider application of animal byproducts, thereby decreasing animal waste generation and protect our environment.

ACKNOWLEDGMENTS

The authors would like to acknowledge the financial support of ACREC (Animal Co-product Research and Education Center) consortium at Clemson University. The authors are also grateful to Kimberly Ivey for her assistance in conducting TGA and FTIR tests.

REFERENCES

(1) Raquez, J.; Del église, M.; Lacrampe, M.; Krawczak, P. Thermosetting (bio) materials derived from renewable resources: a critical review. *Progress in Polymer Science* **2010**, *35*, 487-509.

(2) Dorgan, J. R.; Lehermeier, H. J.; Palade, L.; Cicero, J. Polylactides: properties and prospects of an environmentally benign plastic from renewable resources. *Macromolecular Symposia.* **2001**, 175, 55-66.

(3) Deublein, D.; Steinhauser, A. *Biogas from waste and renewable resources: an introduction*; John Wiley & Sons: 2011; .

(4) Yebi, A.; Ayalew, B.; Pilla, S.; Yu, X. Model-Based Robust Optimal Control for Layer-By-Layer Ultraviolet Processing of Composite Laminates. *Journal of Dynamic Systems, Measurement, and Control* **2017**, *139*, 021008.

(5) Mekonnen, T.; Mussone, P.; Khalil, H.; Bressler, D. Progress in bio-based plastics and plasticizing modifications. *Journal of Materials Chemistry A* **2013**, *1*, 13379-13398.

(6) Zheng, T.; Yu, X.; Pilla, S. Mechanical and moisture sensitivity of fully bio-based dialdehyde carboxymethyl cellulose cross-linked soy protein isolate films. *Carbohydr. Polym.* **2017**, *157*, 1333-1340.

(7) McCluskey, J. J.; Grimsrud, K. M.; Ouchi, H.; Wahl, T. I. Bovine spongiform encephalopathy in Japan: consumers' food safety perceptions and willingness to pay for tested beef. *Aust. J. Agric. Resour. Econ.* **2005**, *49*, 197-209.

(8) Taylor, D. M.; Woodgate, S. L.; Atkinson, M. J. Inactivation of the bovine spongiform encephalopathy agent by rendering procedures. *Vet. Rec.* **1995**, *137*, 605-610.

(9) Chen, H. Functional properties and applications of edible films made of milk proteins. *J. Dairy Sci.* **1995**, *78*, 2563-2583.

(10) Wu, Q.; Yoshino, T.; Sakabe, H.; Zhang, H.; Isobe, S. Chemical modification of zein by bifunctional polycaprolactone (PCL). *Polymer* **2003**, *44*, 3909-3919.

(11) Kim, S.; Sessa, D.; Lawton, J. Characterization of zein modified with a mild cross-linking agent. *Industrial Crops and Products* **2004**, *20*, 291-300.

(12) Sharma, S.; Hodges, J. N.; Luzinov, I. Biodegradable plastics from animal protein coproducts: feathermeal. *J Appl Polym Sci* **2008**, *110*, 459-467.

(13) Mekonnen, T.; Mussone, P.; El‐Thaher, N.; Choi, P. Y.; Bressler, D. C. Thermosetting proteinaceous plastics from hydrolyzed specified risk material. *Macromolecular Materials and Engineering* **2013**, *298*, 1294-1303.

(14) Park, S.; Bae, D.; Rhee, K. Soy protein biopolymers cross-linked with glutaraldehyde. *J. Am. Oil Chem. Soc.* **2000**, *77*, 879-884.

(15) Chen, R. J.; Zhang, Y.; Wang, D.; Dai, H. Noncovalent sidewall functionalization of single-walled carbon nanotubes for protein immobilization. *J. Am. Chem. Soc.* **2001**, *123*, 3838-3839.

(16) González, M. G.; Cabanelas, J. C.; Baselga, J. In *Applications of FTIR on epoxy resins-identification, monitoring the curing process, phase separation and water uptake;* Infrared Spectroscopy-Materials Science, Engineering and Technology; InTech: 2012; .

CHAPTER SIX

SYNTHESIS OF PROPERTIES TUNABLE AND RECYCLABLE NON-ISOCYANATE POLYURETHANE/DGEBA COPOLYMER

ABSTRACT

Epoxy resin-based composites have been widely applied in the automotive industry, initially in making small parts, and later in making whole bodies of components – not just in the auto sector but also in aeronautics, construction and wind energy – as well as alternatives to metals in other sectors. However, recycling of epoxy resin-based composites has gained wide attention in recent times, particularly as the major waste processing method for such composites is landfill. Several alternative recycling pathways have been achieved, such as mechanical, pyrolysis and fluidized bed. However, use of such methods is limited by their application till date only at small scale, highly energy-intensive nature, and damage to environment via other means. Here, we present a new self-healing, repairable, and recyclable epoxy matrix with extendable usage time as well as increased life cycles. Moreover, the introduction of urethane chain into the epoxy matrix made it possible to achieve variable, tunable mechanical properties, with the copolymer possessing the properties of both polyurethane and epoxy. Curing and recycle tests were conducted using a Rubber Process Analyzer for real-time monitoring. This is the first study to report time dependent self-healing process till date.

6.1 Introduction

Conventional thermoset polymers cannot be reprocessed or recycled due to the permanent crosslinking covalent network that causes problems with regard to their waste disposal. However, such covalent bonding polymers usually show extraordinary thermal and mechanical properties compared to traditional thermoplastic materials, because of which they are widely applied in the automotive and even aerospace sectors. Both epoxy and polyurethane (PU) are widely used in manufacturing industries at present, such as in producing coatings, adhesives, sealing materials and individual parts. Epoxy has outstanding adhesive behavior, good chemical resistance, and high mechanical strength, while suffering from brittleness and low elongation at break. In contrast, PU is flexible, elastic and exhibits impressive abrasive resistance, but has low strength. These unique properties inspire the widespread application of polyurethane across a whole host of sectors, ranging from automotive manufacturing to biomedical devices (1, 2). Incorporation of rubber polymers and epoxy emerged as early as 1970s (3). A lot of studies for Epoxy/Polyurethane interpenetrating polymer networks (IPN) emerged subsequently (4, 6). IPN integrates the properties of both PU and epoxy. Traditional PU is prepared by step polymerization of isocyanate and polyols. However, isocyanate is a highly toxic chemical for humans and environment, and thus contrary to the desire for achieving sustainable development. This has led to increased attention on new methods for processing non-isocyanate polyurethane (7, 8). Among those potential pathways, the novel procedure of reaction between cyclic carbonates and amines that are non-toxic and can be designed to be fully biodegradable (9), without using any toxic isocynates

monomers or additives, seems to be a promising alternative (10). Cyclic carbonate rings open, react with alkyl amines (or alcohols) and form hydroxyurethanes. Compared to traditional PU, Non-isocyanate Polyurethanes (NIPUs) possess improved thermal stability, as there are no thermally labile biuret and allophanate to dissolve in organic solvents, while showing higher stiffness and tensile strength (11). After the reaction between cyclic carbonate and alkyl amine is finished, hydroxyl groups are left in the molecule chain that can be further cross-linked with epoxy (12, 13).

Unlike thermoplastic polymers such as polyethylene, polypropylene, traditional epoxy is based on covalent crosslinking network, and the reaction process is irreversible (14). To investigate reprocessing and recyclability of epoxy as well as extend the useful life time of these crosslinked polymers, researchers have introduced reversible chemistry in this field through numerous mechanisms, such as transesterification (15), metathesis of olefins (16), transamination reaction (17) and siloxanes (18). All these mechanisms involve catalysts except transamination. Recently, disulfide covalent bond was introduced into epoxy to achieve self-healing by several researchers and gained a lot of attention due to its low requirement for stimuli. Xu et al. (19) synthesized new polyurethane materials with almost complete crack-healing properties while heating above 80 ℃, while also possessing shape memory effect. Imbernon et al. (20) achieved reprocessable natural rubber via using dithiodibutyric acid (DTDB) as a crosslinker to form DTDB-cured epoxidized natural rubber. Compared to other covalent bonds, such as –C-H, -C-C, -C-N, disulfide bond needs less energy to break, which makes it the first

bond to break when the sample was broken. Hence, moderate temperature is enough for disulfide bond to recombine.

With the introduction of epoxy resin composite into the automotive industry, epoxy resin composite waste management also becomes a rigorous problem (21, 22). Driven by environmental and economic concerns, recycling of epoxy attracts a lot of investigation for past decades, and most of these explorations focus on mechanical or chemical solvent-based fiber recovery (21). Reversible covalent bond can be introduced to overcome this problem from the basis. As is well known, mobility of polymer chain under ambient temperature is extremely limited, and the polymer chain re-crosslinking can be regarded as controlled by diffusion of polymer chain. Thus, chemical re-bonding process is affected by temperature, pressure and other outside factors. In other words, if re-bonding could happen at room temperature, then the crack can exhibit self-healing just after its formation, which extends the service time of the composite part, while helping achieve quicker healing rate at higher temperature.

In this study, a two-step synthetic strategy using non-isocyanate pathway to prepare polyurethane/epoxy copolymer crosslinked networks was introduced, which is also involved with disulfide bond to achieve recycling application. Their thermal and mechanical properties were studied. Reprocessing was monitored by Rubber Process Analyzer machine, which is also the first report to show real-time recycling process.

6.2 Materials and Experimental

6.2.1. Materials

Propylene Carbonate (M = 108 g mol^{-1}), Cystamine Dichlorohydride (M = 225.2 g mol^{-1}, 97 %), 1, 2-Dimethylimidazole (DMI, 98 %, M = 96.13 g mol^{-1}), Bisphenol A diglycidyl ether (DGEBA, M = 340.41 g mol^{-1}), and Sodium Hydroxide (NaOH, M = 40.0 g mol^{-1}) were purchased from VWR, USA. All chemicals were used in as-obtained state without subsequent processing. DI water was used as the aqueous solution for reaction.

6.2.2. Preparation of monomer 3a

Monomer 3a was obtained from the condensation of Propylene Carbonate and Cystamine in water. 0.1 mol Cystamine was added to 50 ml water in a 100 ml glass beaker. 0.2 mol NaOH was added to the mixture and stirred for 30 min. 0.2 mol Propylene Carbonate was then added to the solution and stirred for 2 h at room temperature. The reaction was terminated when complete conversion was indicated by FTIR measurements. The reaction mixture was centrifuged for 10 min under 4000 RPM and supernatant was collected. The supernatant was then vacuum dried for overnight at 60 ℃. The resultant liquid was pure monomer 3a, which was used for synthesis of 5a without any further purification.

6.2.3. Preparation of monomer 3b

Monomer 3b was obtained from the condensation of Propylene Carbonate and Hexamethylenediamine. Propylene Carbonate and Hexamethylenediamine were added to a glass beaker with molar ratio as 2:1. The mixture was heated to 50 ℃ for stirred till the completion of the reaction as measured by FTIR. The resultant product was white and solid under room temperature.

6.2.4. Preparation of copolymer 5a and 5b

Synthesis of 5a (or 5b) was based on the mechanism shown in Scheme 1. 3a (or 3b) and DGEBA were added in a beaker at molar ratio of 1:1. The mixture was placed on a 60 ℃ hot plate and stirred for 10 min. 1 wt. % DMI was added and mixed well to it. The mixture was transferred to silicon mold and heated at 80 ℃ for 8 h. The cured product specimen was prepared in this way.

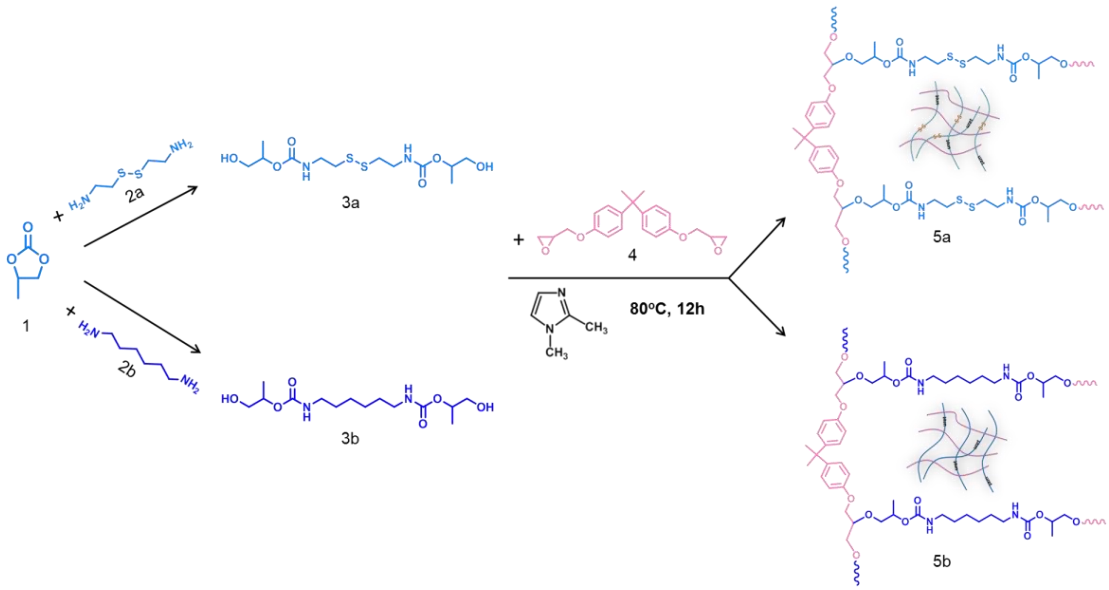

Scheme 6.1 Pathways towards synthesis of 3a, 3b, 5a and 5b

6.2.5. Material characterizations

6.2.5.1. Thermal and Mechanical characterization

TGA and DTG data were collected by TA Q5000 from 25 ℃ to 600 ℃ at heating rate of 10 ℃/min. Tensile modulus of the copolymer was measured using Instron 5500R1125 at room temperature. Statistical average of the measurements on at least five test specimens was taken to obtain the mean value for all tests. Dynamic mechanical tests were carried out on TA Q800. DMA specimens were rectangular shaped with dimensions of 50 mm x 8 mm x 1 mm. Testing was carried out between -100 ℃ and 100 ℃ in 3-point-tension mode in nitrogen atmosphere at 0.1 % amplitude and frequency of 1 Hz.

6.2.5.1. Spectroscopy

FTIR spectra were recorded on Thermo 6700 FTIR at wavelengths ranging from 500cm^{-1} to 4500 cm^{-1}. The number of scans per one recording was 16 and the resolution was 2 cm^{-1}. XPS spectra were recorded on Kratos axis ultra XPS.

6.2.5.1. Curing Dynamics

Curing rheology of 5a and 5b was studied by TA Rubber Process Analyzer. The pressing pressure was 1 bar and 0.1 °rotational angle with 1 Hz frequency.

6.3 Results and Discussion

6.3.1. FTIR and XPS spectra analysis

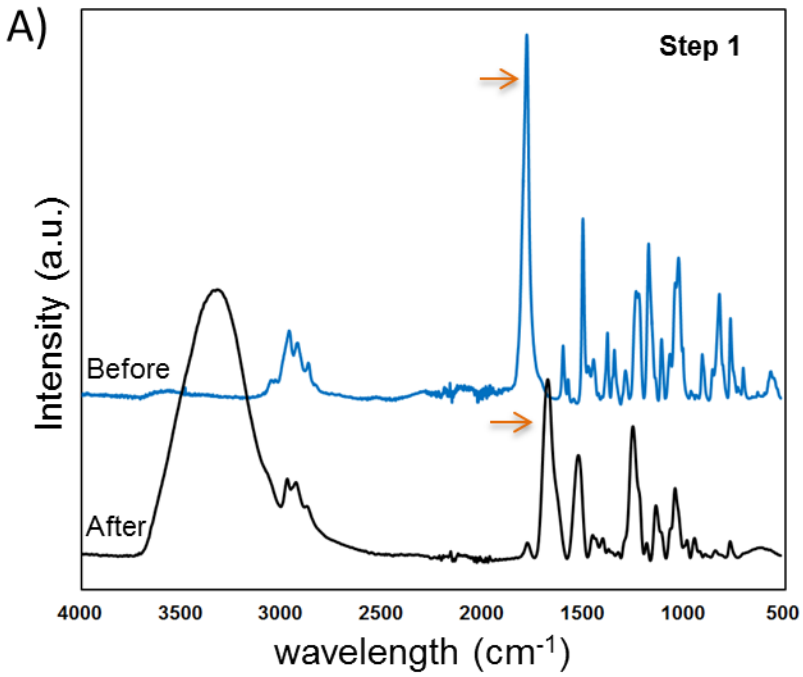

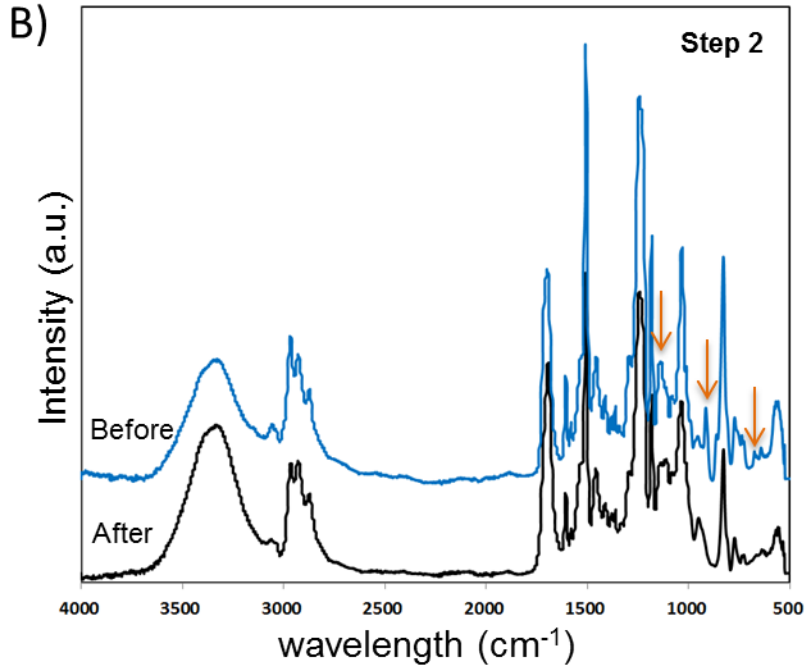
B)
Step 2
Intensity (a.u.)
Before
After
4000
3500
3000
2500
2000
1500
1000
500
wavelength (cm-1)

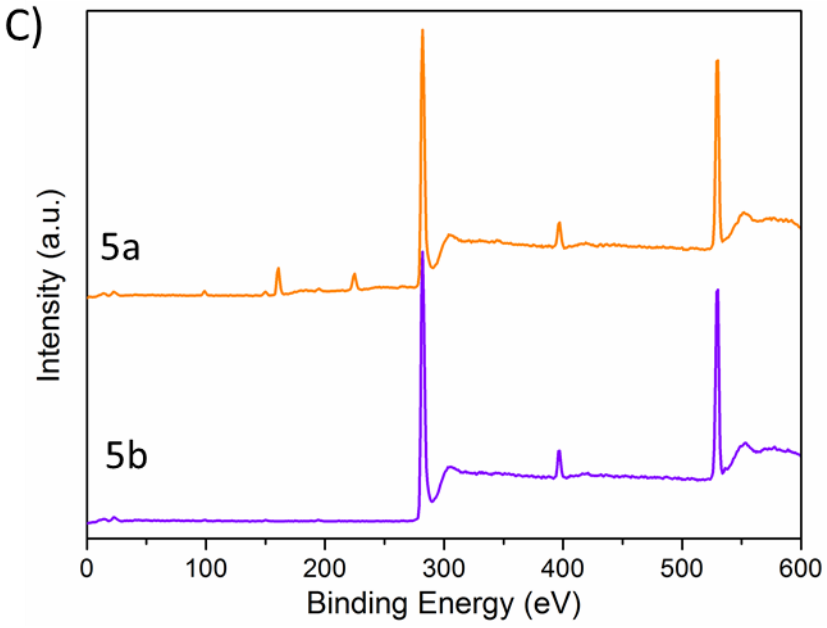
C)
Intensity (a.u.)
5a
5b
0
100
200
300
400
500
600
Binding Energy (eV)

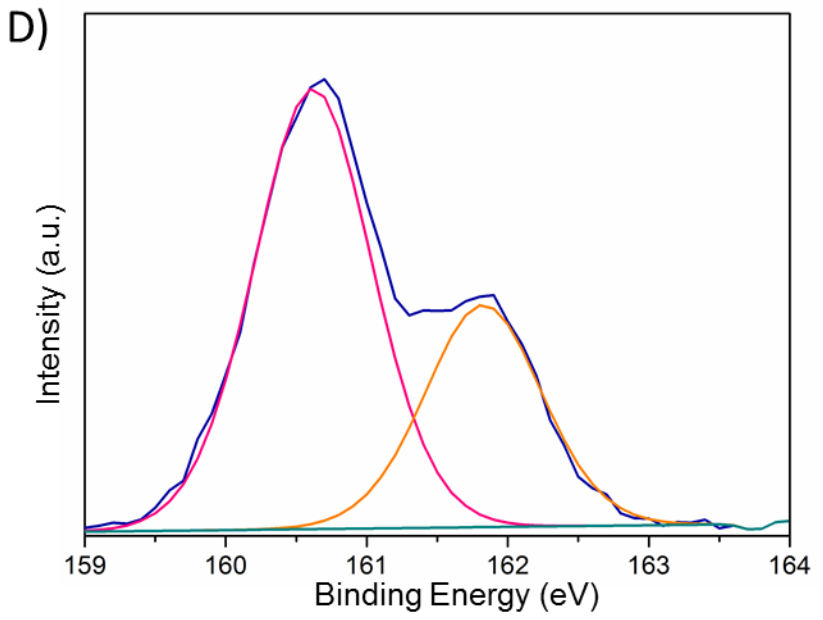

Figure 6.1 FTIR and XPS spectra. A): FTIR spectra for first step reaction of carbonate and diamines 3a. B): FTIR spectra for second step reaction, which is the crosslinking network formation 5a. C): XPS spectra of 5a and 5b. D): S-deconvoluted peak of 5a in the XPS spectra.

Monomers 3a and 3b were synthesized by the carbonate ring opening reaction of Propylene carbonate and diamine under proper pH environment. Formation of urethane group and disappearance of cyclic carbonate group during the reaction were monitored by FTIR, as indicated in Figure 6.1 A). The peak at 1785 cm^{-1} corresponds to the stretching of O-C-O in cyclic carbonate group, which almost disappeared after the reaction completed. Meanwhile, a new peak centered at 1677cm^{-1} appeared after the reaction. This peak corresponds to O=C-N stretching in the urethane group. These changes confirmed the occurrence of successful condensation reaction between Propylene Carbonate and

Cystamine. Fig 6.1 B) shows the difference in functional groups prior to and after crosslinking of 3a by DGEBA. Disappearance of the absorbance peaks centered at 914cm^{-1} could be used to monitor the conversion of epoxy groups. This peak corresponds to C-O-C stretching in DGEBA, which means that all the epoxy rings opened and crosslinked in the polymer networks. The decrease of peak centered at 1240 cm^{-1} refers to the stretching of –OH. It shows that the concentration of –OH decreased after curing.

Fig. 6.1 C) shows the XPS spectra of 5a and 5b. The peak centered at BE = 161 e.v. is responsible for element S and its existence in 5a but not in 5b is evidence that disulfide bond was present even after reaction in 5a. In other words, there is no disulfide bond in 5b, which illustrates the reason why 5b cannot achieve self-healing.

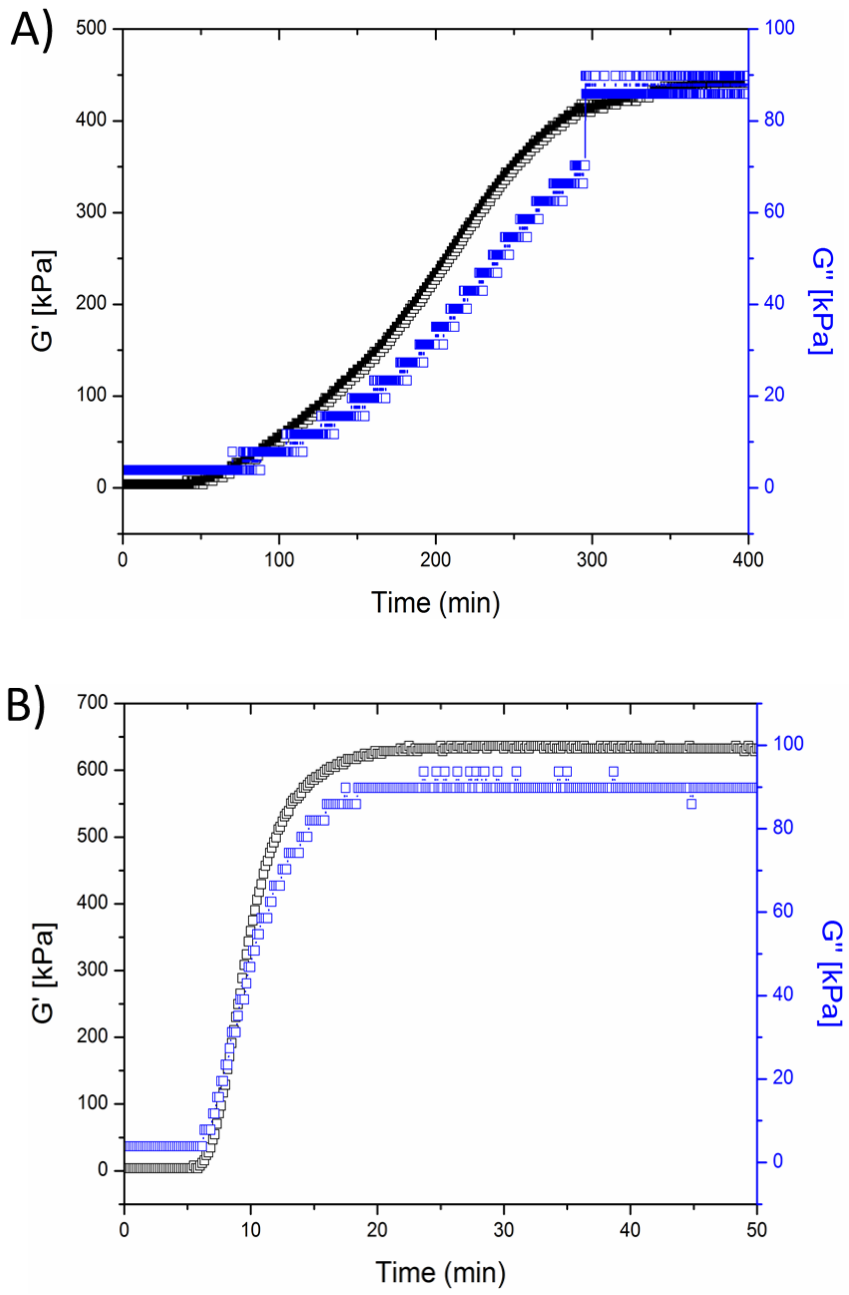

Figure 6.2 Rheometer curing study for A) 5a and B) 5b

Figure 6.2 shows rheometer curing of 3a (or 3b) and DGEBA to form 5a (or 5b) under 100 ℃ until its maximum torque was reached. According to Fig. 6.2 A, the mechanical modulus reaches a plateau at about 350 min, which indicates that polyurethane/epoxy system has reached glassy state. The transition to glassy state occurs gradually as the number of crosslinks rises and molecular mobility becomes increasingly restricted. Similar behavior was observed for 3b and DGEBA just 20 min after the curing started. Several factors, like molecular weight and viscosity, caused the curing time of 5a system to be much longer than that of 5b system. On the other hand, final storage modulus of 5a (450 KPa) was smaller than 5b (650 KPa). This difference was mainly because of the existence of disulfide bond in 5a. Reduction in mechanical properties was also reported in previous disulfide bond-based thermoset materials. (23)

6.3.2. Thermal properties

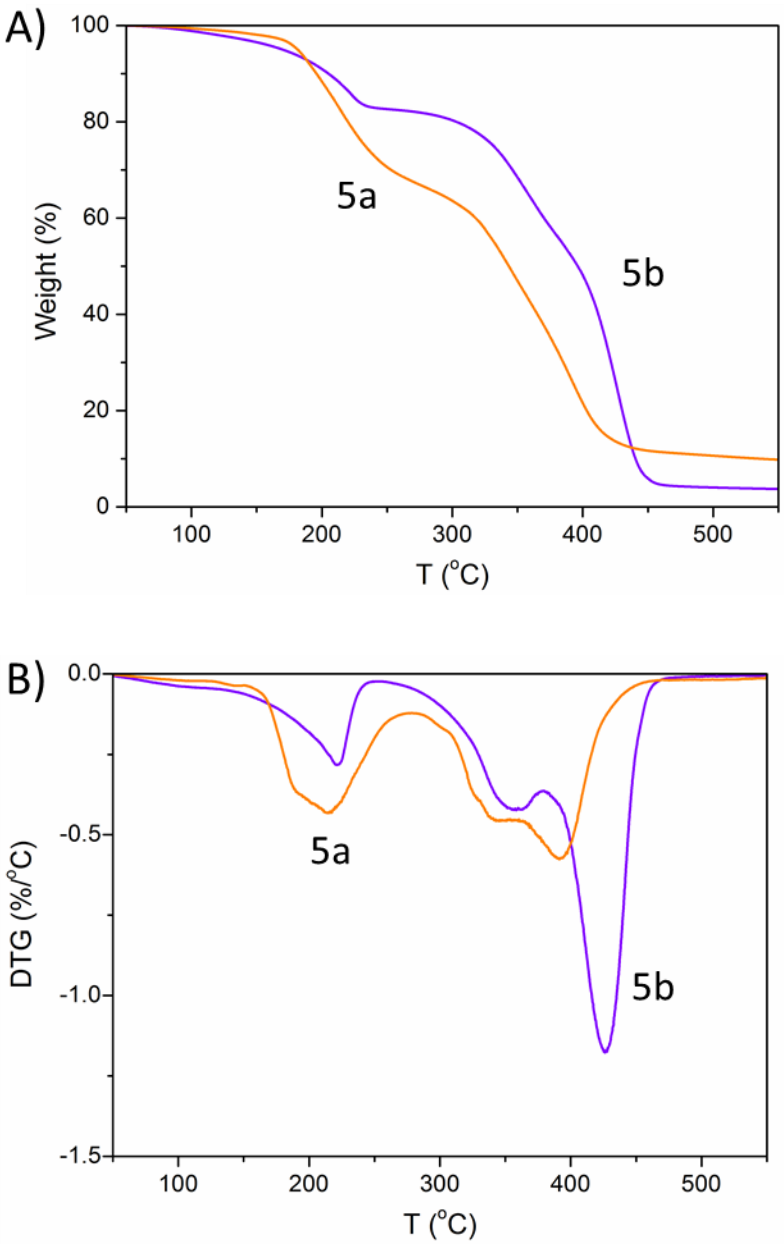

Figure 6.3 TGA and DTG curves of sample 5a and 5b

Table 6.1 TGA and DMA data of the sample 5a and 5b

Sample	T2 % (^{o}C)	Tmax (^{o}C)	% Char (T = 550^{o}C)	Tanδ (^{o}C)	G' /100^{o}C (MPa)
5a	153	394	9.9	50	450
5b	126	428	3.7	60	650

To test whether disulfide bonds result in compromise on thermal stability, the materials were analyzed using TGA. Fig. 3 shows TGA and DTG curves for cured materials. They are observed to be similar for samples 5a and 5b, and all these curves can be divided into three stages. In stage I, a significant weight loss at around 200 ℃ was observed and attributed mainly to the loss of absorbed humidity in the samples. For sample 5a, the weight loss was also partly due to disulfide bond degradation. Both 5a and 5b showed good water absorption. Stage II was observed in DTG curves as a small peak around 325 ℃ to 350 ℃, and is mainly caused by the weight loss of small fragments. Stage III showed onset temperature ～300 ℃. Thermal degradation of urethane linkages and formation of –NCO, primary amines, secondary amines, and the crosslinked network took place in this stage, as found in a previous study (24). In Table 1, thermo-gravimetric parameters have been shown.

6.3.3. Dynamic Mechanical Analysis

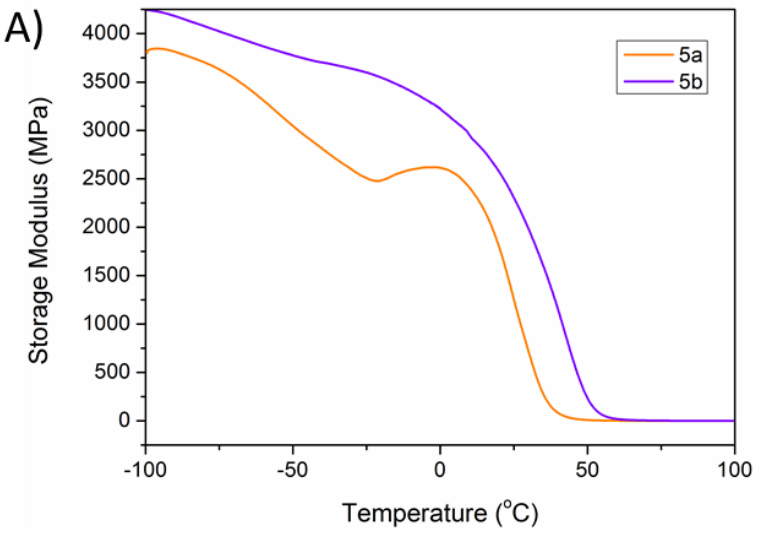
A)
Storage Modulus (MPa)
4000
3500
3000
2500
2000
1500
1000
500
0
-100
-50
0
50
100
Temperature (°C)
5a
5b

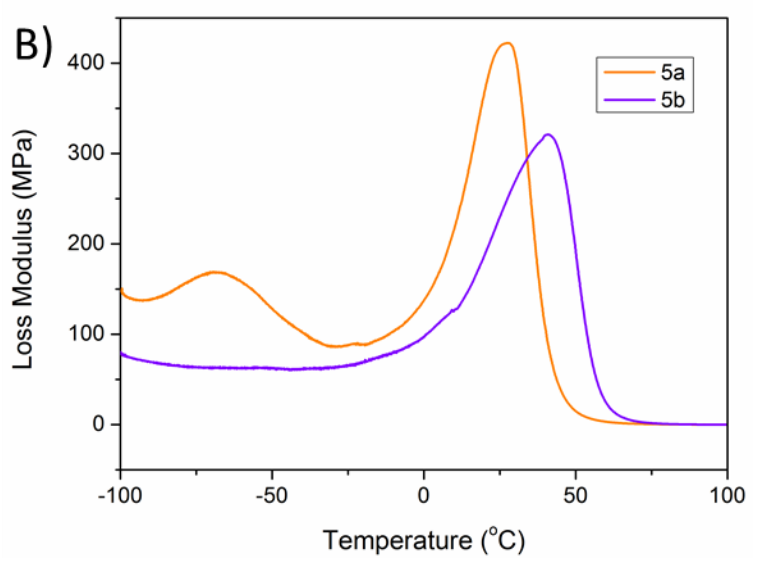
B)
Loss Modulus (MPa)
400
300
200
100
0
-100
-50
0
50
100
Temperature (°C)
5a
5b

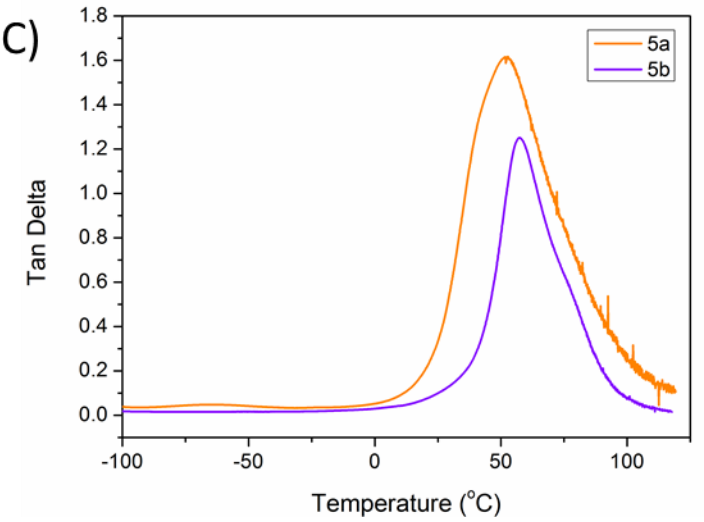

Figure 6.4 DMA plot, storage modulus (A), loss modulus (B) and tan delta (C) of sample 5a and 5b

Dynamic mechanical spectra in the form of plots of storage modulus (E'), loss modulus (E'') and loss factor (tan δ) as functions of temperature are shown in Figure 4 to study thermo-mechanical properties of 5a and 5b. As can be seen, storage modulus of NIPU/Epoxy copolymer without disulfide bonds sample 5b showed decrease with increase in temperature, which is due to the softening of polymer chains by heat. Addition of disulfide bonds to the crosslinked network reduced storage modulus. This result is in accordance with the Rheometer crosslinking result. The temperature at which loss factor curve showed a maximum peak was considered to be glass transition temperature (T_g). According to Fig. 4C, addition of disulfide bonds reduced T_g from 60 ℃ to 50 ℃. This observation proves the fact that addition of disulfide bonds compromises on mechanical and thermal properties.

6.3.4. Tensile properties and reprocess cycles study

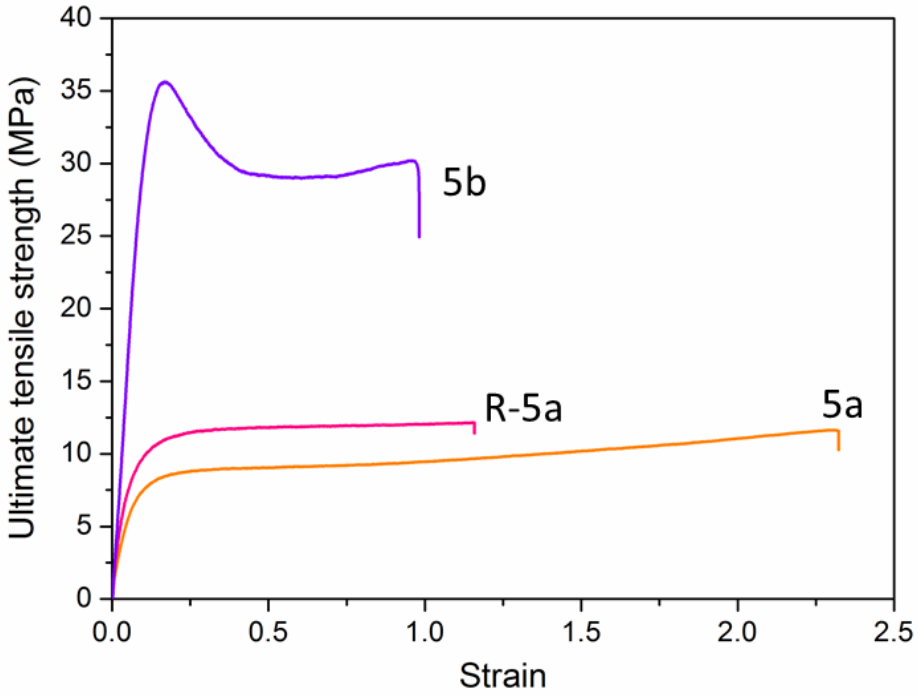

Figure 6.5 Typical strain-stress curves of 5a, 5b and R-5a

Table 6.2 Tensile properties of 5a, 5b, R-5a and R-5b.

Samples	Tensile strength (MPa)	Elongation at break (%)	Young's modulus (MPa)
5a	10.28±2.41	149±64	173±50
5b	33.65±3.71	17±1	352±66
R-5a	12.02±1.79	55±5	180±14
R-5b	-	-	-

Tensile experiments were carried out by an Instron 5500R1125 Electric Universal Machine. Tensile strength, elongation at break, and Young's modulus data are summarized in Table 6.2. As reported, crosslinking density largely affects elongation at break and tensile strength (25). It was observed in this study that the original samples 5a and 5b exhibited totally different strain-stress curves. Ultimate tensile strength of 5a was found to be much smaller than 5b, which again confirms the Rheometer curing data and DMA result that addition of disulfide bonds compromises on mechanical properties of the polymer. Sample 5a showed large elongation (as high as 149 %), which reduced dramatically upon reprocessing, as shown in R-5a curve. This fact may be attributed to the fact that curing density reduces after initial curing. After reprocessing, crosslinking density showed an increase, which also induced increase in ultimate tensile strength. In contrast, sample 5b showed large plastic deformation region, which is different than

traditional epoxy or polyurethane polymers. According to previous studies, it means that sample 5b possesses crystalline part in the matrix (26). This NIPU/Epoxy copolymer shows pretty different properties than other thermoset materials.

6.3.5. Properties tuning

Table 6.3 Ultimate tensile strength, elongation at break and Young's modulus results for samples with different 3b/epoxy monomer ratios

molar ratio		Tensile strength (MPa)	Elongation at break (%)	Young's modulus (MPa)
3b	epoxy			
1	1.0	33.65±3.71	17.0±1.0	352±66
1	1.4	54.97±2.16	17.3±2.2	469±32
1	1.6	81.91±1.36	23.7±2.3	742±57
1	1.8	73.37±10.92	19.0±3.5	695±43
1	2.0	74.96±12.87	20.5±2.2	661±58

Mechanical properties of different monomer ratios (3b/epoxy) have been summarized in Table 6.3. The tested 3b-to-epoxy (DGEBA) molar ratios were 1.0, 1.4, 1.6, 1.8 and 2.0. With higher epoxy ratios, ultimate tensile strength first showed an

increase and then showed minor decrease. The same trend was observed in Young's modulus results. When the 3b/epoxy ratio reaches 1/1.6, the maximum ultimate tensile strength was reached (81.91 ± 1.36 MPa), which is an interesting phenomenon as the elongation at break shows no significant difference for all samples.

6.3.6. Reprocess test

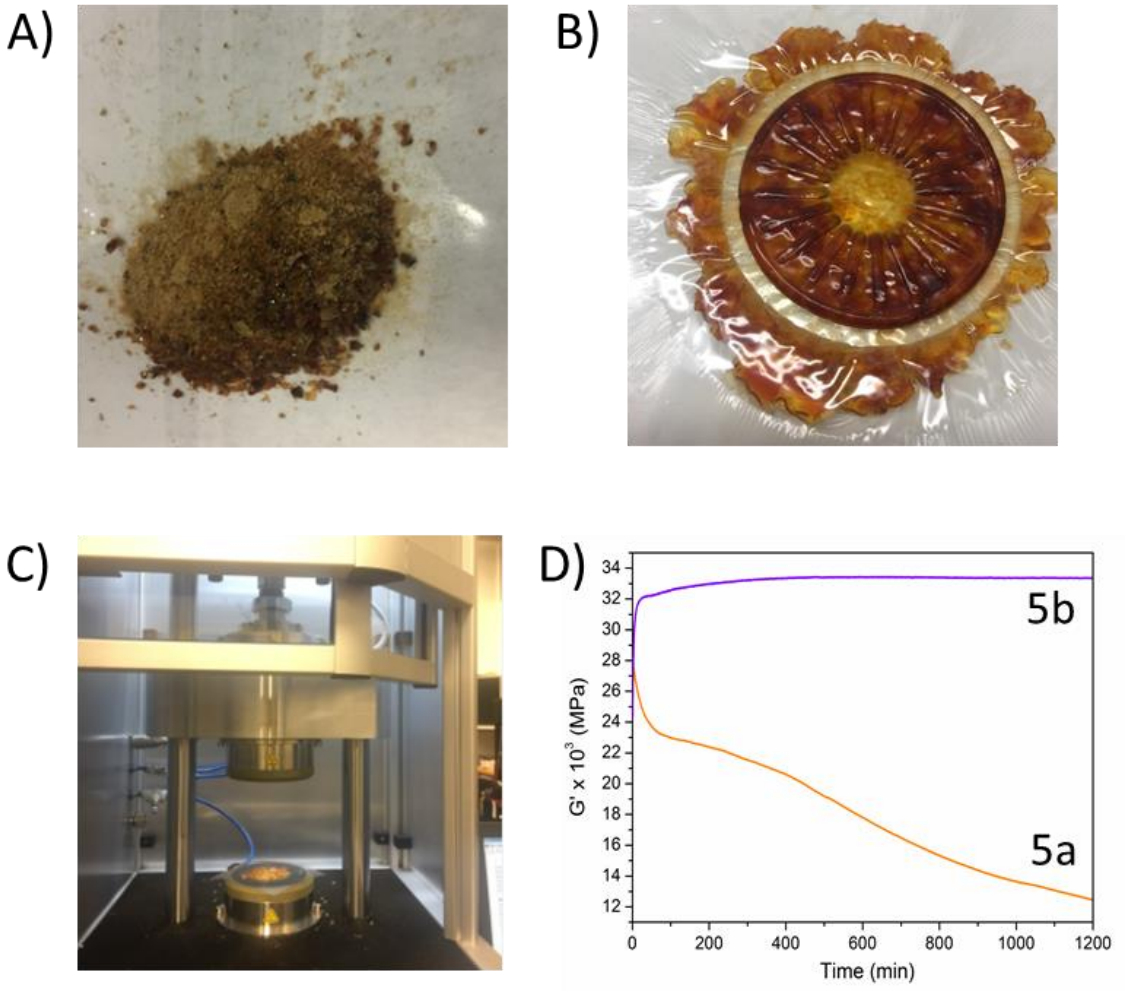

Figure 6.6 SEM images of A) 5a powder and B) reprocessed 5a (R-5a) C) Rubber Process Analyzer machine D) Storage modulus change during reprocessing of sample 5a and 5b.

After testing mechanical properties, samples 5a and 5b were finely ground to powder and reprocessing was finished by placing the powder at a rubber process analyzer

under 1 bar at room temperature for 20 h, at frequency of 1 Hz and strain of 0.1^{o}. Figure 6.6 (A) shows the ground powder of 5a, which is not uniform in size. Figure 6.6 (B) shows reprocessed sample 5a after pressing in room temperature for 20 h. The image clearly shows that sample 5a powder become a whole piece similar to the original color. Figure 6.6 (C) is the Rubber Process Analyzer machine with sample placed between the testing equipment. Recycling process data is summarized in figure 6.6 (D). Storage modulus of reprocessed 5a kept reducing during this time, and sample 5b showed almost similar value of G'. As shown, the modulus decreased when small 5a particles joined together. In contrast, sample 5b maintained the same modulus during this process, and the outcome also showed no rejoining between small particles at all. These results indicate that when disulfide bond was introduced to polyurethane/epoxy networks, reprocessing was also achievable for this thermoset material. Disulfide bond was broken during the grinding process and rejoined when pressed for reprocessing.

6.4 Conclusion

We have developed a two-step synthetic strategy using non-isocyanate pathway to prepare polyurethane/epoxy copolymer crosslinked networks, which was also introduced with disulfide bond to achieve the recycling application. Mechanical and thermal properties of the polymer can be tuned by controlling monomer functional groups, monomer ratios and crosslinking percentage. Moreover, the resultant crosslinked network polymers can undergo reprocessing at room temperature. Recycled samples possess

higher tensile strength than original samples with much smaller elongation. This strategy shows the potential to prepare recyclable polyurethane/epoxy copolymer networks with tunable properties, which is beneficial for the current polyurethane and epoxy industry. The network synthesis process is fully sustainable with the non-isocyanate pathway to prepare urethane monomers. The starting monomers of carbonate, diamine and epoxy can be also produced from bio-based methods. In general, this innovative approach for polymer network formation provides advantages ranging from sustainable resources and methods to tunable properties as well as crosslinked network recycling.

ACKNOWLEDGMENTS

The authors are grateful to Kimberly Ivey for her assistance in conducting TGA and FTIR tests.

REFERENCES

(1) Broos, R.; Herrington, R.; Casati, F. Endurance of polyurethane automotive seating foams under varying temperature and humidity conditions. *Journal of Cellular Plastics* **2000**, *36*, 207-245.

(2) Niu, Y.; Stadler, F. J.; Song, J.; Chen, S.; Chen, S. Facile fabrication of polyurethane microcapsules carriers for tracing cellular internalization and intracellular pH-triggered drug release. *Colloids and Surfaces B: Biointerfaces* , DOI: http://dx.doi.org/10.1016/j.colsurfb.2017.02.018.

(3) Bucknall, C. B.; Yoshii, T. Relationship between structure and mechanical properties in rubber‐toughened epoxy resins. *Polym. Int.* **1978**, *1*0, 53-59.

(4) Vabrik, R.; Czajlik, I.; Tury, G.; Rusznak, I.; Ille, A.; Vig, A. A study of epoxy resin–acrylated polyurethane semi‐interpenetrating polymer networks. *J Appl Polym Sci* **1998**, *6*8, 111-119.

(5) Sharmin, E.; Ashraf, S.; Ahmad, S. Synthesis, characterization, antibacterial and corrosion protective properties of epoxies, epoxy-polyols and epoxy-polyurethane coatings from linseed and Pongamia glabra seed oils. *Int. J. Biol. Macromol.* **2007**, *4*0, 407-422.

(6) Park, S.; Jin, J. Energetic studies on epoxy–polyurethane interpenetrating polymer networks. *J Appl Polym Sci* **2001**, *8*2, 775-780.

(7) Kihara, N.; Kushida, Y.; Endo, T. Optically active poly (hydroxyurethane) s derived from cyclic carbonate and L‐lysine derivatives. *Journal of Polymer Science Part A: Polymer Chemistry* **1996**, *3*4, 2173-2179.

(8) Delebecq, E.; Pascault, J.; Boutevin, B.; Ganachaud, F. On the versatility of urethane/urea bonds: reversibility, blocked isocyanate, and non-isocyanate polyurethane. *Chem. Rev.* **2012**, *11*3, 80-118.

(9) Anastas, P.; Eghbali, N. Green chemistry: principles and practice. *Chem. Soc. Rev.* **2010**, *3*9, 301-312.

(10) David, M. J. *Hydroxy carbamates and process of producing same* **1953**.

(11) Figovsky, O. L.; Shapovalov, L. D. Features of reaction amino‐cyclocarbonate for production of new type nonisocyanate polyurethane coatings. *Macromolecular Symposia.* **200**2, 187, 325-332.

(12) Tundo, P.; Perosa, A.; Zecchini, F. *Methods and reagents for green chemistry*; Wiley Hoboken, NJ: **2007**; .

(13) Bähr, M.; Bitto, A.; Mülhaupt, R. Cyclic limonene dicarbonate as a new monomer for non-isocyanate oligo-and polyurethanes (NIPU) based upon terpenes. *Green Chem.* **2012**, *1*4, 1447-1454.

(14) Kuang, T.; Chen, F.; Fu, D.; Chang, L.; Peng, X.; Lee, L. J. Enhanced strength and foamability of high-density polyethylene prepared by pressure-induced flow and low-temperature crosslinking. *RSC Advances* **2016**, 6, 34422-34427.

(15) Montarnal, D.; Capelot, M.; Tournilhac, F.; Leibler, L. Silica-like malleable materials from permanent organic networks. *Science* **2011**, *334*, 965-968, DOI: 10.1126/science.1212648 [doi].

(16) Connon, S. J.; Blechert, S. Recent developments in olefin cross‐metathesis. *Angewandte Chemie International Edition* **2003**, *42*, 1900-1923.

(17) Denissen, W.; Rivero, G.; NicolaÿR.; Leibler, L.; Winne, J. M.; Du Prez, F. E. Vinylogous urethane vitrimers. *Advanced Functional Materials* **2015**, *25*, 2451-2457.

(18) Zheng, P.; McCarthy, T. J. A Surprise from 1954: siloxane equilibration is a simple, robust, and obvious polymer self-healing mechanism. *J. Am. Chem. Soc.* **2012**, *134*, 2024-2027.

(19) Xu, Y.; Chen, D. A Novel Self‐Healing Polyurethane Based on Disulfide Bonds. *Macromolecular Chemistry and Physics* **2016**.

(20) Imbernon, L.; Oikonomou, E.; Norvez, S.; Leibler, L. Chemically crosslinked yet reprocessable epoxidized natural rubber via thermo-activated disulfide rearrangements. *Polymer Chemistry* **2015**, 6, 4271-4278.

(21) Pimenta, S.; Pinho, S. T. Recycling carbon fibre reinforced polymers for structural applications: Technology review and market outlook. *Waste Manage.* **2011**, *31*, 378-392.

(22) Yebi, A.; Ayalew, B.; Pilla, S.; Yu, X. Model-Based Robust Optimal Control for Layer-By-Layer Ultraviolet Processing of Composite Laminates. *Journal of Dynamic Systems, Measurement, and Control* **2017**, *139*, 021008.

(23) Xu, Y.; Chen, D. A Novel Self‐Healing Polyurethane Based on Disulfide Bonds. *Macromolecular Chemistry and Physics* **2016**.

(24) Javni, I.; Petrović, Z. S.; Guo, A.; Fuller, R. Thermal stability of polyurethanes based on vegetable oils. *J Appl Polym Sci* **2000**, *77*, 1723-1734.

(25) Nielsen, L. E. Cross-linking–effect on physical properties of polymers. **1969**.

(26) G'sell, C.; Hiver, J.; Dahoun, A. Experimental characterization of deformation damage in solid polymers under tension, and its interrelation with necking. *Int. J. Solids Structures* **2002**, *39*, 3857-3872.

CHAPTER SEVEN

SYNTHESIS, ACTIVATION AND APPLICATION OF POLYMER CRYSTAL NANOSHEETS WITH HIGH SURFACE AREA

ABSTRACT

An easy method to prepare graphitic material from synthesized polymer was described in this study. Polyazomethine was synthesized, activated at high temperature, referred to as nitrogen-doped carbon (NC) materials, and then used to purify water. TGA result directs the annealing temperature choice. Raman spectrum confirmed that the material is indeed graphite-similar, having G and D bands at 1584 cm-1 and 1337 cm-1, respectively. Here, Rhodamine B was used to represent the contamination in the water, and the material works efficiently to remove it from the water. The adsorption experiments and BET surface area measurements revealed that 750 ℃ or higher temperature is working efficient to anneal the material.

7.1 Introduction

The advent of graphene lead to a renewed interest in layered two dimensional (2D) material systems. The interest in graphene stems from its fascinating properties including its distinctive band structure, high crystal integrity, high optical absorptivity, tremendous surface area, and exceptional electronic and thermal transport characteristics. (1), which make graphene a fascinating materials with plausible applications in electronics, gas sensors, batteries, supercapacitors, catalyst, biology, and water purification. (2, 3) While

graphene can be considered as the mother of related carbon-based structures such as 3D graphite, carbon nanotube, fullerenes, etc. the lack of a bandgap limits utility, especially when considered for transistor-based electronic applications. Introduction of dopant into graphene matrix is one of the most explored strategy to enhance its properties. Among various dopants, doping graphene with nitrogen is effective to enhance the transport, electrocatalytic, and photoluminescence properties. (4-6). While various direct (CVD, arch discharge etc.) and indirect techniques for the synthesis of N-doped graphene is available, the lack of control over the position of nitrogen inclusion and low doping percentage limits the application guided engineering of this fascinating structures.

Recently, a new class of synthetic materials termed covalent organic frameworks (COFs) emerged with great compositional and structural flexibility. Unlike systems such as graphene, that require high temperature synthesis (≥1000 ℃), COFs can be synthesized through milder organic-chemistry-based techniques. The facile and moderate preparation conditions of COFs lead to greater internal structural flexibility and the opportunity for facile engineering of their molecular architecture including pore size, nature, chemical composition, and placement of functional groups. Such adaptability in design can be achieved by amalgamating the fundamental know-hows of chemistry, surface science, crystal engineering, and polymer technology. Hence, in COFs opportunities exist to integrate and assemble organic units into a predesigned framework with atomic precision. The basic building blocks of COF being light-weight, COFs generally possess low mass densities, high thermal stabilities, and consistent porosity. The design flexibility in COF also allows them to be in two- (2D) or three-dimensional (3D) form based on the building

blocks. When COF are restricted to take the form of 2D sheets they are considered as 2D COFs which can self-assemble to layered structures with periodically aligned columns. Such columnar structures are unique π systems which are difficult to fabricate typical covalent and/or noncovalent approaches. Due to the ordered packing, 2D COFs can conduct energy carriers in the stacking direction, rendering COFs viable candidates for π-electronic, optoelectronics, and photovoltaics applications. Unlike 2D COFS, 3D COFs with extended three dimensional framework that contain sp3 carbon or silane atoms are not generally conductive. However, 3D COFs typically will have high specific surface areas, high porosity, and low densities making them ideal substrates for gas storage, water remediation and catalyst support applications.

For most of the COFs, the basic building block can be considered as a conjugated polymer that can conduct charge carriers due to alternate single and double bonds structure. Due to their excellent electronic, optoelectronic, electrochemical, and non-linear optical properties (7) conjugated polymers attracted widespread interests. Poly(azomethine)s is special category of polycondensation polymer synthesized via reaction between triphenylamine and (heterocyclic) aromatic dialdehydes. Poly(azomethine)s (PAMs) are constructed of nitrogen containing hexagonal rings and the presence of azomethine bond (–N=C–) which is isoelectronic with vinyl analogue, facilitate charge transport through the polymers. Synthesis of PAMs is advantageous compared to traditional conjugated polymers because they can be synthesized through comparatively less expensive noncatalytic process with water as the only by-product. Another advantage of PAM is its highly tunable properties. For example, the bandgap of

the polymer can be easily tuned by changing the aromatic dialdehyde used in the condensation reaction. Polyazomethine, with its extended double bonded structure and associated carrier, chemical, and optical properties, are used as optical pH sensors, detectors, catalyst carriers and light-emitting diodes(7). Controlling the reaction conditions, it is possible to assemble polyazomethine to higher order superstructures. For example Kimura et al. (8) prepared needlelike crystals of polyazomethine through the polycondensation of p-phenylenediamine (PPDA) and 1,4-terephthaldehyde(TPA) in liquid paraffin at 180 ℃. Similarely, Yan et al. (9) synthesized disk-like and protuberance-surface balls of polyazomethine by dynamic exchange controlled reaction of PPDA, TPA and 3,5-Diamino-1,2,4-triazole (DAT), and 2-aminopyridine (AP).

Recent years witnessed a growth in PAMs-based COFs. Assembling of PAMs 2-D and 3-D macromolecular COFs can be carried out by connecting individual PAM chains through weak (such as π-π stacking) or strong interactions (such as covalent bonding) (10). Various PAM-based COF with diverse structure and properties were constructed using different chemical synthetic strategies. However, most of the studies focused on modifying the monomer (with $–NH_2$ and –CHO groups) chemical structures to show different polymer chain morphology, thus to formulate COFs with different porosity, structural regularity, and functionalities (11). While, PAMs in native form and as COFs found various application possibilities, unlike graphenic-materials, the full potential of PAMs remains to be explored. Especially, the phenyl-like ring structure with C=N in PAM could potentially be leveraged to create graphenic or graphite-like materials with tunable porosity, N-doping, and surface area. While various efforts in this direction

has resulted in structures with diverse morphology ranging from discs to highly porous network structures, creating a material system that closely resemble graphite and its perfectly planar sheets remained a challenge. Creating such a structure could lead to isolation of single sheet structures with regular C=N bonds could open up opportunities to unique graphene-like sheets with tunable chemistry and physical, catalytic and transport properties.

In this contribution, we report a novel path way to create graphite-like PAM-based COFs via condensation of p-phenylenediamine and terephthalaldehyde, the simplest of precursors. Unlike any other previously reported PAM-based COF, the as-synthesized PAMs upon drying self-assembled into a COF which closely resembled graphenic layers. The product from the high efficiency synthesis and rapid self-assembly process resembled a porous graphitic structures with individual graphenic planar sheets. The stacking mechanism and the polymer properties are explored. We also devised a facile annealing method to convert the COF to nitrogen-doped graphitic structures with tunable surface area. The annealed materials exhibit ultra-high surface area (~700 m^2/g). We also demonstrate the utility of the fabricated high surface area material for water purification. While this report confined the application to water purification, we expect the material to find high utility in various other area including, electronics or optoelectronics, catalysis, photovoltaics, etc. leading to greater utilization of PAM-based COFs.

7.2 Materials and Methods

7.2.1. Materials

All reagents were purchased from were purchased from commercial sources (VWR, USA) and used without further purification. Terephthalaldehyde, p-phenylenediamine, and methanol were purchased from VWR. Rhodamine B (98%) was purchased from Acros, USA. Deionized water was used in all experiments.

7.2.2. Synthesis of Polyazomethine

Here, 0.3M p-phenylenediamine and 0.3M terephthalaldehyde were dissolved in 150ml methanol separately and then mixed well in a glass beaker. The mixture was left in fume hood to evaporate the methanol. After the reaction finished and all methanol evaporated, the product was then washed with 200ml methanol on the filter paper. The product was then performed annealing processing under 300 ℃, 450 ℃, 600 ℃, 750 ℃ and 900 ℃ for 2 hours (the temperature increase and decrease rate were 10 ℃) under N2 flow. The final carbons were labeled as NC300, NC450, NC600, NC750 and NC900) and kept in dry condition before characterization and water purification measurement.

7.2.3. Material characterization

7.2.3.1. ATR-FTIR spectroscopy

Attenuated Total Reflectance Fourier Transform-Infrared (ATR-FTIR) Spectroscopy was performed on a Thermo-Nicolet Magna 550 FTIR spectrometer in

combination with a Thermo-SpectraTech Foundation Series Diamond ATR accessory with a 50 °angle of incidence.

7.2.3.2. Thermogravimetric analysis (TGA)

TGA measurement was performed using TGA Q5000 instrument. About 5.0 mg sample was heated from room temperature to 1000 ℃ with 10 ℃/min increasing rate under nitrogen atmosphere (25 mL/min) using Al_2O_3 pans.

7.2.3.3. SEM imaging

Surface morphology of polyazomthine, NC300, NC450, NC600, NC750 and NC900 was obtained using Scanning Electron Micrograph (SEM) (Hitachi, S-4800) at an accelerating voltage of 5.0 kV. The pristine polymer, NC300 and NC450 were coated with 2nm gold layer before imaging. The rest were imaged directly.

7.2.3.4. Transmission electron microscopy (TEM)

The TEM investigations for pristine polyazomethine and NC750 were finished with a Hitachi, HD-9500 instrument. The voltage was from 200KV to 500KV. Both the TEM image and live FFT information were collected. All materials are cast in the epoxy first and then cut to 80nm thickness sheets for observation.

7.2.3.5. X-ray Powder Diffraction (XRD)

Rigaku Ultima III X-ray diffractometer (XRD) equipped with a primary monochromator and Cu Kα source. The XRD patterns were collected with a step size of 0.05° in the 2θ angular range from 10° to 50° and an acquisition time of 2 h.

7.2.3.6. Raman spectroscopy

Raman measurements were performed on a Jobin Yvon Horiba – LabRam confocal Raman spectrometer equipped with an Olympus BX40 microscope. As a light source a 632 nm HeNe laser was used. The spectra were collected from 100 to 300 nm.

7.2.3.7. X-ray photoelectron spectroscopy (XPS)

The X-ray photoelectron spectroscopy was performed with Kratos axis ultra XPS.

7.2.4. Surface area measurement

Nitrogen adsorption isotherms were collected at -196 ℃ using a Quantachrom Autosorb 1Q apparatus. The samples were degassed at 100 ℃ overnight before adsorption measurement. The specific surface areas were calculated using the Brunauer-Emmett-Teller (BET) equation (P/Po=0.05-0.20).

7.2.5. Water purification capacity measurement

Batch adsorption experiments were carried out at room temperature to investigate the adsorption behaviors of rhodamine B to NC300, NC450, NC600, NC750 and NC900. The Rhodamine B water solution was prepared with a concentration of 0.132mg/ml.

1mg/ml, 2mg/ml, 3mg/ml and 6mg/ml pristine and annealed polyazomethine/ Rhodamine B solution were prepared and stirred (200rpm) under room temperature. The Rhodamine B concentration in the mixture was monitored by Ultraviolet-Visible spectrometer (UV-Vis) (VWR UV-6300PC Spectrophotometer). The mixture was centrifuged and supernatant was measured by the UV-Vis for every 10min. The total observation time was 1hour. The adsorption capacities of the adsorbents were calculated according to the equation of

Capacity of Rhodamine B/carbon material (mg/mg) = $\frac{\mathbf{A_o - A_t}}{\mathbf{A_o}} * \frac{\mathbf{C_R}}{\mathbf{C_{NC}}}$

Where, Ao and At represent the original and t time UV-Vis absorbance values.

CR and CNC are the concentration of Rhodamine B and nitrogen-doped carbon materials.

7.3 Results and discussion

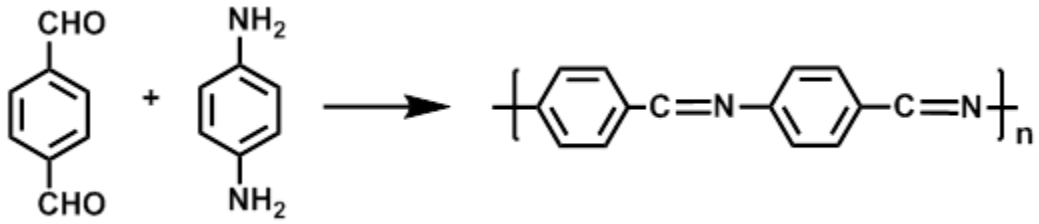

Figure 7.1 The reaction mechanism and product images

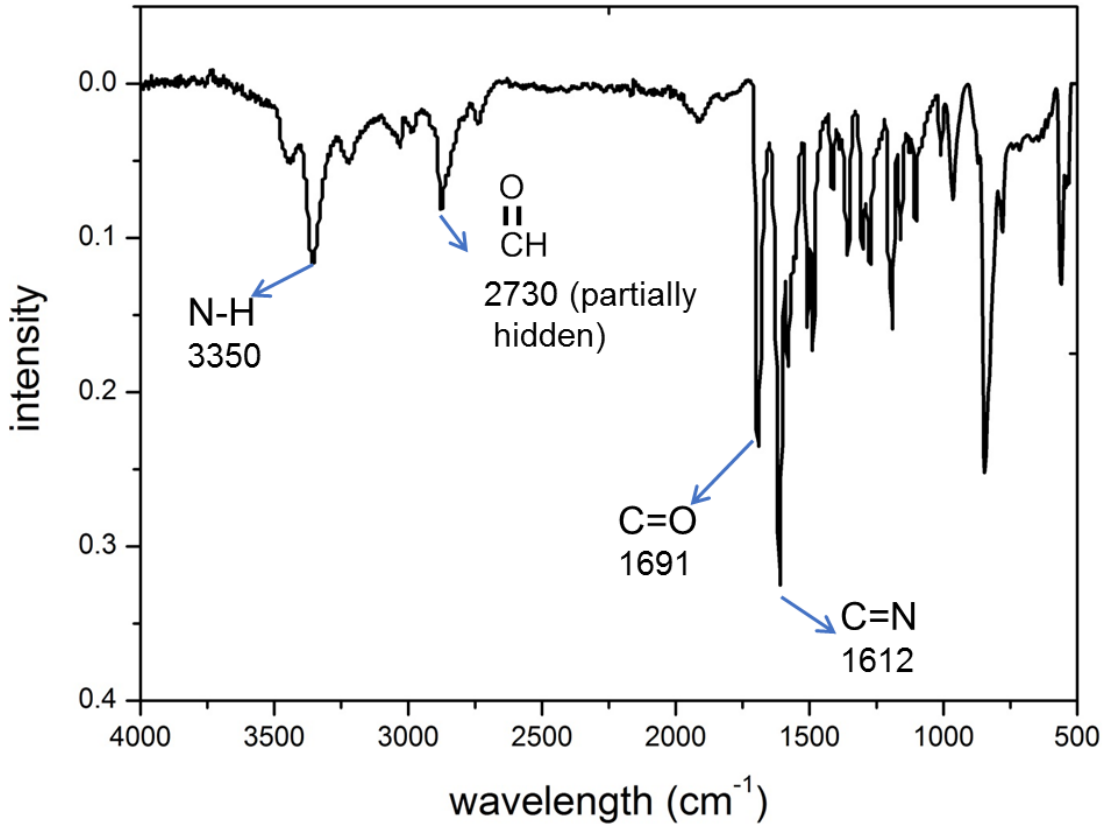

Figure 7.2 FT-IR spectrum of Polyazomethine

The formation of imine functional group is confirmed to be formed between p-phenylenediamine and terephthalaldehyde by FTIR spectra showed in Figure 7.2. The big band at ~1612 cm-1 in the spectrum corresponds to CH=N of azomethine, which is an evidence to show imine group formed during the condensation reaction. There is also a smaller band at ~1691 cm-1, which is responsible for unreacted aldehydes and synthesized polymer molecular chain ends. The ~2730 cm-1 peak is corresponding to the aldehyde stretching, which has partially hidden. The ~3350 cm-1 peak is attributed to the secondary amine stretching. The IR measurements show that polyazomethine was synthesized successfully, in the form of crystal, but the molecular weight is not quite high (12). The photos show the color of the polymer is orange and black after annealing.

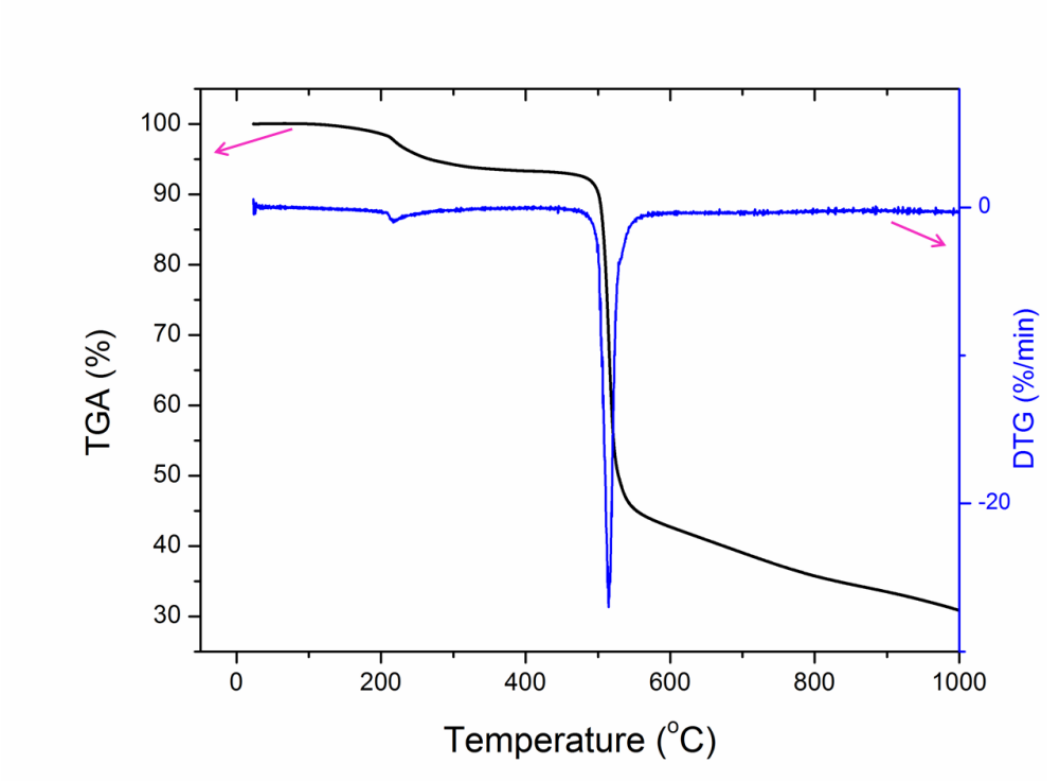

Figure 7.3 TGA and DTG curve for polyazomethine from 0 to 1000 ℃ under N_2

TGA was performed to study the thermal stability of Polyazomethine in the N_2 atmosphere from room temperature to 1000 ℃ (Fig. 7.3). The TGA curve shows two weight loss stages. The first stage starts at ~100 ℃ till ~300 ℃ with a plateau at ~214 ℃ in the DTG curve, which should be attributed to the release of adsorbed moisture and water formed by the further condensation reaction between p-phenylenediamine and terephthalaldehyde. The total weight loss during this stage is around 6.4%. This result is consistent with imine-linked amorphous and porous polymer (13, 14) It confirms that the amine and aldehyde are able to condense with heat treatment. The second giant and sharp mass loss of ~55% between ~440 ℃ and ~540 ℃ could be ascribed to the combustion of polymer in N_2, which matches well with previous study (15)

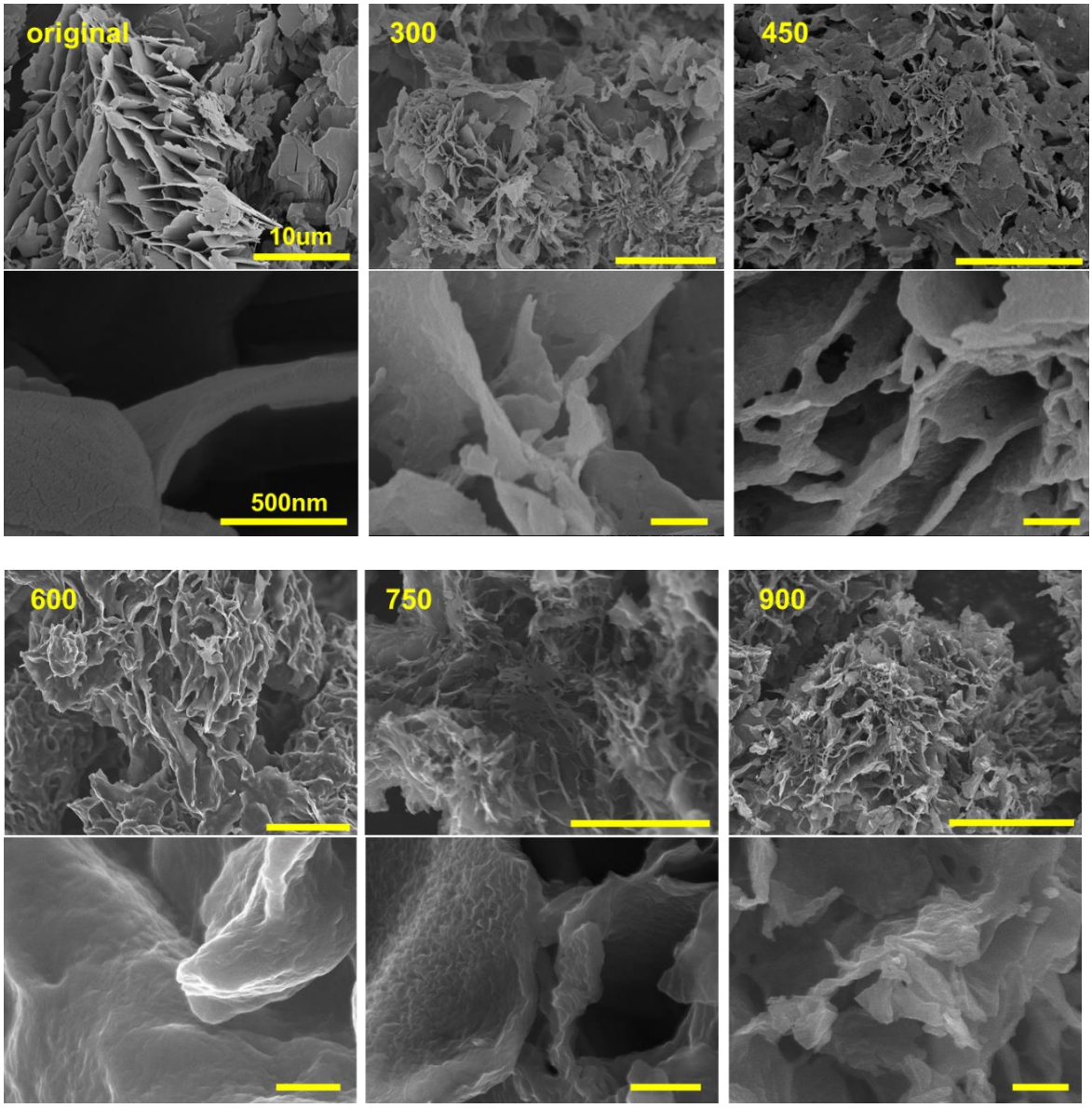

Figure 7.4 SEM images for the original synthesized polymer and the N-doped carbon materials annealed at 300 ℃, 450 ℃, 600 ℃, 750 ℃ and 900 ℃

Figure 7.4 shows the morphology of the original synthesized polymer and the N-doped carbon materials which is from synthesized polyazomethine annealed at 300 ℃, 450 ℃, 600 ℃, 750 ℃ and 900 ℃ under 10um and 500nm scale bars. The synthesized

polymer shows crystalline-similar structure and macro size porous morphology. The formation of this crystalline structure is due to the dynamic covalent chemistry controlled condensation reaction of p-phenylenediamine and terephthalaldehyde and the conjugation of the linear polyazomethine molecule chains during evaporation (16). As presented in SEM images, the N-doped carbon material shows nanosheet structure and the average nanosheet thickness is less than 50nm. In this way, all annealing resulting carbon particles possess thin nature and high aspect ratio structure. On the other side, obvious defected surface feature of the nanosheet was observed from the SEM images. Both of these features increase the surface area efficiently. Original polyazomethine shows a typical crystalline structure with nanosheet thickness less than 50nm. After annealing, this crystalline structure was destroyed and the nanosheet structure was kept. The formation of nanosheet surface defects results from the high temperature annealing activation, which reaches the maximum density in NC-750 sample. When the temperature is higher than 750 ℃, some defects on the samples became porous, which reduce the surface area. The NC-750 SEM image shows the high porous, amorphous and partially collapsed structure. These results are consistent with the trend of decreasing carbon yields by the increased activation temperature shown in TGA result and the following water purification data.

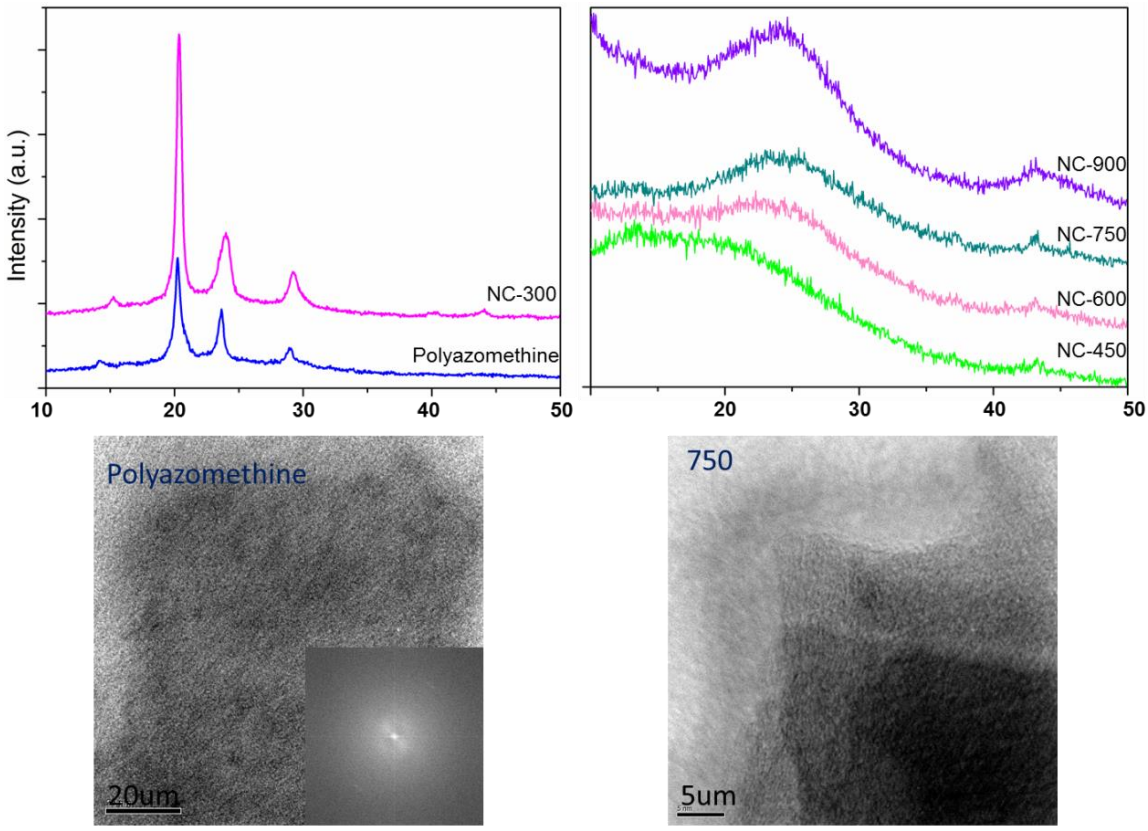

Figure 7.5 XRD and TEM spectra for polyazomethine, NC-300, NC-450, NC-600, NC-750, NC-900

The powder X-ray diffraction (XRD) patterns of pristine and Nitrogen-doped carbon materials from annealing polyazomethine under different temperatures are depicted in Figure 7.5. Four sharp peaks were observed in the polyazomethine and NC-300 at 2θ of 14.4 °, 20.3 °, 23.7 ° and 29.0 °, which is highly consistent with the results of polyazomethine crystalline structure reported by Pron et al (17) and Yamashita et al (18). These peaks are ascribed to (111), (110), (200) and (210) diffractions respectively. The crystalline structure was kept when the annealing temperature increased as high as 300 ℃. When the annealing temperature increases from 450 to 900 ℃, a very broadening peak

was observed in the XRD spectra centered at 2θ of ～24 °, which is attributed to (002) diffractions. Another much narrower peak was centered at 2θ of ～44 °and it is responsible for the (100) diffractions. The second peak achieved highest intensity compared to others for NC-900. These two bands indicate the formation of graphitic structure in the carbon materials for NC-450, NC-600, NC-750 and NC-900. The graphite percentage was achieved maximum when the annealing temperature was 900 ℃ (19).

Moreover, the high-resolution TEM (HRTEM) image and FFT result shows that the polyazomethine has high regulated structure. The NC-750 carbon materials also shows high regulate micropores. These high regulation structure results are in agreement with the XRD spectrums.

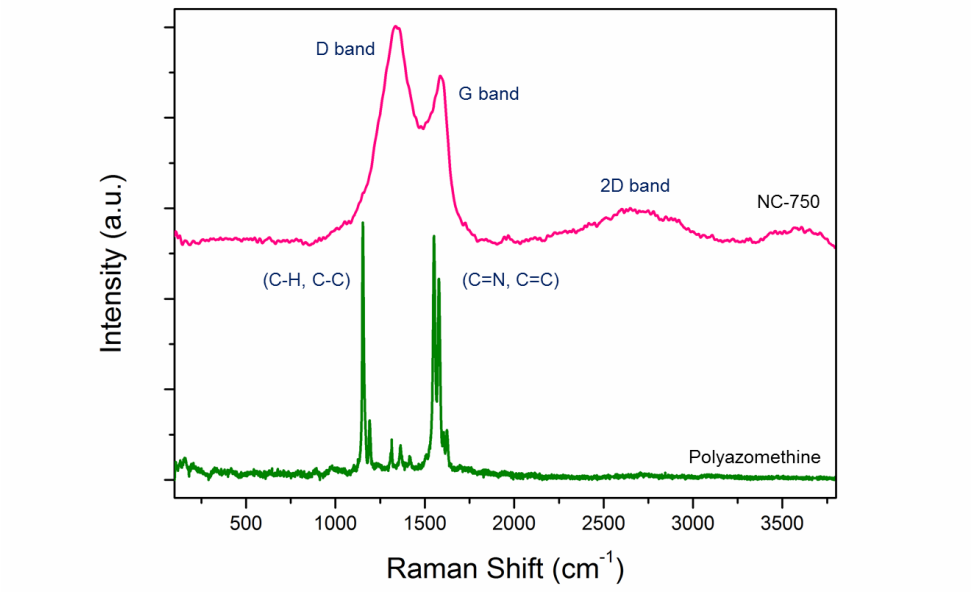

Figure 7.6 Raman spectra for polyazomethine and NC-750

Figure 7.6 shows the Raman spectrum of polyazomethine and NC-750. The NC-750 shows evidently D, G and 2D bands at 1337 cm-1, 1584 cm-1 and 2700 cm-1 respectively. The D band in NC-750 suggests the presence of high density defect sites, (20, 21) which increases the surface area efficiently, and it is beneficial for water purification. The G band at 1584 cm-1 suggests the formation of graphite-similar structure after high temperature annealing. The 2D band in NC-750 at 2700 cm-1 suggests the graphitic sp2 materials and shows the existence of single layer graphene-like structure in the materials. The Raman spectra of Polyazomethine further confirmed the imine group formed by condensation of p-phenylenediamine and terephthalaldehyde (22).

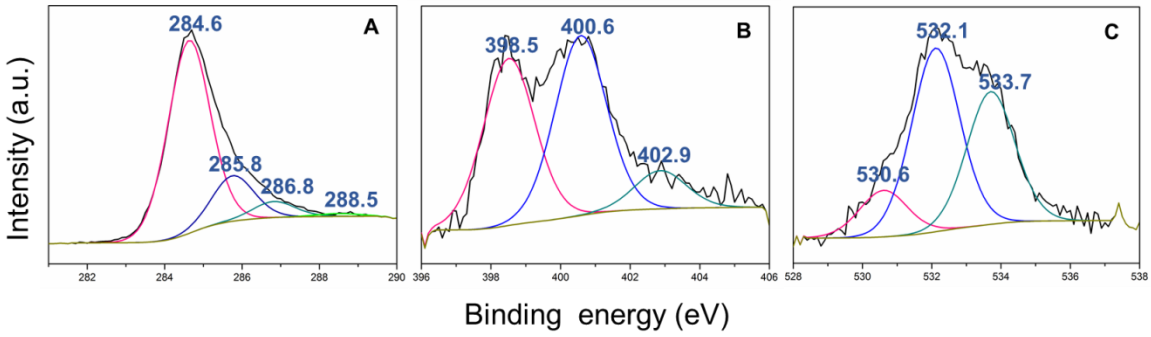

Figure 7.7 A, B and C show the deconvoluted XPS of carbon, nitrogen and oxygen, respectively (NC-750).

The existence of various functionalities is evident in the XPS spectrum shown in figure 7.7. The presence of high percentage of nonoxygenated C 1s (peak centered at 284.6 eV in figure 7.7A) is a sign of extended carbon backbone. Oxygenated C as C-O

(peak at 288.5 eV) is due to the presence of oxygen functionality. The peak of BE=284.6 is sp3 C. The peak centered at binding energy of 286.8eV shows the presence of C=N. It means amide group formed during the reaction. As well known, the peak of C-N is overlaid with C-O around the binding energy at BE=288.5eV. The presence of functional oxygen group is also responsible for water contamination adsorption (23)(24)(25). Deconvolution of the O 1s spectrum (figure 7.7 B) gives three components: the first component centered around 530.6eV, the second around 532.1 eV and the third around 533.7 eV, they are corresponding to N-C=O, C=O and C-O entities, respectively. The N 1s peaks are centered at 398.5eV, 400.6eV and 402.9eV, and they are expected to represent the -N=C-, -N+H- and =N+H- functional groups. The NC-750 XPS results confirmed that imine group was formed in original synthesized polymer and it demonstrated successful doping of N into carbon materials.

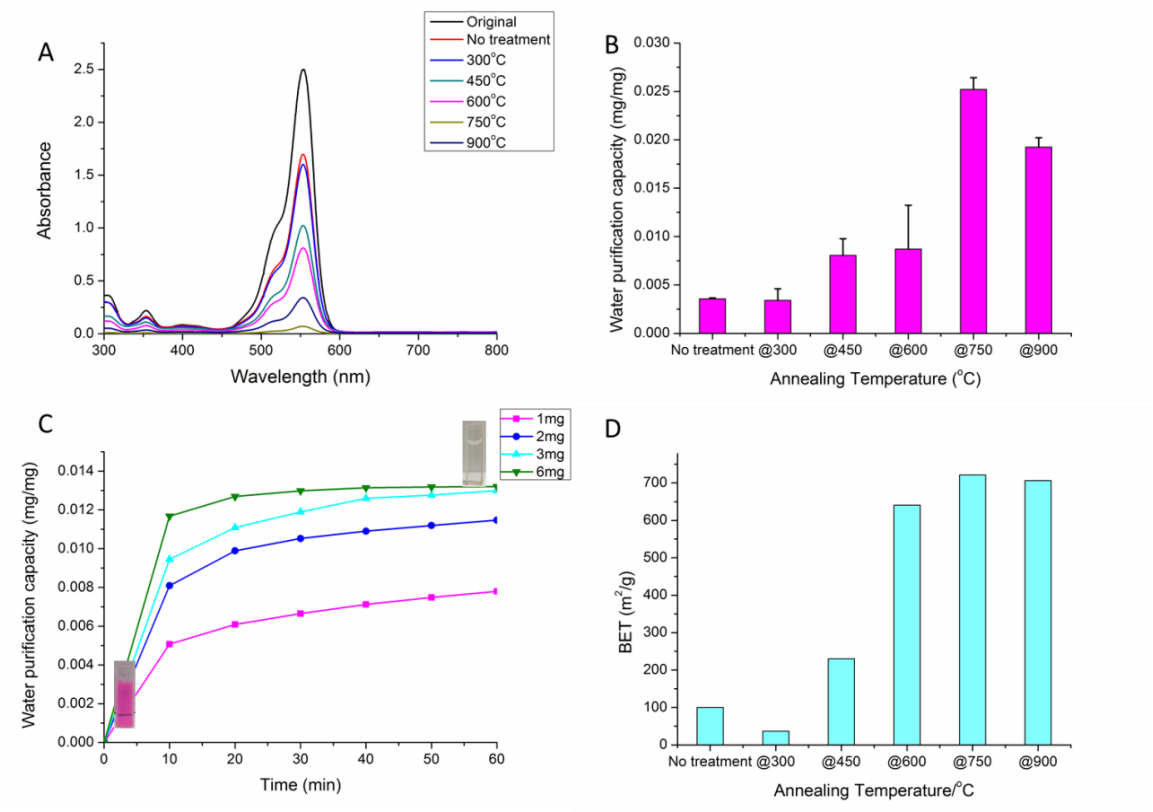

Figure 7.8 UV-vis spectra showing (A) the typical UV-visible spectrum curves after Rhodamin B removal by 1mg/ml polyazomethine and annealed material under different temperature after 60 mins stirring. (B) The water purification capacity (C) The time dependent curves for NC-600. (D) The BET surface area for NC under different annealing temperatures

Water purification capacity measurement experiments were conducted as a function of carbon materials concentration and service time in adsorption of Rhodamin B (chosen as model contaminants) from water. The data obtained from the study are summarized in Figure 7.8.

Figure 7.8A shows the UV-Visible absorbance from 300nm to 800nm wavelength of original polymer, NC-300, NC-450, NC-600, NC-750 and NC-900 purified water for 60min. The peak at 550nm refers to the typical Rhodamine B absorbance peak. The peak height is relevant to the Proportional to the Rhodamine B concentration in the solution. For 1mg/ml carbon materials, the peak value achieves the minimum for NC-750. The no treatment polymer purified water achieved highest peak value and the NC-300 one is very close to it. There is dramatic decrease from NC-300 to NC-450. This result is corresponding to the Raman result that when the temperature is 300 ℃, the material does not carbonize. The peak value, which equals to the contamination concentraion, decreased gradually when the temperature increased from 450 ℃ to 750 ℃, but it has some reduction from 750 ℃ to 900 ℃.

All the peak values were collected and calculated to show the effect of annealing temperature to the water purification capacity (Figure 7.8 B). Evidently, the capacity achieves the maximum when the annealing temperature is 750 ℃. This means the surface area of NC-750 is maximum at this point. The capacity shows some decrease for higher temperature at 900 ℃. Figure 7.8 C represents the effect of purification time and concentration of carbon materials to the water purification capacity for NC-600. The purification rates decreased after 20mins and became stable after 30mins for all different concentrations. Both the 3mg and 6mg achieved the maximum at 60mins since the solution became totally colorless and all Rhodamine B was absorbed. Figure 7.8 D shows the BET surface area of polyazomthine, NC-300, NC-450, NC-600, NC-750 and NC900.

The surface area starts increase from 450 ℃ and achieved maximum at 750 ℃, which is corresponding to the water purification capacity results.

7.4 Conclusion

We have demonstrated a one-step method to synthesize and activate polyazomethine and obtained a graphite-similar structure nitrogen-doped materials. It was found that the water contamination adsorption capacity of the carbon materials was greatest when the annealing temperature was 750 ℃. The BET surface area data from N_2 adsorption experiments confirmed the hypothesis that the surface area difference reduced to the capacity difference. In all, the N-doped carbon material based on polyazomethine shows great potential for water purification.

ACKNOWLEDGEMENT

The authors are grateful to Kimberly Ivey for her assistance in conducting TGA and FTIR tests.

REFERENCE

(1) Geim, A. K.; Novoselov, K. S. The rise of graphene. *Nature materials* **2007**, *6*, 183-191.

(2) Avouris, P. Graphene: electronic and photonic properties and devices. *Nano letters* **2010**, *10*, 4285-4294.

(3) Schedin, F.; Geim, A.; Morozov, S.; Hill, E.; Blake, P.; Katsnelson, M.; Novoselov, K. Detection of individual gas molecules adsorbed on graphene. *Nature materials* **2007**, *6*, 652-655.

(4) Wei, D.; Liu, Y.; Wang, Y.; Zhang, H.; Huang, L.; Yu, G. Synthesis of N-doped graphene by chemical vapor deposition and its electrical properties. *Nano letters* **2009**, *9*, 1752-1758.

(5) Wei, D.; Liu, Y.; Wang, Y.; Zhang, H.; Huang, L.; Yu, G. Synthesis of N-doped graphene by chemical vapor deposition and its electrical properties. *Nano letters* **2009**, *9*, 1752-1758.

(6) Qu, L.; Liu, Y.; Baek, J.; Dai, L. Nitrogen-doped graphene as efficient metal-free electrocatalyst for oxygen reduction in fuel cells. *ACS nano* **2010**, *4*, 1321-1326.

(7) Iwan, A.; Sek, D. Processible polyazomethines and polyketanils: from aerospace to light-emitting diodes and other advanced applications. *Progress in Polymer Science* **2008**, *33*, 289-345.

(8) Kimura, K.; Zhuang, J.; Shirabe, K.; Yamashita, Y. Preparation of needle-like poly (azomethine) crystals by means of reaction-induced crystallization of oligomers. *Polymer* **2003**, *44*, 4761-4764.

(9) Yan, Y.; Chen, L.; Dai, H.; Chen, Z.; Li, X.; Liu, X. Morphosynthesis of nanostructured polyazomethines and carbon through constitutional dynamic chemistry controlled reaction induced crystallization process. *Polymer* **2012**, *53*, 1611-1616.

(10) Ding, S.; Wang, W. Covalent organic frameworks (COFs): from design to applications. *Chem. Soc. Rev.* **2013**, *42*, 548-568.

(11) Schwab, M. G.; Hamburger, M.; Feng, X.; Shu, J.; Spiess, H. W.; Wang, X.; Antonietti, M.; Müllen, K. Photocatalytic hydrogen evolution through fully conjugated poly (azomethine) networks. *Chemical Communications* **2010**, *46*, 8932-8934.

(12) Kimura, K.; Zhuang, J.; Shirabe, K.; Yamashita, Y. Preparation of needle-like poly (azomethine) crystals by means of reaction-induced crystallization of oligomers. *Polymer* **2003**, *44*, 4761-4764.

(13) Wang, J.; Senkovska, I.; Oschatz, M.; Lohe, M. R.; Borchardt, L.; Heerwig, A.; Liu, Q.; Kaskel, S. Imine-linked polymer-derived nitrogen-doped microporous carbons with excellent CO2 capture properties. *ACS applied materials & interfaces* **2013**, *5*, 3160-3167.

(14) Wang, J.; Liu, Q. An efficient one-step condensation and activation strategy to synthesize porous carbons with optimal micropore sizes for highly selective CO 2 adsorption. *Nanoscale* **2014**, *6*, 4148-4156.

(15) Uribe-Romo, F. J.; Hunt, J. R.; Furukawa, H.; Klöck, C.; O'Keeffe, M.; Yaghi, O. M. A crystalline imine-linked 3-D porous covalent organic framework. *J. Am. Chem. Soc.* **2009**, *131*, 4570-4571.

(16) Iwan, A.; Sek, D. Processible polyazomethines and polyketanils: from aerospace to light-emitting diodes and other advanced applications. *Progress in Polymer Science* **2008**, *33*, 289-345.

(17) Łużny, W.; Stochmal-Pomarzańska, E.; Proń, A. Structural properties of selected poly (azomethines). *Polymer* **1999**, *40*, 6611-6614.

(18) Kimura, K.; Zhuang, J.; Shirabe, K.; Yamashita, Y. Preparation of needle-like poly (azomethine) crystals by means of reaction-induced crystallization of oligomers. *Polymer* **2003**, *44*, 4761-4764.

(19) Gupta, S. S.; Sreeprasad, T. S.; Maliyekkal, S. M.; Das, S. K.; Pradeep, T. Graphene from sugar and its application in water purification. *ACS applied materials & interfaces* **2012**, *4*, 4156-4163.

(20) Eckmann, A.; Felten, A.; Mishchenko, A.; Britnell, L.; Krupke, R.; Novoselov, K. S.; Casiraghi, C. Probing the nature of defects in graphene by Raman spectroscopy. *Nano letters* **2012**, *12*, 3925-3930.

(21) Beams, R.; Can çado, L. G.; Novotny, L. Raman characterization of defects and dopants in graphene. *Journal of Physics: Condensed Matter* **2015**, *27*, 083002.

(22) Tseng, R. J.; Baker, C. O.; Shedd, B.; Huang, J.; Kaner, R. B.; Ouyang, J.; Yang, Y. Charge transfer effect in the polyaniline-gold nanoparticle memory system. *Appl. Phys. Lett.* **2007**, *90*, 053101.

(23) Warta, C. L.; Papadimas, S. P.; Sorial, G. A.; Suidan, M. T.; Speth, T. F. The effect of molecular oxygen on the activated carbon adsorption of natural organic matter in Ohio river water. *Water Res.* **1995**, *29*, 551-562.

(24) Yu, F.; Ma, J.; Wu, Y. Adsorption of toluene, ethylbenzene and m-xylene on multi-walled carbon nanotubes with different oxygen contents from aqueous solutions. *J. Hazard. Mater.* **2011**, *192*, 1370-1379.

(25) Derylo-Marczewska, A.; Buczek, B.; Swiatkowski, A. Effect of oxygen surface groups on adsorption of benzene derivatives from aqueous solutions onto active carbon samples. *Appl. Surf. Sci.* **2011**, *257*, 9466-9472.

CHAPTER EIGHT

CONCLUSIONS AND FUTURE WORK

In this dissertation, the animal protein based thermoset plastics were investigated with several different resin systems, like DGEBA, WPU and WEP. The thermal and mechanical properties were investigated for all the animal protein based plastics. All these researches explored new economic value added animal byproduct based materials. However, there is still a long way to go to promote the wide application of such plastics into industries. Obstacles could be the odor of the animal protein, the moisture absorption, the color of the final product, the thermal and mechanical properties limitations, etc. To introduce the animal protein plastics into industries, the researchers have to put more efforts to overcome these problems.

Another aspect is for the recyclable non-isocyanate based polyurethane/DGEBA copolymer study, the researchers have achieved mechanical properties tunable copolymer with the combining property of polyurethane and epoxy, the thermoset material, which is most importantly, could be recycled. However, there are still uncontrolled factors like copolymer water-resistance, which is due to abundant –OH groups that exist in the final product. In future, we still need to work on better design of the molecule structure and experimental pathways to obtain higher water resistance final product to satisfy different applications.

2D Covalent Organic Frameworks have been studied with the simplest example, that the polyazomethine was synthesized; annealed and sustainable applications such as water

purification and gas storage capacity were detected. It approved our hypothesis that the material has larger surface area after thermal annealing. In future, there is still a lot work to do to enlarge the molecule structure to 3D scale with more complicated functional groups and molecule architectures, which may show huge potential for electro-conductivity or photo-conductivity applications.